Chapter 2

Chemistry Climate Models and Scenarios

Lead authors: Olaf Morgenstern, Marco Giorgetta & Kiyotaka Shibata

Contributing authors: Hideharu Akiyoshi, John Austin, Andreas Baumgaertner, Slimane Bekki, Peter Braesicke, Christoph Brühl, Martyn Chipperfield, Martin Dameris, Sandip Dhomse, Stacey Frith, Hella Garny, Andrew Gettelman, Steven Hardiman, Michaela Hegglin, Doug Kinnison, Jean-François Lamarque, Elisa Manzini, Martine Michou, Eric Nielsen, Giovanni Pitari, David Plummer, Eugene Rozanov, John Scinocca, Dan Smale, Susan Strahan, Matthew Toohey, Wenshou Tian

Summary

This chapter provides ancillary information regarding the models participating in CCMVal-2, the model simulations conducted, forcings used, and diagnostics produced by the simulations. We outline the general problems associated with modelling and predicting chemistry and climate of the stratosphere. We briefly review the major components that make up modern climate-chemistry models (CCMs), addressing dynamics, radiation, chemistry, and transport. A section is devoted to introducing the 16 different models (counting nearly identical models as one) with a focus on new developments since CCMVal-1. Furthermore, we describe the reference simulations performed for CCMVal-2, the associated external forcing fields, and the deviations of the individual model setups from the definitions. We document the diagnostic output fields that modellers have produced from their simulations.

Morgenstern et al. (2010) have published a shortened version of this chapter.

2.1 Introduction

CCMVal makes use of Chemistry Climate Models (CCMs) to simulate the general circulation and the chemistry of the atmosphere from 1960 to about 2100. This period is characterized by marked changes in atmospheric composition and associated climate change. There are two interconnected developments shaping these 140 years: On the one hand, during the 20th century anthropogenic activities caused an approximate 6-folding of stratospheric chlorine (WMO, 2007, assuming CH_3Cl to be the only natural source of stratospheric chlorine), and an approximate doubling of bromine, which led to a thinning of the ozone layer everywhere and the occurrence of the ozone hole over Antarctica (Molina and Rowland, 1974; Farman *et al*., 1985). When these effects were beginning to be identified, a political process was set in motion which resulted the Montreal Protocol and subsequent amendments. Thanks to these interventions, stratospheric halogen levels have peaked around the year 2000 and are anticipated to undergo a slow recovery spanning the 21st century.

On the other hand, other human activities have caused a substantial increase of greenhouse gases. Climate change has now been unambiguously identified, and with "very high confidence" (IPCC, 2007) linked to these human activities. In the stratosphere, climate change is intricately linked to ozone abundances, through a variety of feedback processes involving temperature, transport, ultraviolet (UV), and the influence of non-halogen ozone depletion cycles involving hydrogen and nitrogen radicals (Waugh *et al*., 2009, and references therein).

Hence during the period covered by CCMVal-2, human influence on the stratosphere is thought to undergo a transition from a past dominated by ozone-depleting substances, particularly chlorofluorocarbons (CFCs), to a future increasing affected by greenhouse gases (GHGs) and climate change.

Within the CCMVal-2 project, chemistry-climate models (CCMs) are used to assess the evolution of the stratosphere under the influence of these two processes, and also taking into account natural perturbations due to volcanoes and solar variability. A comprehensive CCM would consist of a climate model and a chemistry scheme, where the climate model describes the atmosphere – ocean – land system and the different feedbacks determining the magnitude of climate change, and the chemistry scheme processes transported substances and feeds back to the circulation *via* chemical modification of radiatively active substances. One such model (see below) is participating in CCMVal-2; it is expected that in the near future more such models will reach maturity.

The first round of CCMVal (CCMVal-1), performed in 2006, produced an assessment of stratospheric climate-chemistry modelling (Eyring *et al*., 2006, 2007) which will form a basis of comparison for the present study, CCMVal-2 (Eyring *et al*., 2008). Several problems were encountered during CCMVal-1. In particular, only two models covered the whole of the 21st century producing 6 simulations; other models only covered the period to 2050 or earlier (Eyring *et al*., 2007). Considering the large differences in global ozone between models and relative to observations for the core period (1980-2025; Eyring *et al*., 2007), the ozone forecast to 2100 produced by CCMVal-1 must be considered uncertain. Serious model problems were identified, *e.g*., halogen non-conservation (Eyring *et al*., 2007) leading to erroneous ozone depletion, particularly at high latitudes, temperature biases (Eyring *et al*., 2006), and errors in the transport formulation (Eyring *et al*., 2006). Since then, modelling groups have had a few years to address these problems. Moreover, since CCMVal-1, progress in computing capacity has enabled modellers to perform longer and more simulations or, in some cases, to expand the complexity of the models (see below). Thus now more models have completed the long simulations, some performing ensemble calculations, and the designs of many models have been improved (see below) to address the problems identified in CCMVal-1.

2.2 Climate change in CCMVal-2

The experimental design for this evaluation does not require interactive coupling of the atmospheric CCM to an ocean GCM. This constitutes the most important simplification in the current report, and thus all but one model do not account for changes in surface temperature caused by changes in stratospheric composition. Instead, these CCMs prescribe sea surface temperature (SST) and sea ice cover from climate model simulations that were forced by the same observed or projected GHG concentrations. All CCMVal-2 integrations of the 21st century use the middle-of-the-road Special Report on Emission Scenarios (SRES) A1b scenario (IPCC 2001; Section 2.5.3.2). Considering that A1b is only one of the possible scenarios, and that recent CO_2 emissions are larger than foreseen in A1b (Global Carbon Budget, 2009; Le Quéré *et al*., 2009), the lack of consideration of other scenarios needs to be considered when interpreting the current results. Moreover, the impact of climate change on the CCMVal-2 predictions depends not only on the direct radiative impact of GHGs, but also on the realism of the associated parent AOGCM whose SSTs and sea ice are used. Biases in the ocean surface conditions (see below), as well as lacking feedback of ozone-induced climate change onto the ocean in most models, complicate the interpretation of climate change in the CCMs considered here. As noted before, the next generation of CCMs will likely comprise more models incorporating an interactive ocean.

2.3 Major components of chemistry climate models and their coupling by transport and radiation

The major building blocks of CCMs comprise the dynamical core, diabatic physics (*e.g.*, radiation), the transport scheme, and the chemistry and microphysics modules associated with chemical composition change. These major components are linked by feedback processes, whereby dynamics and radiation interact, radiation and chemistry interact through photolysis and GHG and aerosol forcing, and dynamics affects chemistry through the transport of chemical constituents and impacts on temperature and moisture. A schematic depiction of a CCM is given in **Figure 2.1**.

Table 1.1 (Chapter 1) introduces the models participating in CCMVal-2 with associated institutions, principal investigators, and key references. **Table 2.1** lists the main components of these models. Several models share a common heritage. For example, the E39CA, EMAC, and (Niwa-)SOCOL models are all based on the ECHAM GCM. Likewise, the UMETRAC, UMSLIMCAT, and UMUKCA models are based on the Unified Model (UM). However, both ECHAM and the UM have undergone substantial development in recent years, such that models based on the newer versions of these models (EMAC, UMUKCA) may behave quite differently from those based on the older versions (E39CA, (Niwa-)SOCOL, UMETRAC, UMSLIMCAT). CAM3.5 and WACCM are both based on CAM/CLM. The other models may be regarded as independent; however, models often share approaches to certain problems with other models (see below).

2.3.1 Dynamics

2.3.1.1 Dynamical cores and model grids

Dynamical cores describe the temporal evolution of wind, temperature and pressure, or equivalent convenient variables, under the influences of inertia in a rotating framework, gravity and various diabatic forcings. The development of dynamical cores was initially strongly pushed by the needs of numerical weather prediction (NWP), with an emphasis on accurate and highly efficient numerical methods for solving, in most cases, the primitive equations (PEs). An important breakthrough was achieved by the spectral transform method (*e.g.*, Holton, 1992), which for a relatively small number of degrees of freedom allowed accurate and numerically very efficient simulations of baroclinic waves of major concern in NWP. Hence, this method is also frequently used in atmospheric general circulation models for climate research, because of its advantageous performance at low resolution; it is used by roughly half of the CCMVal-2 models (CCSRNIES, CMAM, CNRM-ACM, E39CA, EMAC, MRI, (Niwa-)SOCOL, ULAQ; **Table 2.2**). The transport equation is however not easily treated in a spectral coordinate system, due to the occurrence of numerical artifacts, hence some "hybrid" models using the spectral transform method perform transport of chemical constituents in physical space (E39CA, EMAC, MRI, (Niwa-)SOCOL; **Tables 2.3** and **2.4**). Likewise, parameterised and explicit physical processes are difficult to implement in spectral models.

Almost all of the remaining models use a regular

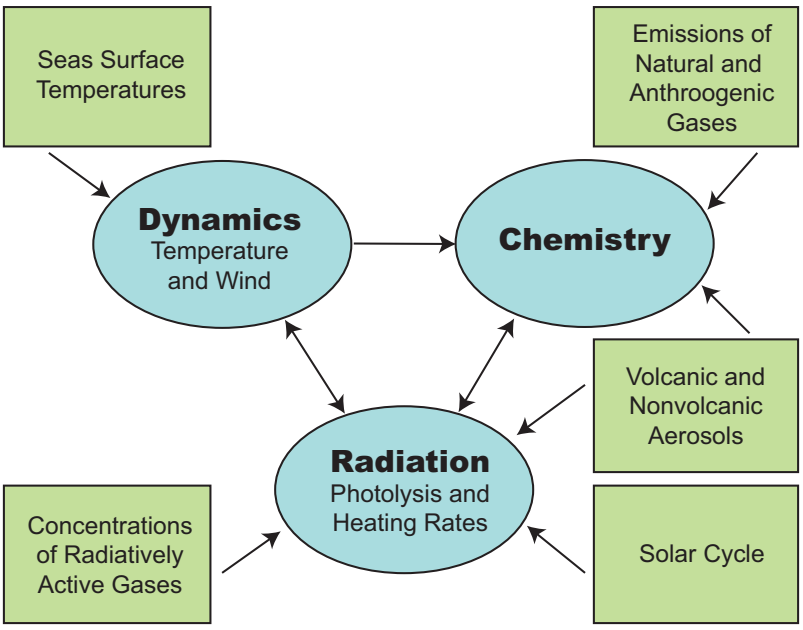

Figure 2.1: Basic structure of a CCM and external forcings (reproduced from WMO, 2007).

Table 2.1: Main structure of CCMs (names of main sub-models), for the atmosphere, ocean, land, transport, and chemistry. F = offline forcing.

CCM	Atmospheric. GCM	Ocean GCM	Land model	Reference	Transport model for meteorol. active constituents	Transport model for chemically active constituents	Chemistry scheme
AMTRAC3	AM3	N/A	LM3		AM3	AM3	*Austin (1991)*
CAM3.5	CAM	N/A	CLM		CAM	CAM	WACCM + reduced HCs
CCSRNIES	CCSR/NIES AGCM 5.4g	N/A	CCSR/NIES AGCM 5.4g	*Numaguti et al. (1997)*	CCSR/NIES AGCM 5.4g	CCSR/NIES AGCM 5.4g	*Akiyoshi (2000), Nagashima et al. (2002) Akiyoshi et al. (2009)*
CMAM	AGCM3	Modified NCOM 1.3	CLASS 2.7		AGCM3 spectral	AGCM3 spectral	*deGrandpré et al. (2000) plus updates*
CNRM-ACM	ARPEGE-Climate version 4.6	N/A	ISBA	*Déqué (2007); Teyssèdre et al (2007)*	Déqué (2007)	*Williamson and Rasch (1989)*	REPROBUS: *Lefèvre, (1994)*
E39CA	ECHAM4	N/A	ECHAM4	*Roeckner et al. (2004)*	ECHAM4	ATTILA (*Reithmeier and Sausen, 2002*)	CHEM *(Steil et al., 1998)*
EMAC	ECHAM5	N/A	ECHAM5		ECHAM5	ECHAM5	MECCA1 *(Sander et al., 2005)*
GEOSCCM	GEOS5	N/A	CLSM	*Koster et al. (2000)*	GEOS5	GEOS5	*Stratchem (Douglass et al., 1997; Kawa et al., 2002)*
LMDZrepro	LMDz	N/A	ORCHIDEE (F)		*Hourdin et al. (2006)*	*Hourdin and Armengaud (1999)*	*Lefevre et al. (1998)*
MRI	MJ98	N/A			MJ98	MJ98	*Shibata et al. (2005)*
Niwa-SOCOL SOCOL	MAECHAM4	N/A	ECHAM4		MAECHAM4	Hybrid (SLS+SOMC) *Zubov et al. (1999)*	MEZON *(Egorova et al., 2003)*
ULAQ	ULAQ-GCM	N/A	N/A		ULAQ-CTM	ULAQ-CTM	*Pitari et al. (2002)*
UMETRAC	HadAM3 L64	N/A	MOSES-1		UM 4.5	UM 4.5	*Austin and Butchart (2003)*
UMSLIMCAT	HadAM3 L64	N/A	MOSES-1		UM 4.5	UM 4.5	*Tian and Chipperfield (2005)*
UMUKCA-METO UMUKCA-UCAM	HadGEM-A	N/A	MOSES-2		UM 6.1	UM 6.1	*Morgenstern et al. (2009)*
WACCM	CAM	N/A	CLM		CAM	CAM	*Kinnison et al. (2007)*

Table 2.2: Governing equations and horizontal discretizations of dynamical cores. QG = quasi-geostrophic. PE = primitive equations, NH = non-hydrostatic. STL = spectral transform linear, STQ = spectral transform quadratic, F[D,V,E]LL = finite [difference, volume, elements] on lat-lon grid. T42 approximately corresponds to 2.8º x 2.8º, T30 to 3.75º x 3.75º.

CCM	Gov. equations	Horizontal Discretization	Truncation/ resolution	Comments
AMTRAC3	PE	FV Cubed sphere	variable, ~200 km	Most results are interpolated to 2º×2.5º grid.
CAM3.5	PE	FVLL	1.9 (lat) x 2.5 (lon)	
CCSRNIES	PE	STQ	T42	
CMAM	PE	STQ	T31	For dynamics
CNRM-ACM	PE	STL	T42/T63	The linear T63 and the quadratic T42 grids both have a resolution of 2.8° × 2.8°.
E39CA	PE	STL	T30	
EMAC	PE	STQ	T42	
GEOSCCM	PE	FVLL	2˚(lat) x 2.5˚(lon)	
LMDZrepro	PE	FVLL	2.5˚(lat) x 3.75˚(lon)	Arakawa-C
MRI	PE	STQ	T42	
Niwa-SOCOL SOCOL	PE	STL	T30	
ULAQ	QG	STL	R6 / 11.5˚(lat) x 22.5˚(lon)	Dynamical core, radiation
UMETRAC UMSLIMCAT	PE	FDLL	2.5˚(lat) x 3.75˚(lon)	Arakawa-B
UMUKCA-METO UMUKCA-UCAM	NH	FDLL	2.5˚(lat) x 3.75˚(lon)	Arakawa-C
WACCM	PE	FVLL	1.9 (lat) x 2.5 (lon)	

Table 2.3: Additional horizontal grids in CCMs. CCMs not listed here do not use additional grids.

CCM	Grid	Comments
CCSRNIES	Quadratic Gaussian	for physics and chemistry
CMAM	STL	for physics and chemistry
CNRM-ACM	T42 Gaussian T21 Gaussian	Dynamics and transport Chemistry
E39CA	T30 Gaussian	Physics, chemistry, etc.
EMAC	Quadratic Gaussian equivalent to T42	Physics, chemistry, etc.
GEOSCCM	Catchment	*Koster et al. (2000)*
MRI	Quadratic Gaussian Reduced by a quarter	Dynamics + physics + chemistry Radiation
ULAQ	10˚(lat) x 22.5˚(lon)	Chemistry, aerosols

Table 2.4: Transport scheme, by tracer. FV = finite volume. FFSL = flux-form semi-Lagranian. SL = semi-Lagrangian. STFD = spectral transform and finite difference. FFEE = flux form Eulerian explicit.

CCM	Physical tracers	Water vapour	Other chemical tracers	References
AMTRAC3	FFSL	FFSL	FFSL	*Lin (2004)*
CAM3.5	FFSL	FFSL	FFSL	*Lin (2004); Rasch et al. (2006)*
CCSRNIES	STFD	STFD	STFD	*Numaguti et al. (1997)*
CMAM	Spectral	Spectral – log(q)	Spectral	
CNRM-ACM	SL cubic	SL cubic	SL cubic	*Déqué (2007); Williamson and Rasch (1989)*
E39CA	Semi-Lagrangian	ATTILA	ATTILA	*Reithmeier and Sausen (2002)*
EMAC	FFSL	FFSL	FFSL	*Lin and Rood (1996)*
GEOSCCM	FFSL	FFSL	FFSL	*Lin and Rood (1996)*
LMDZrepro	FV	FV	FV	*Hourdin and Armengaud (1999)*
MRI	STFD	STFD	Hybrid SL quintic and PRM	*Shibata and Deushi (2008b)*
Niwa-SOCOL SOCOL	semi-Lagrangian	semi-Lagrangian	Hybrid	*Zubov et al. (1999); Williamson and Rasch (1989)*
ULAQ	FFEE	FFEE	FFEE	
UMETRAC UMSLIMCAT		Quintic FV	Quintic FV	*Gregory and West (2002)*
UMUKCA-METO UMUKCA-UCAM	SL, quasi-cubic	SL. Hor.: Quasi-cubic. Vert.: quintic	Same as water vapour	*Priestley (1993)*
WACCM	FFSL	FFSL	FFSL	*Lin (2004)*

Table 2.5: Vertical grid: Grid type: L=Lorenz, CP=Charney Phillips, O = other. TP = terrain following hybrid pressure; TA = terrain following hybrid altitude. NTP = non-terrain following pressure.

CCM	Grid type, number of levels	Uppermost computational level	Top of model	Coordinate system
AMTRAC3	L48	0.017 hPa	0.01 hPa	TP
CAM3.5	L26	3.5 hPa	2.2 hPa	TP
CCSRNIES	L34	0.012 hPa	0.01 hPa	TP
CMAM	O71	0.00081 hPa		TP
CNRM-ACM	L60	0.07 hPa	0 hPa	TP
E39CA	L39	10 hPa	Not 0	TP
EMAC	L90	0.01 hPa	0 hPa	TP
GEOSCCM	L72	0.015 hPa	0.01 hPa	TP
LMDZrepro	L50	0.07 hPa	0 hPa	TP
MRI	L68	0.01 hPa	0 hPa	TP
Niwa-SOCOL/SOCOL	L39	0.01 hPa	0 hPa	TP
ULAQ	CP26	0.04 hPa	Not 0	Log-NTP
UMETRAC/UMSLIMCAT	L64	0.01 hPa	0.0077 hPa	TP
UMUKCA-METO/UMUKCA-UCAM	CP60	84 km	84 km	TA
WACCM	L66	5.96×10^{-6} hPa	4.5×10^{-6} hPa	TP

Table 2.6: Vertical resolution: Number of full levels for p_s = 1013.25 hPa at sea level, between p_s and 850 hPa, between 850 hPa and 300 hPa, between 300 hPa and 100 hPa, between 100 and 1 hPa, above 1 hPa.

CCM	p_s – 850 hPa	850 – 300 hPa	300 – 100 hPa	100 – 1 hPa	Above 1 hPa	Comments
AMTRAC3	8	9	7	15	9	
CAM3.5	4	7	7	8	0	
CCSRNIES	4	5	6	13	6	
CMAM	10	12	7	20	22	
CNRM-ACM	12	15	8	21	4	
E39CA	5	11	15	8	0	
EMAC	4	11	12	48	15	
GEOSCCM	10	18	7	23	14	
LMDZrepro	7	11	8	20	4	
MRI	6	7	6	42	7	
Niwa-SOCOL/SOCOL	5	6	5	15	8	
ULAQ	1	2	3	12	8	
UMETRAC/UMSLIMCAT	4	13	9	24	14	
UMUKCA-METO/UMUKCA-UCAM	8	13	7	22	10	US standard atmosphere
WACCM	4	7	7	21	27	

latitude-longitude grid, favoured because it allows for a straightforward discretization of the governing equations on a single grid. Disadvantages are a non-uniform resolution and special treatments required at the poles (*e.g.*, Lanser *et al.*, 2000, Table 2.2). Only the AMTRAC3 model uses neither of the above discretization methods. AMTRAC3 uses a "cubed sphere" grid (Putman and Lin, 2007; Adcroft *et al.*, 2007), based on projecting the edges of a cube onto a sphere around its centre.

The dynamical cores of most CCMs are based on the primitive equations (*e.g.*, Holton, 1992), with terrain-following hybrid-pressure as the vertical coordinate (**Table 2.5**). The MetOffice's New Dynamics Unified Model (UMUKCA-METO, UMUKCA-UCAM) solves a non-hydrostatic set of equations (Davies *et al.*, 2005), although UMUKCA is used at a resolution that would justify the hydrostatic approximation. This also results in UMUKCA being the only model using hybrid-height as the vertical coordinate system (*i.e.*, near the surface, the model levels follow the orography, but in the stratosphere are pure height levels; Tables 2.2 and 2.5). The ULAQ CCM uses a geostrophic set of equations (Pitari, 1993), resulting in stronger constraints to simulated dynamics than in the other CCMs (Table 2.2). Also ULAQ use non-terrain following pressure (Table 2.5). Vertical resolution can also play a major role in model performance, *e.g.*, in representing the QBO (see below) or transition regions such as the tropopause. CCMVal-2 models exhibit a wide range of vertical resolutions. For example, the region between 100 and 1 hPa is covered by between 8 and 48 levels (**Table 2.6**).

2.3.1.2 Horizontal diffusion

Diffusion is generally split into horizontal and vertical components. Horizontal diffusion is often used as closure for the discretized horizontal dynamics, which accumulates energy at the resolution limit. Depending on the dynamical core, this is achieved implicitly (GEOSCCM, UMUKCA) or explicitly using a horizontal diffusion term or a form of spectral damping (all other CCMVal-2 models). Due to the lack of a general theory of turbulence, horizontal diffusion schemes vary a lot in their characteristics, but achieve the main purpose of suppressing dynamical instabilities with the least possible impact on large scale features of the general circulation. Models with spectral transform dynamics often apply high-order diffusion operators to be scale selective (CNRM-ACM, E39CA, EMAC, (Niwa-)SOCOL), while those grid-point models requiring explicit diffusion rely on low-order operators, which can be realised with small stencils (CAM3.5, LMDZrepro, WACCM; **Table 2.7**), .

"Sponges", *i.e.* increased diffusivity near the model top, are often necessary to reduce the artificial reflection of atmospheric waves off the model top, and are used in the majority of CCMVal-2 models. Depending on the formulation of the sponge, its effects may however extend to lower layers and violate angular momentum conservation (Shepherd *et al.*, 1996; Shepherd and Shaw, 2004; Shaw *et al.*, 2009). Such effects can be avoided if the sponge does not affect the zonal-mean structures (EMAC, CMAM). Some models do not use a sponge at the model

Table 2.7: Horizontal diffusion

CCM	Order of diff. scheme	Linear	Damping time of smallest scales (h)	Range of sponge layer	Reference	Comment
CAM3.5	2	Yes	Wavenumber-Dependent	≤14 hPa	*Collins et al. (2004)*	Divergence Damping
CCSRNIES	4	Yes	18	Sponge	*Numaguti et al. (1997)*	
CMAM			13.9		*Koshyk and Boer (1995)*	Modified Leith diff.
CNRM-ACM	6	Yes			*Yessad (2001)*	
E39CA	10 (2 at top)		9	≤20 hPa	*Roeckner et al. (1996); Land et al. (2002)*	
EMAC	10	No	9	Sponge	*Roeckner et al. (2003)*	
GEOSCCM	N/A	N/A	N/A	No sponge		No explicit diffusion
LMDZrepro	2			Sponge	*Hourdin et al. (2006)*	
MRI	4	Yes	18 (p>150hPa) 100 (p<100hPa)	No sponge	*Shibata and Deushi (2008a)*	
Niwa-SOCOL SOCOL	10	No	6	0.01 hPa (top level)	*Manzini and McFarlane (1998)*	
ULAQ	N/A	Yes	12	Sponge	*Pitari et al. (2002)*	
UMETRAC UMSLIMCAT		No		≤0.017 hPa		
UMUKCA-METO UMUKCA-UCAM	N/A	N/A	N/A	No sponge	*McCalpin (1988)*	No explicit diffusion
WACCM	2	Yes	Wavenumber-Dependent	≤1.6-5 hPa	*Collins et al. (2004)*	Divergence Damping

top (GEOSCCM, MRI, UMUKCA; Table 2.7). Further aspects of numerical diffusion are discussed below in the context of advection schemes (Section 2.3.4.1).

2.3.1.3 The Quasi-Biennial Oscillation

The Quasi-Biennial Oscillation (QBO) is the major dynamical mode of variability of the tropical stratosphere and gives rise to QBO signals in circulation and chemistry in many other regions of the atmosphere (Baldwin *et al.*, 2001). The QBO results from wave mean-flow interaction, which reinforces the westerly and easterly jets of the QBO and causes their downward propagation against the general upwelling in the tropical stratosphere. In recent years, a number of climate models have simulated the QBO (Takahashi, 1999; Scaife *et al.*, 2000; Giorgetta *et al.*, 2002; McLandress, 2002). However, the simulation of the QBO in atmospheric GCMs or CCMs is still a major challenge (Giorgetta *et al.*, 2006). The major difficulty in simulating the QBO arises from the imperfect representation of tropical convection, which in reality excites a broad spectrum of vertically propagating waves. While CCMs can resolve the large-scale portion of this spectrum, if a suitable vertical resolution is used, a realistic excitation of these waves also depends strongly on the spatial and temporal characteristics of the simulated tropical convective clouds, and therefore on the parameterisation of these clouds (Horinouchi *et al.*, 2003). The contribution of unresolved waves to the wave mean-flow interaction in the QBO shear layers depends entirely on parameterisations of gravity waves. While the simulation of the wave mean-flow interaction is considered to be the biggest challenge, the tropical upwelling also needs to be well simulated, to allow for a realistic quasi-biennial period of the equatorial oscillation in zonal wind (Giorgetta *et al.*, 2006).

Table 2.8: Usage of QBO nudging in CCMVal-2 simulations: CCM name; experiments run with QBO nudging; variable that is nudged, '<x>' indicates that the nudging is applied on the zonal-mean of the variable x, while 'x' indicates local nudging; time scale in (days) used for the nudging in the core of the QBO domain; latitude range in °latitude where the nudging is applied; height range of the QBO nudging in hPa or km for pressure or height based vertical coordinate systems, respectively. Models not listed here do not impose a QBO but may have an internally generated QBO.

CCM	Experiments including QBO nudging	Nudged variable	Time scale (day)	Latitude range (°)	Pressure range (hPa)	Comments
CAM3.5	REF-B1	u	10	22°S-22°N	90 – 3 hPa	
CCSRNIES	REF-B1	<u>	5	Tropics	Mid-stratosphere	
E39CA	REF-B1, SCN-B2d	u	7	20°S-20°N	90 – 10 hPa	*Giorgetta and Bengttson (1999)*
EMAC	REF-B1	u	58	7°S-7°N	50 – 15 hPa	
Niwa-SOCOL SOCOL	REF-B1	u	7	10°S-10°N (full), 20°S-10°S, 10°N-20°N (tapered)	90 – 3hPa	*Giorgetta (1996)*
ULAQ	REF-B1	rel. vorticity	10	23°S–23°N	107 – 2.8 hPa	
WACCM	REF-B1	u	10	22°S-22°N	90-3 hPa	

Among the CCMs used for CCMVal-2, EMAC, the UM based models (UMETRAC, UMSLIMCAT, and UMUKCA; Scaife *et al*., 2000), and MRI spontaneously simulate the QBO (Chapter 8). The other models either do not include QBO nudging (AMTRAC3, CMAM, LMDZrepro) and produce no QBO, or the appearance of the QBO depends entirely on the assimilation of the equatorial zonal wind to externally given QBO wind profiles (CAM3.5, CCSRNIES, E39CA, SOCOL, Niwa-SOCOL, ULAQ, WACCM; **Table 2.8**). EMAC also applies nudging in its simulations of the past, in order to synchronise its internally generated QBO with observations. The nudging time scale is typically chosen between 5 and 10 days, *i.e*., on the time scale of large scale equatorial waves, whose unrealistic representation (due to insufficient vertical resolution and / or excitation by tropical weather) is the primary reason for the absence of a QBO in some CCMs. In EMAC, however, the time scale is 58 days, hence much longer than the time scales of the driving wave spectrum, and the nudging domain is more restricted than in the other models (**Table 2.8**).

QBO nudging has however limitations:

1. By construction, the nudging of zonal wind introduces localized momentum sources and sinks, thus violating the internal momentum budget of the atmosphere.
2. The QBO is an internal mode of variability, but nudging makes the QBO dependent on boundary conditions. This will destroy any internal variability arising from two-way interaction with the extra-tropics (Anstey *et al*., 2010).
3. Nudging generally results in a realistic zonally averaged structure of the QBO, but does not repair the potentially deficient wave structures. QBO nudging can therefore contribute to QBO signals related to zonal mean effects, but not to QBO signals dependent on waves, *e.g*., eddy fluxes of tracers.
4. Simulations covering the future cannot use nudging to observations.

2.3.1.4 Gravity wave drag

Gravity wave drag (GWD) is among the drivers of meridional overturning in the middle atmosphere, a.k.a. the Brewer-Dobson Circulation (McIntyre, 1995), and of the QBO (Section 2.3.1.3). The small spatial scales and complications due to wave breaking require their effects to be parameterised. Gravity waves are excited by tropospheric processes, mainly flow over topography and frontal and other forms of convection. Hence GWD parameterisations are usually divided into two parts, orographic and non-orographic. CAM3.5, CNRM-ACM, and WACCM link GWD to tropospheric convection (Bossuet *et al*., 1998; Richter *et al*., 2009; **Table 2.9**); in the other models, this link is not incorporated. McLandress and Scinocca (2005) examine the impacts on middle-atmosphere dynamics of three different GWD schemes (Hines, 1997a,b; Alexander and Dunkerton, 1999; Warner and McIntyre, 2001), variants of

Table 2.9: Orographic and non-orographic gravity wave drag.

CCM	Reference for orographic GWD	Sources for nonorographic GWG	Launch level for prescribed gravity waves	Latitude range for param. gravity waves	Reference for nonorographic GWD
AMTRAC3	*Pierrehumbert (1986)*	parameterised	~tropopause	90°S-90°N	*Alexander and Dunkerton (1999)*
CAM3.5	*McFarlane (1987)*	Parameterised using deep convective heating and frontal zones	ground (orog. waves); 100 hPa (deep convection); 500 hPa (fronts)	90°S-90°N	*Richter et al. (2009)*
CCSRNIES	*McFarlane (1987)*	Parameterised	Parameterised	90°S-90°N	*Hines (1997b)*
CMAM	*Scinocca and McFarlane (2000)*	Specified generalised Desaubies	100 hPa (non-orographic)	All	*Scinocca (2003)*
CNRM-ACM	*Lott (1997)*	Convection	N/A	90°S-90°N	*Bossuet (1998)*
E39CA	*Miller et al. (1989)*	None			
EMAC	*Lott (1999); Lott and Miller (1997)*	Parameterised	640 hPa	90°S-90°N	*Hines (1997a,b)*
GEOSCCM	*McFarlane (1987)*	Parameterised	100 hPa	90°S-90°N	*Garcia and Boville (1994)*
LMDZrepro	*Lott and Miller, (1997); Lott (1999); Lott et al. (2005)*	Parameterised	Surface	90°S-90°N	*Lott et al. (2005) (based on Hines (1997a,b))*
MRI	*Iwasaki et al. (1989)*	Parameterised	Lowest level	Uniform + tropical enhancement	*Hines(1997b)*
Niwa-SOCOL SOCOL	*McFarlane (1987), Manzini and McFarlane (1998)*	Parameterised	~700Pa	90°S-90°N, Tapered response based on latitude	*Hines (1997b); Charron and Manzini (2002)*
ULAQ		N/A	N/A	N/A	
UMETRAC	*Gregory et al. (1998)*	Parameterised			*Scaife et al. (2000)*
UMSLIMCAT	*Webster et al., (2003)*	Parameterised			*Scaife et al. (2000)*
UMUKCA-METO UMUKCA-UCAM	*Webster et al. (2003)*	Prescribed	Parameterised	90°S-90°N	*Scaife et al. (2000)*
WACCM	*McFarlane (1987)*	Parameterised using deep convective heating and frontal zones	ground (orog. waves); 100 hPa (deep convection); 500 hPa (fronts)	90°S-90°N	*Richter et al. (2009)*

which are widely used across the CCMVal-2 models (Table 2.9). The three schemes, when employed in a comparable way, produce very similar dynamical responses despite differences in the dissipation mechanisms. This suggests that differences in responses to GWD are mainly due to adjustable parameters in the schemes, such as the properties of the launch spectrum or the launch height, but not the dissipation mechanism. E39CA does not have a representation of non-orographic GWD because of the low top in this model. ULAQ represents the effect of GWD through Rayleigh friction (Table 2.9), which violates momentum conservation (Shepherd and Shaw, 2004). Momentum conservation can also be violated in flux-based GWD parameterisations if momentum flux is allowed to escape out the top of the model domain (Shaw and Shepherd, 2007).

2.3.2 Radiation

Radiative processes lead to additional challenges in the development of CCMs, especially concerning the solar UV radiation relevant for dynamics and chemistry. Traditionally separate radiative transfer schemes are used for shortwave heating and photolysis; this is the case in all CCMVal-2 models except CCSRNIES (Akiyoshi *et al*., 2009) and WACCM (Kinnison *et al*., 2007). Radiative transfer schemes for shortwave heating often use relatively broad spectral bands covering the solar spectrum from the near infrared to the UV, and include scattering by air molecules and cloud and aerosol particles (*e.g*., Edwards and Slingo, 1996). Radiative transfer schemes used for photolysis (Section 2.3.3.5) need to resolve the UV spectrum much better, and scattering may be treated differently (*e.g*., Lary and Pyle, 1991). All models use the two-stream approximation for short-wave radiation (a common simplification used in radiative transfer modelling; **Table 2.10**). An inspection of the number of spectral bands, both in the shortwave and the longwave part of the spectrum (**Table 2.11**), reveals substantial differences in spectral resolution. Models that cover the upper atmosphere (WACCM, CMAM) also include chemical heating (*i.e*. the heating produced by some exothermic / endothermic chemical reactions, which is typically ignored at lower levels; Marsh *et al*., 2007) and non-local thermodynamical equilibrium (LTE) effects, produced *e.g*., by excitation of vibrational states of molecules under conditions of low collision probability (low density; Kockarts, 1980; Fomichev *et al*., 1998). A more detailed discussion on radiation in CCMVal-2 models, including an offline comparison of the models' radiation schemes, is the subject of Chapter 3.

2.3.3 Chemistry and composition

2.3.3.1 Stratospheric chemistry

Tables 2.12 and **2.13** summarize broadly the scopes of the different chemical schemes in use for CCMVal-2. More detail is in the online supplement. All models participating in CCMVal-2 employ an inorganic chemistry scheme including chlorine chemistry; all but the E39CA model also contain an explicit representation of bromine chemistry. In the E39CA model, bromine chemistry is parameterised (supplement to Stenke *et al*., 2009). The number and type of source gases for chlorine and bromine varies greatly between models. Lumping (*i.e*., adding the halogen atoms of those source gases not represented in the chemistry schemes to those that are, with similar lifetimes) is used widely across the CCMVal-2 models (Section 2.5.2.2); only AMTRAC3, CCSRNIES, CNRM-ACM, (Niwa-) SOCOL, and UMETRAC do not use it. Particularly for UMSLIMCAT and UMUKCA this has a big impact on the few halogen sources gases (CFC-11, CFC-12, CH_3Br) represented in their schemes (Chipperfield, 1999). AMTRAC3 and UMETRAC do not transport the halogen source species directly, but the local rates of change of inorganic chlorine and bromine are calculated using tabulated functions of the derivatives of the source molecules with respect to the age of air (Austin and Butchart, 2003). Although modellers have been asked to update their kinetics data to JPL (2006), few have done so completely and most use a mixture of different sources (Table 2.12; Chapter 6). A detailed assessment of chemistry in CCMVal-2 models, including a comparison with a benchmark photochemical steady-state (PSS) model, is the subject of Chapter 6. Also a comprehensive listing of reactions can be found there.

2.3.3.2 Tropospheric chemistry

The major target of CCMVal-participating models is currently not the troposphere but the stratosphere; hence tropospheric chemistry is simplified or absent in most models. This is motivated by the success *e.g*., of stratospheric chemistry-transport models in broadly reproducing stratospheric ozone without considering tropospheric chemistry (*e.g*., Chipperfield, 1999). However, the absence of tropospheric chemistry in most CCMVal-2 models must be regarded as a limitation. Only CAM3.5, EMAC, and ULAQ include a comprehensive representation of tropospheric chemistry (Table 2.13); these models are however characterized by low resolution (ULAQ), a low model top (CAM3.5), or few simulations (EMAC). This reflects the added cost imposed by tropospheric chemistry. In the other models, tropospheric composition is handled in a variety of ways: Introduction of background tropospheric

Table 2.10: Shortwave radiation. 2-s: Two-stream.

CCM	Reference	Description	Clouds	Spectral interval boundaries (nm)	Gas abs.
CAM3.5	*Briegleb et al. (1992); Collins et al. (2004)*	Δ-Eddington 2-s	Random / max. overlap	19 intervals (>200nm); <200nm consistent with photolysis.	O_2, O_3, CO_2, H_2O
CCSRNIES	*Nakajima and Tanaka (1986); Nakajima et al. (2000)*	2-s	random overlap	[200,217],[217,233],[233,278],[278,290],[290,303],[303,317],[317, 690],[690,2500],[2500,4000]	O_2, O_3, CO_2, H_2O
CMAM	*Fouquart and Bonnel (1980); Fomichev et al. (2004)*	Δ 2-s	Maximum or random overlap	[250,690],[690,1190],[1190,2380],[2380,4000]; Separate parameterizations for near-IR CO2 [1200,4300] above 1 hPa and O2 absorption in SRC [125-175] and SRB [175-205] above 0.25 hPa	O_2, O_3, CO_2, H_2O
CNRM-ACM	*Morcrette (1990, 1991)*	Fourquart-Morcrette 2-s	maximum random overlap	[250,680], [680,4000]	O_3, H_2O, O_2, CO_2, CH_4, N_2O
E39CA	*Fouquart and Bonnel (1980)*	Δ 2-s	Maximum to random overlap	[245-685]	O_2, O_3, CO_2, H_2O
EMAC	*Nissen et al (2007) ; Fouquart and Bonnel (1980) ; Roeckner et al. (2003)*	Δ 2-s	Maximum to random overlap	121.6], [125,175], [175,205], [206,244], [244,278], [278,362], [362,683] (49 bands), [690,1190], [1190,2380], [2380,4000]	O_2, O_3, CO_2, H_2O
GEOSCCM	*Chou and Suarez (1999); Sud et al. (1993); Chou et al. (1997)*	Δ-Eddington 2-s	Maximum random overlap	[175-225],[225-245],[245-260],[280-295], [295-310], [310-320], [320-400], [400-700], [700-1220], [1220-2270], [2270-10000]	O_2, O_3, CO_2, H_2O
LMDZrepro	*Fouquart and Bonnel (1980)*	2.s	Maximum or random overlap	[250,680], [680,4000]	O_2, O_3, CO_2, H_2O
MRI	*Briegleb et al. (1992); Shibata and Uchiyama (1992)*	Δ 2-s. DOM	Maximum to random overlap	[200,245], [245,265], [265,275], [275,285], [285,295], [295,305], [205,350], [350,700], [700,5000], [2630-2860], [4160-4550]	O_2, O_3, CO_2, H_2O
Niwa-SOCOL SOCOL	*Fouquart and Bonnel (1980); Egorova et al. (2004)*	Δ 2-s	Maximum or random overlap	[250-680],[680-4000]; parameterization for O2 and O3 absorption in L-α [121-122], SRB [175-205] and HC [200-250]	O_2, O_3, CO_2, H_2O
ULAQ	*Lacis et al. (1992); Pitari (1993); Pitari et al. (2002)*	Δ-Eddington 2-s	Maximum random overlap	21 intervals [135, 175]; 14 intervals [175, 200]; 19 intervals [200, 245]; 19 intervals [245, 320]; 11 intervals [320, 690]; 16 intervals [690, 10000]	O_2, O_3, CO_2, H_2O, NO_2
UMETRAC UMSLIMCAT	*Edwards and Slingo (1996); Zdunkowski et al. (1982); Zhong et al. (2001)*	2-s	Maximum to random overlap	[116,175], [175,200], [200,245], [245,320], [320,690], [320,690], [690,1190], [1190,2380], [2380,10000]	O_2, O_3, CO_2, H_2O
UMUKCA-METO UMUKCA-UCAM	*Edwards and Slingo (1996; Zdunkowski et al. (1982); Zhong et al. (2008)*	2-s.	Maximum to random overlap	[200,320], [320,690], [320,690], [690,1190], [1190,2380], [2380,10000]	O_2, O_3, CO_2, H_2O
WACCM	*Briegleb et al. (1992); Collins et al. (2004)*	Δ-Eddington 2-s	Random / max. overlap	19 intervals (>200nm); <200nm consistent with photolysis	O_2, O_3, CO_2, H_2O

Table 2.11: Longwave radiation.

CCM	Reference	Description	Spectral interval boundaries (μm)	Gas abs.	Chem. heating	Non-LTE
CAM3.5	*Collins et al. (2004)*	Broad Band Approach	*Collins et al. (2004)*	H_2O, CO_2, O_3, CH_4, N_2O, F11, F12, NO	NO	NO
CCSRNIES	*Nakajima et al. (2000)*	Discrete ordinate and k-distribution	[4.00,5.00], [5.00,7.14], [7.14,9.09], [9.09,10.1], [10.1,13.0], [13.0,18.2], [18.2,25.0], [25.0,40.0], [40.0,200]	H_2O, CO_2, O_3, CH_4, N_2O, CFCs	NO	NO
CMAM	*Morcrette (1991); Fomichev et al. (2004)*	>39 hPa: 2-s; < 6.7 hPa: Matrix param. 6.7-39: Merging region	Below 39 hPa: [6.9,8.0 : 3.5,5.3], [9.0,10.3], [10.3,12.5 : 8.0,9.0], [12.5,20.0], [20.0,28.6], [28.6,10000 : 5.3,6.9]; Above 6.7 hPa: 15 μm CO_2, 9.6 μm O_3 and rotational H_2O bands	Below 39 hPa: H_2O, CO_2, O_3, CH_4, N_2O, F11, F12; Above 6.7 hPa: H_2O, CO_2, O_3	YES	YES (CO_2, O_3, O_2)
CNRM-ACM	*Morcrette (1990, 1991)*	FMR ; 2-stream	[28.6,]+[5.3,6.9], [20.0,28.6], [12.5,20],[10.3,12.5]+[8,9],[9 ,10.3], [6.9,8]+[3.5,5.3]	O_3, H_2O, CO_2, CH_4, N_2O, F11	NO	NO
E39CA	*Morcrette (1991)*	Broad-band flux emissivity method in six spectral intervals	[3.55,8], [8,10.31], [10.31,12.5], [12.5,20], [20,28.57], [28.57,1000]; wavenumbers 0 to 2.82 x 10^5 m^{-1}	H_2O, CO_2, O_3, CH_4, N_2O, F11, F12	NO	NO
EMAC	*Roeckner et al. (2003); Mlawer et al. (1997)*	Correlated-k method, RRTM	[3.3,3.8], [3.8,4.2], [[4.2,4.4], [4.4,4.8], [4.8,5.6], [5.6,6.8], [6.8,7.2], [7.2,8.5], [8.5,9.3], [9.3,,10.2], [10.2,12.2], [12.2,14.3], [14.3,15.9], [15.9,20], [20,40], [40,1000]	H_2O, CO_2, O_3, CH_4, N_2O, F11, F12	NO	NO
GEOSCCM	*Chou et al. (2001)*	k-distribution and table look-up	[29.4,10000], [18.5,29.4], [16.1,18.5], [13.9,16.1], [12.5,13.9], [10.2,12.5], [9.09,10.2], [7.25,9.09], [5.26,7.25], [3.33,5.26]	H_2O, CO_2, O_3, F11, F12, F22, CH_4, N_2O	NO	NO
LMDZrepro	*Morcrette (1991)*	Broad-band flux emissivity method in six spectral intervals	[3.55,8], [8,10.31], [10.31,12.5], [12.5,20], [20,28.57], [28.57,1000]; wavenumbers 0 to 2.82 x 10^5 m^{-1}	H_2O, CO_2, O_3, CH_4, N_2O, F11, F12	NO	NO
MRI	*Shibata and Aoki (1989)*	Multi-parameter-random model	20-550-800-1200-2200 cm^{-1}; [4.55,8.33], [8.33,12.5], [12.5,18.2], [18..2,50]	H_2O, CO_2, O_3, CH_4, N_2O	NO	NO

Table 2.11 continued.

CCM	Reference	Description	Spectral interval boundaries (µm)	Gas abs.	Chem. heating	Non-LTE
Niwa-SOCOL SOCOL	*Morcrette (1991)*	Broad-band approach	[6.9-8 & 3.5-5.3], [9-10.3], [10.3-12.5 & 8-9], [12.5,20], [20,28.6], [28.6, 10000 & 5.3,6.9]	CH_4, N_2O, F11, F12, CO_2, H_2O, O_3	NO	NO
ULAQ	*Andrews et al. (1987) Lacis et al. (1992); Pitari (1993)*	Broad Band Approach	[18.2,28.6], [12.5,18.2], [8.3,12.5], [3.3,7.5]	H_2O, CO_2, O_3	NO	NO
UMETRAC UMSLIMCAT	*Edwards and Slingo (1996), Zdunkowski et al. (1982), Zhong and Haigh (2001)*	2-s.	[28.6,10000], [18.2,28.6], [12.5,18.2], [13.3,16.9], [8.33,12.5], [8.93,10.1], [6.67,8.33], [8.93,10.1], [6.67,8.33], [5.26,6.67], [3.34,5.26]	H_2O, CO_2, O_3, CH_4, N_2O, F11, F12	NO	NO
UMUKCA-METO UMUKCA-UCAM	*Edwards and Slingo (1996), Zdunkowski et al. (1982)*	2-s.	[25,10000], [18.2,25], [12.5,18.2], [13.3,16.9], [8.33,12.5], [8.93,10.1], [7.52,8.33], [6.67,7.52], [3.34,6.67]	H_2O, CO_2, O_3, CH_4, N_2O, F11 (rescaled), F12 (rescaled)	NO	NO
WACCM	*Collins et al. (2004)*	Broad Band Approach	*Collins et al. (2004)*	H_2O, CO_2, O_3, CH_4, N_2O, F11, F12, NO	*Marsh et al. (2007)*	*Fomichev et al. (1998), Kockarts (1980)*

chemistry/methane oxidation (AMTRAC3, CCSRNIES, E39CA, MRI, (Niwa-)SOCOL, UMETRAC, UMUKCA, WACCM); relaxation of tropospheric ozone and/or other constituents to a climatology (AMTRAC3, GEOSCCM, CNRM-ACM, LMDZrepro, UMETRAC); or the treatment of chemical species as passive tracers below a level (CMAM, UMSLIMCAT; Table 2.13).

2.3.3.3 Mesospheric and upper atmospheric chemistry and physics

Processes specific to the upper atmosphere include ion chemistry, solar particle precipitation associated with NO_x production, and other effects. Mesospheric NO_x production is thought to affect NO_y abundances in the stratospheric polar vortex (Vogel *et al.*, 2008) although its magnitude is uncertain and dependent on solar activity. Only WACCM has explicit representations of these upper-atmospheric processes (Garcia *et al.*, 2007). EMAC (Baumgaertner *et al.*, 2009), MRI, and WACCM treat the production of NO_x by cosmic rays and solar particles in the mesosphere; the CMAM model takes this into account by imposing an upper boundary condition (at ~95 km) for NO_x of 1 ppmv.

2.3.3.4 Time-integration of chemical kinetics

Homogeneous reactions (*i.e.*, reactions between free-moving gas phase molecules) are represented by simultaneous first-order, first-degree, homogeneous ordinary differential equations and thus their solutions are generally not chaotic (Shepherd, 2003). This sets them apart from the chaotic properties of atmospheric dynamics. However, chemical reactions are stiff in that the lifetimes of individual species vary by many orders of magnitude (*e.g.*, Jacobson, 1999). To obtain stable and accurate solutions for such stiff chemical equations, different numerical methods have been used in atmospheric chemistry. Most popular is the family method (*e.g.*, Ramaroson *et al.*, 1992; Douglass

and Kawa, 1999), adopted by all CCMVal-2 models except CAM3.5, CMAM, EMAC, (Niwa-)SOCOL, UMUKCA, and WACCM. This method relies on the fact that there are groups (families) of gases, namely the odd oxygen (O_x), odd hydrogen (HO_x), odd nitrogen (NO_x), chlorine (ClO_x), and bromine (BrO_x) families, within which family members are linked by fast reactions (meaning that equilibrium assumptions can be made), but the lifetimes of the families as a whole are much longer. As a result, families are treated as long-lived species and can be integrated with a longer time step. Indeed, the family method is accurate for moderate- and low-stiffness systems, but, to be so, the families need to be carefully set up and validated. The grouping of species into families for chemistry does not need to correspond to any grouping adopted for transport (de Grandpré *et al*., 1997; Dameris *et al*., 2005).

By contrast, the non-families methods, used by CAM3.5, CMAM, EMAC, (Niwa-)SOCOL, UMUKCA, and WACCM (Kinnison *et al*., 2007; Morgenstern *et al*., 2009), make no such *a priori* assumption about lifetimes. Advantages of non-families chemistry include the possibility to extend the chemistry scheme into the upper atmosphere (above approximately 60 km, where the chemical equilibrium assumption underlying the family formulations is not valid). Solvers in this category comprise a Rosenbrock-type predictor-corrector method (EMAC), a combined explicit-implicit backward-Euler method (CAM3.5, CMAM, WACCM), and the Newton-Raphson iterative method ((Niwa-)SOCOL, UMUKCA).

2.3.3.5 Photolysis

There are two methods for the calculation of photolysis rates, the online and the offline (look-up table) methods. Offline methods involve filling, for every photolysis reaction included in the model, a table of photolyis rates as functions of pressure, solar zenith angle (SZA), with SZAs up to 100º taken into consideration, overhead ozone column, and often temperature (*e.g*., Lary and Pyle, 1991; **Table 2.14**). SZAs larger than 90º are important for polar spring ozone depletion triggered by solar radiation which reaches the stratosphere earlier than the Earth's surface, due to the Earth's curvature. The tables are filled offline or once at the start of a simulation. Interpolation then yields the photolysis rates at any time and location of the model simulation. This method is computationally efficient; however, it usually limits the number and types of physical effects that can be considered. For example, surface albedo, clouds, and aerosols are often assumed uniform (*e.g*., Chipperfield, 1999). If solar cycle effects are included, the photolysis tables need to be updated periodically, or the phase of the 11-year cycle needs to be among the interpolation parameters (AMTRAC3).

By contrast, models using online photolysis schemes (CAM3.5, CCSRNIES, EMAC, E39CA, WACCM) evaluate the radiative transfer equation at the time of simulation, accounting in addition for variations in cloudiness, albedo, and solar output (Landgraf and Crutzen, 1998; Bian and Prather, 2002) which are usually ignored by offline photolysis methods. As noted before, CCSRNIES and WACCM treat photolysis and shortwave radiation consistently, whereas the other models calculate shortwave radiation and photolysis separately, possibly leading to inconsistencies. A detailed investigation of photolysis in CCMVal-2 models is the subject of the PHOTOCOMP study (Chapter 6).

2.3.3.6 Heterogeneous reactions and PSC microphysics

On the surfaces of liquid and solid particles, certain chemical reactions proceed efficiently between gas molecules and adsorbed or substrate molecules in the surface layer. Such reactions are called heterogeneous. The heterogeneous reactions are described by a first-order loss process for the gas reactant, and the rate constant is proportional to the thermal velocity of the gas molecules, the particulate surface area density, and an uptake coefficient. The uptake coefficient is dimensionless with a value between 0 and 1, and typically depends on temperature and pressure (JPL, 2006).

In the CCMVal-2 models, two types of particles, sulfate aerosols and polar stratospheric clouds (PSCs), are considered in the stratosphere. Sulfate aerosols result from oxidation of sulfur-containing precursors (*e.g*., OCS) during volcanically clean periods; in addition, explosive volcanic eruptions can cause temporary increases in the sulfate aerosol abundance by orders of magnitude (*e.g*., Robock, 2002). The absence of representations of stratospheric aerosol physics and chemistry in CCMVal-2 models means that sulfate aerosol needs to be externally imposed (Section 2.5.3.4). PSCs, on the other hand, are internal variables, and there are large differences among CCMs for their treatments, regarding their formation mechanisms, types, and sizes (**Tables 2.15** and **2.16**). All CCMs include water-ice PSCs and some form of sulfate aerosol; all except CMAM (Hitchcock *et al*., 2009) furthermore include $HNO_3 \cdot 3\,H_2O$ (nitric acid trihydrate, NAT). Heterogeneous reactions also differ between CCMs. The most important reactions for chlorine activation, and N_2O_5 hydrolysis leading to HNO_3 formation (Table 2.15, columns 2-5) are present in all models. The treatment of reactions involving bromine is less consistent; this may be because heterogeneous activation of bromine is less important than that of chlorine due to the absence of a photochemically stable inorganic reservoir for bromine (as is HCl for chlorine; Brasseur *et al*., 1999).

The conditions at which PSCs are condensed and evaporated vary, not only for water-ice PSCs but also for

Table 2.12: Chlorine, bromine, and NMHC source gases, type of chemical scheme, origin of kinetic and photolysis data. NMHC source gases are primary organic species with more than 1 carbon atom per molecule. Lumping means replacing unrepresented with represented species for chemistry. F10 = CCl_4. F11 = $CFCl_3$. F12=CF_2Cl_2. F113 = $CF_2ClCFCl_2$. F114 = $(CF_2Cl)_2$. F115 = CF_2ClCF_3. F123 = $CHCl_2CF_3$. F21 = $CHFCl_2$. F22 = CHF_2Cl. F141b = CH_3CFCl_2. F142b = CH_3CF_2Cl. H1211 = CF_2ClBr. H1301 = CF_3Br.

CCM	Chlorine source gases	Bromine source gases	NMHC source gases	Chemical scheme	Origin of kinetic data	Lumping (YES/NO)
AMTRAC3	parameterised	parameterised	None	*Austin and Wilson (2006)*		NO
CAM3.5	F10, F11, F12, F113, F22, CH_3CCl_3, CH3Cl	CH_3Br, H1211, H1301	C_5H_8, $C_{10}H_{16}$, anthropogenic VOCs	Stratosphere: WACCM Troposphere: *Lamarque et al. (2008), updated to JPL (2006)*	*JPL (2006)*	YES
CCSRNIES	F11, F12, F113, F22, CH_3Cl, CH_3CCl_3	H1211, H1301, CH_3Br, $CHBr_3$	None	N_2O-CH_4-CO-H_2O-families (O_x, HO_x, NO_x, CHO_x, ClO_x, BrO_x)	*JPL (2006)*	NO
CMAM	F10, F11, F12, F22, CH_3CCl_3, CH_3Cl	CH_3Br	None	CH_4-CO-NO_x-ClO_x-BrO	*JPL (2006)*	YES (halocarbons)
CNRM-ACM	F10, F11, F12, F113, CH_3CCl_3, CH_3Cl, F22, H1211	CH_3Br, H1211, H1301	N/A	REPROBUS *Lefèvre (1994)*	*JPL (2006)*	NO
E39CA	F10, F11, F12, CH_3Cl, CH_3CCl_3	parameterisation (*Stenke et al., 2009*)	None	CHEM (*Steil et al., 1998*)	*JPL (2002)*	YES
EMAC	F10, F11, F12, CH_3CCl_3, CH_3Cl, H1211	CH_3Br, H1301, H1211	C_2H_6, C_2H_4, C_3H_6, C_4H_{10}, CH_3CHO, CH_3COCH_3, CH_3OH, HCHO	MECCA1	*JPL (2002)*	C_4+; F113, F114, F115, F22, F141, F142 are lumped with F12
GEOSCCM	F10, F11, F12, F113, CH_3CCl_3, CH_3Cl, F22, F142b, F141b	CH_3Br, H1301, H1211, H2402	None	*Douglass et al. (1997); Kawa et al. (2002)*	*JPL (2002)*	YES
LMDZrepro	F10, F11, F12, F113, F22, CH_3CCl_3, CH_3Cl	H1211, H1301, CH_2Br_2, CH_3Br	None	CH_4-CO-NO_x-ClO_x-BrO_x	*JPL (2006)*	YES
MRI	F10, F11, F12, CH_3Cl, H1211	CH_3Br, H1211, H1301	None	CH_4-CO-NOx-ClOx-BrO_x	*JPL (2006)*	YES
Niwa-SOCOL SOCOL	F10, F11, F12, F113, F114, F115, CH_3CCl_3, F22, F141b, F142b, CH_3Cl, F21, F123	$CHBr_3$, CH2Br_2, CH_3Br, H1211, H1301	None	CH_4-CO-NO_x-ClO_x-O_x-BrO_x	*JPL (2002, 2006), IUPAC (2004, 2005)*	No

CCM	Chlorine source gases	Bromine source gases	NMHC source gases	Chemical scheme	Origin of kinetic data	Lumping (YES/NO)
ULAQ	F10, F11, F12, F113, F114, F115, F22, F141B, F142B, F123, CH_3CCl_3, CH_3Cl, H1211	H1211, H1301, CH_3Br	C_2H_6, C_3H_6, C_2H_4, C_5H_8, $C_{10}H_{16}$, Other NMHC	N_2O-CH_4-CO-families (NO_x, NO_y, Cl_y, Br_y, HO_x, CHO_x, SO_x)	*JPL (2006)*	YES (for other NMHCs)
UMETRAC	Parameterised	Parameterised	None	CH_4-CO-NO_x-ClO_x-BrO_x	*JPL (2002)*	NO
UMSLIMCAT	F11, F12 (scaled)	CH_3Br (scaled)	None	CH_4-CO-NO_x-ClO_x-BrO_x	*JPL (2002, 2006)*	YES
UMUKCA-METO	F11, F12 (scaled)	CH_3Br (scaled)	None	CH_4-CO-NO_x-ClO_x-BrO_x	*JPL (2006); Chipperfield (1999)*	YES
UMUKCA-UCAM	F11, F12 (scaled)	CH_3Br (scaled)	None	CH_4-CO-NO_x-ClO_x-BrO_x	*JPL (2002); IUPAC (2003)*	YES
WACCM	F10, F11, F12, F113, F22, CH_3CCl_3, CH_3Cl	CH_3Br, H1211, H1301	None	*Kinnison et al. (2007)*	*JPL (2006)*	YES (for other halocarbons)

NAT and STS, between CCMs (Table 2.16). The simplest assumption is that PSCs are formed at the saturation points of HNO_3 over NAT and H_2O over water-ice. This assumption is made in most CCMVal-2 CCMs. By contrast, the ULAQ model does not assume thermodynamic equilibrium and thus allows for supersaturation and other non-equilibrium effects. ULAQ has 9 tracers each for size-resolved NAT and ice (Pitari *et al*., 2002). CAM3.5 and WACCM also allow for supersaturation of up to 10 times saturation but do not transport a separate NAT tracer (Garcia *et al*., 2007). GEOSCCM accounts for non-equilibrium by using a NAT tracer. In EMAC, NAT forms only on ice or pre-existing NAT (Buchholz, 2005).

The equilibrium assumption only defines the mass of condensed PSC; assumptions about size distributions and particle shapes need to be made to derive surface area densities. The assumed size distribution affects the PSCs sedimentation velocities, *i.e*., the rates of de-/rehydration and de-/renitrification, particularly in the case of large particles. The denitrification through PSC sedimentation contributes to the enhancement of polar stratospheric ozone loss in spring by inhibiting the formation of the $ClONO_2$ reservoir. All CCMs except CMAM include this process (Table 2.16) although sedimentation velocities differ a lot between models.

2.3.3.7 Boundary conditions, emissions and surface sinks

Different methods are used to impose source gases at the Earth's surface. For reproducing the past, GHGs and ODSs (CO_2, N_2O, CH_4, CFCs, halons) are prescribed at the surface using observed global-mean surface abundances (Section 2.5.3.2). The same holds true for the future except for that here the abundances are based on future projections. This method assures the source gas abundances near the surface to be close to the desired values. Diagnosed fluxes associated with the prescribed surface abundances may however deviate substantially from those derived from emission inventories; this would indicate a mismatch in lifetime for such a species between the CCM and the assessment model used to calculate the scenario. Models with an explicit or simplified treatment of tropospheric chemistry usually impose explicit emissions (fluxes) for higher organic species (represented in CAM3.5, EMAC, and ULAQ), NO_x, CO, and/or CH_2O (Table 2.13). Emissions aloft by lightning (Price and Rind, 1992 or 1994, Müller and Brasseur, 1995, or Grewe *et al*., 2001) or aircraft are also represented to a varying degree in those models (Table 2.13). Emissions of SO_2, dimethyl sulfide (DMS) and NH_3 associated with tropospheric aerosol are represented in CAM3.5, EMAC, ULAQ, UMETRAC, and UMUKCA.

There are two types of deposition in the troposphere, dry deposition and wet deposition. Dry deposition may be

Table 2.13: Species with surface emissions, aircraft emissions; lightning emission of NO_x, wet and dry deposition. NO = nitrogen oxide. NI = not included.

CCM	Surface emission	Aircraft em.	Lightning NOx	Wet deposition	Dry deposition	Comment
AMTRAC3	NI	NI	NI	NI	NI	Trop. NO_x climatology imposed
CAM3.5	paraffin, olefin, terpene, BC, C_2H_4, CH_2O, CH_3CHO, CO, DMS, C_5H_8, NH_3, NO, OC, SO_2, C_7H_8, dust, SS	CO, NO	NO	Yes	Yes	
CCSRNIES	NI	NI	NI	Yes	Yes	
CMAM	NI	NI	NI	NI	Yes	
CNRM-ACM	NI	NI	NI	NI	NI	Below 577 hPa relaxation to ground values (τ=7 days)
E39CA	NO, NO_2	NO, NO_2	*Grewe et al. (2001)*	Yes	Yes	
EMAC	CO, NO, C_2H_6, C_2H_4, C_3H_6, C_4H_{10}, CH_3CHO, CH_3COCH_3, CH_3OH, CH_2O, SO_2, NH_3	NO	*Tost et al. (2007); Price and Rind (1994)*	Yes	Yes	
GEOSCCM	NI	NI	parameterised	NI	NI	
LMDZrepro	NI	NI	NI	NI	NI	Zonally invariant composition imposed below 400 mb
MRI	CO	NO	NO	Yes	Yes	
Niwa-SOCOL SOCOL	CO, NO_x	NO_x	*Müller and Brasseur (1995)*	Yes HNO_3	Yes	Deposition: *Seinfeld (2006)*. HCl, HBr, $ClONO_2$ imposed at surface
ULAQ	NO_x, CO, NMHC, SO_2, DMS	H_2O, NO_x, CO, SO_2, BC, SO_4	*Grewe et al. (2001)*	Yes	Yes	
UMETRAC	SO_2, DMS	NI	NI	No	No	
UMSLIMCAT	NI	NI	NI	No	No	LBCs imposed for all species
UMUKCA-METO	NO, CH_2O, CO, SO_2, DMS, NH_3	NO	*Price and Rind (1992)*	Yes	Yes	Erroneous washout imposed for inorganic halogens
UMUKCA-UCAM	NO, CH_2O, CO, SO_2, DMS, NH_3	NO	*Price and Rind (1992)*	Yes	Yes	0 boundary conditions for inorganic halogens imposed
WACCM	NO, CH_2O, CO	NO	*Price and Rind (1992)*	Yes	Yes	Includes SPE emissions of HO_x and NO_x

represented by a deposition velocity for a particular surface and gas so that a deposition flux is the product of deposition velocity and abundance (*e.g.*, Walcek *et al.*, 1986). Dry deposition is an important component of the tropospheric ozone budget (*e.g.*, Hough, 1991). Wet deposition, on the other hand, involves the scavenging of gases by cloud droplets. Hydro-halogens such as HCl and HBr dissolve well in water; this makes wet depositions of these species the dominant sink for Cl_y and Br_y. Similarly, the wet deposition of HNO_3 is a major sink of NO_y.

The removal of inorganic halogen is handled in different ways in the models. All models (except AMTRAC3, CMAM, CNRM-ACM, GEOSCCM, LMDZrepro, UMETRAC and UMSLIMCAT; Table 2.13) incorporate explicit washout (at least for some species). In some models removal is represented by relaxing species to a background tropospheric climatology (CNRM-ACM, LMDZrepro, UMETRAC). In the case of UMUKCA-UCAM, removal of inorganic halogens is achieved by imposing zero surface boundary conditions for these species (Morgenstern *et al.*, 2009). By contrast, UMUKCA-METO has explicit washout for these species *albeit* incorporated incorrectly. With the exception of CMAM, the same models that include washout also include dry deposition; for CMAM only dry deposition is included.

2.3.4 Transport

2.3.4.1 Advection

Advection is one of the major processes determining the distribution of chemical species, particularly in the lower stratosphere, where the chemical lifetimes of long-lived species are much longer than the dynamical (transport) lifetimes, as manifested, for example, by the tape-recorder signal of H_2O in the equatorial lower stratosphere (Mote *et al.*, 1996), and by the "mixing barriers" in the subtropics and around the winter pole (*e.g.*, Shepherd, 2003). The distribution of chemical species, and the age of air, are sensitive to the details of advection schemes (*e.g.,* Eluszkiewicz *et al.*, 2000; Gregory and West, 2002; Rasch *et al.*, 2005; Chipperfield, 2006; Struthers *et al.*, 2009). In addition, inconsistencies may arise from the different discretization of the continuity equation and the tracer transport equation, as shown for example by Jöckel *et al.* (2001). Some CCMs (CNRM-ACM, E39CA, LMDZrepro, MRI, and (Niwa-)SOCOL; Table 2.1) also use different advection schemes for meteorological (*i.e.,* momentum, heat, water) and chemical tracers, resulting in different numerical diffusivities for tracers advected by different schemes, and possible inconsistencies. Several types of advection schemes are used in the CCMVal-participation models, namely finite volume, spectral, semi-Lagrangian, flux-form semi-Lagrangian, and fully Lagrangian schemes.

Spectral advection in the horizontal and finite difference advection in the vertical (CCSRNIES, CMAM) conserves species mass, but requires careful attention to avoid the development of sharp gradient in species distribution and to fill negative values (de Grandpré *et al.*, 2000).

Semi-Lagrangian schemes can be used with relatively long time steps without compromising stability. Also semi-Lagrangian schemes are advantageous when a large number of tracers needs to be advected (such as in CCMs) because a major fraction of the cost is independent of the number of tracers. However, these schemes may be overly diffusive (*e.g.*, Eluszkiewicz *et al.*, 2000) due to an interpolation step necessary to project tracers from the departure points onto the arrival points. This diffusive property can be improved through higher-order interpolation, *e.g.*, quintic (MRI, UMUKCA; Priestley, 1993; Table 2.4). However, the better accuracy of higher-order interpolation comes at the price of numerical artifacts, such as overshoots and undershoots (similar to those found in spectral advection) that require special treatment. Also, some semi-Lagrangian schemes exhibit tracer non-conservation (*e.g.*, Rasch *et al.*, 2005), requiring an unphysical correction. Flux-form semi-Lagrangian advection is considered relative accurate; however, in practice little difference has been found between flux-form semi-Lagrangian and spectral advection schemes (Eyring *et al.*, 2006; Shepherd, 2007). Flux-form schemes are used in a number of models (AMTRAC3, CAM3.5, EMAC, GEOSCCM, LMDZrepro, WACCM). They can be made to conserve tracers (Rasch *et al.*, 2005). Many models in this category (AMTRAC3, CAM3.5, EMAC, GEOSCCM, WACCM) use formulations after Lin and Rood (1996 or 1997) or Lin (2004). LMDZrepro, UMETRAC, and UMSLIMCAT use finite-volume advection schemes (Hourdin and Armengaud, 1999; Gregory and West, 2002).

The E39CA model uses a fully Lagrangian approach to constituent transport, thereby avoiding the interpolation step needed in semi-Lagrangian methods (Reithmeier and Sausen, 2002; Stenke *et al.*, 2008). This method is not subject to numerical diffusion, thus allowing for a specification of explicit, physically motivated diffusion to represent mixing between neighbouring parcels. This explicitly defined diffusion may be much smaller than numerical diffusion found in other schemes. The ATTILA scheme in E39CA does not include parcel merging or parcel splitting, implying very different concentrations of parcels in the stratosphere compared to parcels in the lower troposphere (*i.e.,* effectively decreasing resolution with height). This main disadvantage needs to be weighed against the gain of controlled diffusion.

Table 2.14: Photolysis. SZA: Solar zenith angle. OC: ozone column. L-α: Lyman-α, 121.6 nm.

CCM	Reference for scheme	References for cross section	Online	Spectral range (nm)	Average resolution (nm)	Max. SZA (degrees)	Temperature range (K)	Interpolation parameters
AMTRAC3	*Austin et al. (1987)*	*JPL (2006)*	NO	175-700,L-α	0.5-10 (158 bands)	up to 100	200-300	T, p, SZA, OC
CAM3.5	*Kinnison et al. (2007)*	*JPL (2006); Burkholder et al. (1990)*	YES	200-750	~2-5 (200-400nm; 10-50 (>400nm).	97	150-350	T, p, SZA, OC, albedo
CCSRNIES	*Kurokawa et al. (2005); Akiyoshi et al. (2009)*	*JPL (2006)*	YES	177.5-690, L-α	0.90-2.35 (S-R bands); 12.1-372 (>200nm)	96	195-300	N/A
CMAM	*de Grandpré et al. (2000)*	*JPL (2006)*	NO	121-852.5; 165 bands	4.4 (1.6-10)	100	Variable	p, SZA, OC
CNRM-ACM	TUV 4.1a *(Madronich and Flocke, 1998)*	*JPL (2006)*	NO	116-850	0.01 (S-R bands); 0.1 (L-α); 1 (elsewhere)	95	187-288	p, SZA, OC
E39CA	*Landgraf and Crutzen (1998)*	*JPL (1997)*	YES	175-683 (8 bands)	1-5 for pre-calculation of coefficients, 8-260 for bands (with scattering)	93 (*Lamago et al., 2003*)	Variable	N/A
EMAC	*Landgraf and Crutzen (1998); Zdunkowski et al. (1980); Allen and Frederick (1982); Koppers and Murtagh (1996)*	*JPL (1997) ; Talukdar et al. (1998) ; Roehl et al. (2002); Blitz et al. (2004)*	YES	175-683 (8 bands), L-α	1-5 for pre-calculation of coefficients, 8-260 for bands (with scattering)	94.5	Variable	Online, with clouds and ozone
GEOSCCM	*Douglass et al., (1997)*	*JPL (2002)*	YES	176.2-310 (50 bands); 310-450 (28 bands); 652.5; L-α	176.2-310: 2.775 nm; 310-450: 5 nm	94	148-348	T, p, SZA, OC
LMDZrepro	*Madronich and Flocke (1998)*	*JPL (2006)*	NO	121-750	116-124: 0.1nm; 124-175: 1nm; 175-205: 0.01nm; 205-850: 1nm	95	Variable	Z, SZA, ozone column
MRI	*Shibata et al. (2005)*		NO	116.3-735; 171 bands	0.7-5.0	96	253-293	T, p, SZA, OC

CCM	Reference for scheme	References for cross section	Online	Spectral range (nm)	Average resolution (nm)	Max. SZA (degrees)	Temperature range (K)	Interpolation parameters
Niwa-SOCOL SOCOL	*Rozanov et al. (1999)*	*JPL (2006); IUPAC (2004, 2005)*	YES (LUTs)	121-750, 73 bands	1-160; median: 5 nm	98	Variable	SZA, OC, oxygen total column
ULAQ	*NASA (1993)*	*JPL (2006)*	YES	135-850	0.7-5.0	94	Variable	Online
UMETRAC	*Austin et al. (1987)*		NO	175-700,L-α	0.5-10 (158 bands)	up to 100	200-300	T, p, SZA, OC
UMSLIMCAT	*Lary and Pyle (1991); Chipperfield (1999)*	*JPL (2002)*	NO	175-850,L-α	4.3	98	Variable	T, p, SZA, OC
UMUKCA-METO UMUKCA-UCAM	*Lary and Pyle (1991); Chipperfield (1999)*	*Chipperfield (1999)*	NO	175-850,L-α	4.3	98	Variable	T, p, SZA, OC
WACCM	*Kinnison et al. (2007)*	*JPL (2006); Burkholder et al. (1990)*	YES	120-750	~1-2 (SRC, SRB), ~2-5 (200-400nm; 10-50 (>400nm)	97	150-350	T, p, SZA, OC, albedo

2.3.4.2 Convective transport and turbulent mixing of chemical species

Convection and turbulence rapidly mix air and chemical species vertically, and thus they are important for the distribution of chemical species. Such processes are of interest not just in the troposphere, but also in the middle atmosphere (*e.g.*, associated with gravity wave breaking). Turbulent mixing works predominantly within the planetary boundary layer (below ~2000m), and convective transport is the dominant process mixing air between the planetary boundary layer and the free troposphere, thereby playing a crucial role for long-range transport such as intercontinental and hemispheric transport. In particular, deep cumulus convection uplifts the chemical species in the boundary layer directly to the upper troposphere through detrainment, giving large effects on tropospheric ozone (*e.g.,* Lawrence *et al*., 2003). Entrainment of mid-level air and downdraft associated with detrained air in a convective cell also contribute to the vertical mixing of chemical species. However, since most CCMVal-2 models do not include detailed tropospheric chemistry, sophisticated schemes are often not required for convective transport and turbulent mixing. (See online supplement for more details). Also the CCMVal-2 reference simulations (Section 2.5.2) do not consider very short-lived halogen species (VSLS) which would be sensitive to the details of convection.

2.4 CCMVal-2 models and development since CCMVal-1

Several models that were used for CCMVal-1 are used here again for CCMVal-2. Sometimes the name of the CCM has remained the same, although developments have taken place. In other cases, a new model name is used and a predecessor model was used for CCMVal-1.The purpose of this section is therefore to provide a basic description of each model and a detailed list of differences versus the CCMVal-1 version.

2.4.1 AMTRAC3 (known as AMTRAC in CCMVal-1)

AMTRAC3 is an improved version of AMTRAC (Austin and Wilson, 2006). The major model differences are incorporation of the 'cubed sphere' dynamical core (Putman and Lin, 2007) as well as convection (Phillips and Donner, 2006) and aerosol changes in preparation for IPCC AR5. These changes have led, in particular, to increased stratospheric water vapour amounts in much better agreement with observations. Chlorine and bromine source gases are not explicitly modelled. The parameterisation for the production of inorganic chlorine and bromine

Table 2.15: Heterogeneous reactions. LSA: liquid stratospheric aerosol. LTA: liquid (sulfuric) tropospheric aerosol. N: NAT. I: ice. SO_4: sulfate. SAD: Sulfuric acid dihydrate. STS: supercooled ternary (H_2SO_4 / HNO_3 / H_2O) solution. LA: liquid aerosol

CCM	$ClNO_3$ + H_2O	$ClNO_3$ + HCl	HOCl + HCl	N_2O5 + H_2O	N_2O_5 + HCl	B_rNO_3 + H_2O	HOBr + HCl	$ClNO_3$ + HBr	$BrNO_3$ + HCl	HOBr + HCl	HOBr + HBr	$ClNO_2$ + H_2O	$ClNO_2$ + HCl	HOCl + HBr
AMTRAC3 UMETRAC	SAD/N/I	SAD/N/I	SAD/N/I	SAD/ N/I	N/I	N/I	N/I				SAD/ N/I			N/I
CAM3.5	N/STS/I	N/STS/I	N/STS/I	N/STS/I		STS/I	STS/I	N/STS/I						
CCSRNIES	N/I/LSA	N/I/LSA	N/I/LSA	N/I/LSA	N/I	N/I/LSA	N/I/LSA	N/I	N/I	N/I/LSA	N/I/ LSA			N/I/ LSA
CMAM	STS/I	STS/I	STS/I	SO_4/ STS/I		SO_4/ STS	STS/I							
CNRM-ACM	N/I/ LSA	N/I	N/I	N/I/LSA	N/I	N/I				N/I	N/I	N/I	N/I	
E39CA	N/I/LSA	N/I/LSA	N/I/LSA	N/I/LSA	N/I/ LSA									
EMAC	N/I/LSA	N/I/LSA	N/I/LSA	N/I/ LSA/ LTA		N/I/LSA	N/I/LSA		N/I	N/I/ LSA				
GEOSCCM	I/N/LSA	I/N/LSA	I/N/LSA	I/N/LSA	I/N/ LSA	I/N/LSA								
LMDZrepro	LA/N/I	LA/N/I	LA/N/I	LA/N/I	N/I	LA/N/I	LA/N/I				I			
MRI	N/I/SO_4	N/I	N/I	N/I/SO_4	N/I	SO_4	N/I							
Niwa-SOCOL SOCOL	LSA/N/I	LSA/N/I	LSA/N/I	LSA/ N/I		LSA/I	LSA/I							
ULAQ	N/I/SAD	N/I	N/I/SAD	N/I/ SAD	N/I	N/I/ SAD	N/I/ SAD		N/I	N/I/ SAD				
UMSLIMCAT	N/STS/I	N/STS/I	N/STS/I	N/STS/I	N/I					N/STS/I	N/ STS/I			
UMUKCA-METO UMUKCA-UCAM	N/I/SO_4	N/I	N/I/SO_4	N/I/SO_4	N/I									
WACCM	N/STS/I	N/STS/I	N/STS/I	N/STS/I		STS/I	STS/I	N/STS/I						

used in AMTRAC3 has been modified, *versus* AMTRAC. Essentially, the effective photolysis rates of the CFCs have been decreased in the lower stratosphere and increased in the tropical middle stratosphere. The other major change in the photochemistry is that the scattering calculation in the photolysis lookup table has been corrected (L. Horowitz, personal communication), leading to higher ozone amounts in the lower stratosphere in better agreement with observations. Finally, the positions of the model vertical levels have been adjusted to provide increased stratospheric resolution, at the expense of decreased mesospheric resolution. The new model physics and dynamics have required a new tuning (*i.e.*, a reduction) of the parameterised non-orographic gravity wave forcing.

Changes since CCMVal-1:

- Cubed sphere dynamics
- Improved CFC parameterisation
- Improved photolysis rates *etc*., as in descriptive section.

2.4.2 CAM3.5

CAM3.5 is a version of the recently updated Community Atmosphere Model (Gent *et al*., 2009) with interactive chemistry in the troposphere (including aerosols) and stratosphere. This setup is equivalent to CAM3 (Lamarque *et al*., 2008). The main difference over the latter version is the inclusion of the new gravity-wave drag parameterization from Richter *et al*. (2010), similar to WACCM (see below).

CAM3.5 did not participate in CCMVal-1.

2.4.3 CCSRNIES

The CCSR/NIES GCM originates from an NWP model obtained from the Japan Meteorological Agency. Some improvements of the codes and an extension of the heights up to the stratosphere were made (Numaguti, 1993; Numaguti *et al*., 1995; Takahashi, 1996, 1999; Nakajima *et al*., 2000). The chemical module for stratospheric gas phase reactions was developed by Akiyoshi (2000) and incorporated in a CCSR/NIES GCM with a top boundary in the mesosphere (Takigawa *et al*., 1999; Nagashima *et*

Table 2.16: Microphysics of polar stratospheric clouds (PSCs). EQ = thermodynamic equilibrium with gaseous HNO_3 / H_2SO_4 / H_2O assumed. HY = non-equilibrium / hysteresis considered.

CCM	Sedimentation velocity (mm/s)	Thermodynamics	Transported PSC tracers	References / comments
AMTRAC3 UMETRAC	NAT: 0.14; NAT/ice: 12.7	EQ	None	
CAM3.5	NAT / ice but not STS	NAT: HY; ice: EQ	None	*Kinnison et al. (2007)*
CCSRNIES	NAT/ICE, dep. on mode radius	EQ	None	
CMAM	No sedimentation	EQ	None	
CNRM-ACM	NAT/ice: mean value around 17.3	EQ	None	
E39CA	Varies by particle size (*Steil et al., 1998*)	HY	NAT + HNO3, ice	
EMAC	*Buchholz (2005)*	NAT: HY; ice: EQ	NAT	
GEOSCCM	Varies by particle size	HY	NAT, ice	
LMDZrepro	*Lefèvre et al. (1998)*	EQ	None	
MRI	NAT: 0.17, ice:17.4	EQ	None	
Niwa-SOCOL SOCOL	*Schraner (2008)*	EQ	None	*Carslaw et al. (1995)*
ULAQ	Function of size bin	HY	9 NAT + 9 ice	
UMSLIMCAT UMUKCA-METO UKUKCA-UCAM	NAT: 0.46; NAT/ice: 17.3	EQ	None	
WACCM	NAT / ice but not STS.	NAT: HY; ice: EQ	NAT	*Kinnison et al. (2007)*

al., 2002). The heterogeneous chemistry module originates from a box model version of SLIMCAT model (Carslaw *et al*., 1995; Sessler *et al*., 1996). Recent updates including bromine chemistry, heterogeneous reactions, Schumann-Runge bands, atmospheric sphericity, and non-orographic GWD were made before participating in CCMVal (Akiyoshi *et al*., 2004; Kurokawa *et al*., 2005; Akiyoshi *et al*., 2009).

Changes since CCMVal-1: None

2.4.4 CMAM

CMAM is an upwardly extended version of the spectral CCCma third generation atmospheric GCM (Scinocca *et al*., 2008). The model's resolution increases monotonically from roughly 100 m near the surface to around 900 m around the extra-tropical tropopause to 2.5 km in the stratosphere and middle atmosphere. REF-B2 simulations (see below) were coupled to the NCOM 1.3 ocean general circulation model (OGCM) (Gent 1998; Arora *et al*., 2009). The OGCM employes a horizontal resolution of 1.86º with 29 levels with a 50 m upper layer and 300 m layers in the deep ocean. CMAM includes a comprehensive representation of stratospheric chemistry with all the relevant catalytic ozone loss cycles (de Grandpré *et al*., 1997). Sedimentation/denitrification and NAT formation are not included (Hitchcock *et al*., 2009). The chemistry is fully interactive with the radiation code (de Grandpré *et al*., 2000). An upper boundary condition (at ~95 km) of 1 ppmv is imposed for NO_x to account for mesospheric NO_x production by cosmic rays and solar particles.

Changes since CCMVal-1:

Probably the biggest development is that CMAM has been coupled to an ocean GCM (see above). Coupling to the ocean required retuning the model cloud and aerosol forcing for energy balance. This appears to have substantially increased the planetary wave forcing in the NH winter, such that even with observed SSTs the vortex is now too warm, SSWs are too frequent, and the Brewer-Dobson circulation is stronger. In coupled mode the troposphere warms at a rate comparable to that projected in the CMAM CCMVal-1 contribution, though the rate of acceleration of the Brewer-Dobson circulation is faster. This is the subject of further investigation. Thus, the price paid for this initial coupling to the ocean has been a degradation of the dynamical aspects of the simulations.

Further changes between CCMVal-1 and CCMVal-2 include: CCl_4, CH_3CCl_3, HCFC-22, and CH_3Cl have been added to the chemistry scheme, including lumping with non-represented source gases. Reactive chlorine (Cl_y) had been advected as a single family in CMAM for CCMVal-1. For CCMVal-2, HCl was advected separately from the other Cl_y species, allowing for a more realistic activation of chlorine in the polar vortex. Within the polar vortex, particularly over the Antarctic, problems were identified with the local conservation of NO_y by advection due to the particular partitioning of HNO_3 and NO_x during polar night. The sum of HNO_3, NO_x and HNO_4, the three advected species in CMAM that carry NO_y, has been constrained by the addition of an additional advected tracer (NO_y) that is the sum of the three.

Gas-phase (but not heterogeneous) chemical reaction rates and photolysis rates were updated to JPL (2006). The photolysis look-up table underwent a variety of improvements which included: increased number of solar zenith angle look-up points in the table, for improved photolysis rates at twilight, the change to a more up-to-date solar flux input (SOLARIS), a revised wavelength grid for improved rates in the mesosphere, and the correction of various programming errors (fix for the excessive transmission of UV to the Earth's surface and overestimated photolysis rates for O_2, CFCs, H_2O, and N_2O in the troposphere and lower stratosphere). An interpolation procedure in the longwave scheme was changed which caused the CCMVal-1 simulations to under-estimate the impact of the CO_2 increase in the recent past (Jonsson *et al*., 2009). For REF-B1 (see below), solar variability is now included in CMAM in both J-value and solar heating calculations. To include solar variability in J-values, the look up table approach was modified. Solar variability in solar heating is calculated as an additional term and includes treatment in 8 spectral bands between 121 and 300 nm. The vertical diffusivity for tracers is enhanced in the upper stratosphere and mesosphere to crudely account for missing dissipation associated with gravity-wave breaking.

2.4.5 CNRM-ACM

The dynamical GCM ARPEGE-Climat 4.6 (Déqué, 2007) is coupled to the atmospheric chemistry scheme described by Teyssèdre *et al*. (2007). The composition module uses its own transport scheme. CCMVal-2 simulations have been performed with horizontal resolutions differing between dynamics and chemistry to reduce computation cost. The vertical resolutions of dynamics and chemistry are identical.

CNRM-ACM did not participate in CCMVal-1.

2.4.6 E39CA (known as E39C in CCMVal-1)

The coupled chemistry-climate model ECHAM4.L39(DLR)/CHEM/-ATTILA (hereafter referred to a E39CA) is an upgraded version of ECHAM4.L39(DLR)/CHEM (E39C). E39CA consists of the dynamic part ECHAM4 and the family-based chemistry module CHEM. Chemical and hydrological tracers are transported using

the purely Lagrangian scheme ATTILA which is strictly mass conserving and numerically non-diffusive.

Changes since CCMVal-1:

- Introduction of ATTILA, see above.
- Introduction of parameterised bromine-catalysed ozone loss (Stenke *et al*., 2009).

2.4.7 EMAC

The ECHAM5/MESSy Atmospheric Chemistry (EMAC) model is a numerical chemistry and climate simulation system that includes sub-models describing tropospheric and middle atmosphere processes (Jöckel *et al*., 2006). It uses the first version of the Modular Earth Submodel System (MESSy1) to link multi-institutional computer codes. The core atmospheric model is ECHAM5 (Roeckner *et al*., 2003). For the present study we applied EMAC (ECHAM5 version 5.3.01, MESSy version 1.6) in the T42L90MA-resolution (Giorgetta *et al*., 2006). EMAC includes a representation of mesospheric NO_x production by cosmic rays and solar particles.

EMAC replaces the MAECHAM4CHEM CCM that was used in CCMVal-1.

2.4.8 GEOSCCM

GEOSCCM couples the Goddard Earth Observing System (GEOS) version 5 AGCM (Reineker *et al*., 2008) to an updated version of the Douglass *et al*. (1997) stratospheric chemistry mechanism. The GEOS-5 AGCM uses a flux-form semi-Lagrangian dynamical core (Lin, 2004) with a quasi-Lagrangian vertical coordinate (Lin and Rood, 1997) that allows for accurate computation of vertical motions. The stratospheric chemistry package includes a comprehensive suite of chemicals and chemical reactions thought to be important in the stratosphere. The photochemistry code is based on the family approach, as described by Douglass and Kawa (1999). Constituent advection also uses the Lin (2004) transport scheme. GEOSCCM does not use explicit diffusion and also does not impose a sponge at the model top. Tropospheric ozone is relaxed to a climatology (Logan, 1999).

Changes since CCMVal-1:

- Transition from GEOS-4 to the Earth System Modeling Framework (ESMF)-compliant GEOS-5
- New versions of several physical processes, most importantly moist physics, have been implemented (Bacmeister *et al*., 2006; Rieneker *et al*., 2008).
- A catchment approach (Koster *et al*., 2000) is now used to model the land-surface.

2.4.9 LMDZrepro

The LMDz-REPROBUS CCM (Jourdain *et al*., 2008) couples interactively the vertically extended version of the LMDz 4th-generation GCM (Lott *et al*., 2005) and the stratospheric chemistry module of the REPROBUS CTM (Lefèvre *et al*., 1998). LMDz is the atmospheric component of the IPSL Earth System model. The chemistry module contains a detailed description of stratospheric chemistry. It calculates the chemical evolution of 55 species using 160 gas-phase reactions and 6 heterogeneous reactions with sedimentation taken into account. Radiation is based on Morcrette (1989).

Changes since CCMVal-1:

- Improved convection scheme (Kerry-Emmanuel)
- Improved composition climatology for NO_x, CO, and O_3 below 400 hPa (Savage *et al*., 2004)
- Updated chemistry to JPL (2006)
- Improved PSC scheme including a bimodal size distribution of PSC particles.

2.4.10 MRI

MRI-CCM is an upgraded version of the MRI-CTM (Shibata *et al*., 2005; Shibata and Deushi, 2008). The dynamical core of MRI-CCM is based on the spectral global model MJ98 (Shibata *et al*., 1999) at a triangular truncation of T42 used for CCM simulations. The model employs hybrid-pressure coordinates in the vertical with 68 layers, the thickness of which is about 500 m between 100 and 10 hPa with tapering off below and above the levels, respectively. Explicit bi-harmonic horizontal diffusivity is weaker in the middle atmosphere than in the troposphere to allow for a representation of the QBO (Shibata and Deushi, 2005a). Transport of chemical species is performed using a hybrid semi-Lagrangian scheme satisfying the continuity equation (see below). The chemistry module comprises full stratospheric chemistry including the relevant heterogeneous reactions on PSCs and sulfate aerosols, and also a simplified representation of tropospheric chemistry.

Changes since CCMVal1:

- Implementation of a new hybrid semi-Lagrangian scheme. The new scheme is semi-Lagrangian with a quintic interpolation in the horizontal, but flux form in the vertical, wherein advection is calculated with the piecewise rational method (PRM) (Xiao and Peng, 2004).

2.4.11 SOCOL and Niwa-SOCOL

SOCOL (Egorova *et al*., 2005) is a combination of the GCM MA-ECHAM4 (Manzini *et al*., 1997) and the

CTM MEZON (Rozanov *et al*., 1999; Egorova, 2003). MEZON has the same vertical and horizontal resolution as MA-ECHAM4 (used in CCMVal-1) and in addition includes a comprehensive representation of stratospheric chemistry. An extensive evaluation of SOCOL (Egorova *et al*., 2005; Eyring *et al*., 2006, 2007) led to the development of SOCOL version 2.0 (Schraner *et al*., 2008) used here.

Niwa-SOCOL differs from SOCOL regarding to the lower boundary conditions and some details of photochemistry. Due to these minor differences Niwa-SOCOL simulations should not be regarded as ensemble members of SOCOL.

Changes since CCMVal-1:

- The list of ODS is extended to 15 for chemistry, while for transport they are still clustered into three tracers;
- Inclusion of HNO_3 uptake by aqueous sulfuric acid aerosols;
- NAT particle number densities are limited by an upper boundary of $5e10^{-4}$ cm^{-3} to take into account that observed NAT clouds are often strongly supersaturated;
- All considered species are transported;
- The mass correction after the semi-Lagrangian transport step is applied to the chlorine, bromine and nitrogen families instead of their individual members, and to ozone only between 40°S and 40°N to avoid artificial mass loss in the polar areas;
- The water vapour removal by the highest ice clouds (100 hPa – CPT) is now explicitly taken into account to prevent an overestimation of stratospheric water content.

2.4.12 ULAQ

ULAQ-CCM is a low-resolution CCM. Dynamical fields (streamfunction, velocity potential and temperature) are taken from the output of a simplified spectral circulation model (GCM) adopting the quasi-geostrophic approximation (rhomboidal truncation with six waves and six components per wave). The effect of gravity wave breaking is simulated *via* Rayleigh friction. Pitari *et al*. (2002) describe details of the coupling between GCM and CTM (Eyring *et al*., 2006). A flux-form Eulerian fully explicit advection scheme is used. Medium and short-lived chemical species are grouped in families (O_x, NO_y, NO_x, HO_x, CHO_x, Cl_y, Br_y, SO_x, aerosols, ice cloud particles). The size distribution of sulphate and PSCs is calculated online using an interactive and mass conserving microphysics code for aerosol formation and growth.

Changes since CCMVal-1:

- Inclusion of QBO nudging.
- Inclusion of upper tropospheric cirrus ice particles.
- Upgrade of tropospheric chemistry (NMHC).

2.4.13 UMETRAC

UMETRAC is a vertically extended version of the Met Office's HadAM3 Unified Model (UM) version 4.5, combined with a stratospheric chemistry package. Chemistry is treated in a somewhat simplified way with release of inorganic chlorine and bromine from the organic reservoir calculated as functions of age of air.

Changes since CCMVal-1:

- An artificial increase of CFC photolysis rates, used in CCMVal-1 to correct the inorganic chlorine loading, has been dropped.

2.4.14 UMSLIMCAT

UMSLIMCAT (Tian and Chipperfield, 2005) uses the stratospheric chemistry scheme from the SLIMCAT offline CTM (Chipperfield, 2006) coupled to a vertically extended version of the Met Office's HadAM3 UM version 4.5. The stratospheric water vapour is coupled to the UM's humidity field.

Changes since CCMVal-1:

- Chemical kinetics were updated to JPL (2006).
- The number of solar flux bands in the model's radiation scheme was changed from 3 to 6.
- A time varying solar flux with an 11-year solar cycle was incorporated.

2.4.15 UMUKCA-METO and UMUKCA-UCAM

UMUKCA is a vertically extended version of the Met Office's UM 6.1 in a configuration similar to HadGEM1 (Johns *et al*., 2006) combined with the UKCA stratospheric chemistry module (Morgenstern *et al*., 2008, 2009). The model does not use the hydrostatic approximation and uses a non-families formulation of chemistry. UMUKCA does not impose explicit diffusion and also does not have a sponge layer. Chemical water vapour production or loss is ignored in the hydrology scheme and instead a parameterisation of methane oxidation (Untch *et al*., 1998) is used. Also water vapour is imposed at the tropical tropopause, meaning that UMUKCA does not have a tape recorder signal in the water vapour field. The two model versions used here differ in the use of some chemical kinetic data, the treatment of removal of inorganic halogen compounds in the troposphere, and stratospheric aerosol radiative heating in REF-B1 (see below). In UMUKCA-METO, washout of inorganic halogen is incorporated incorrectly. In UMUKCA-UCAM, instead of explicit washout inorganic halogen is forced to 0 at the surface. UMUKCA-UCAM

Table 2.17: SST and sea ice data sets. Note that CMAM has an interactive ocean.

CCM	SST/sea ice for REF-B0/B1, SCN-B1	SST/sea ice for REF-B2, SCN-B2b/c/d	Reference for SST/sea ice used in REF-B2
AMTRAC3	HadISST1		
CAM3.5	HadISST1	CCSM3	*Collins et al. (2006)*
CCSRNIES	HadISST1	MIROC / IPCC-AR4	*Shiogama et al. (2005); Nozawa et al. (2007)*
CMAM	HadISST1	Interactive	*Arora et al. (2009)*
CNRM-ACM	HadISST1	CNRM-CM3 AR4 A1B	*www-pcmdi.llnl.gov/ipcc/subproject_publications.php*
E39CA	HadISST1	HadGEM1	*Stott et al. (2007)*
EMAC	HadISST1	N/A	N/A
GEOSCCM	HadISST1	CCSM3	*Collins et al. (2006)*
LMDZrepro	AMIP-II	OPA (ocean) LIM (ice)	
MRI	HadISST1(1); MRI-CGCM2.3.2(3)	MRI-CGCM2.3.2	*Yukimoto et al. (2006)*
Niwa-SOCOL	HadISST1	HadISST1:1960-2002 HadGEM1:2003-2100	HadGEM1*: Johns et al. (2006)*
SOCOL	HadISST1	ECHAM5-MPIOM	
ULAQ	HadISST1	CCSM3	*Collins et al. (2006)*
UMSLIMCAT UMUKCA-METO UKUKCA-UCAM	HadISST1	HadGEM1	*Johns et al. (2006)*
WACCM	HadISST1	CCSM3	*Collins et al. (2006)*

does not have heating associated with the presence of stratospheric aerosol.

UMUKCA did not participate in CCMVal-1.

2.4.16 WACCM

WACCM, version 3.5.48, spans the range of altitude from the Earth's surface to the lower thermosphere. WACCM is a fully interactive model with a comprehensive range of radiatively active gases (Sassi *et al*., 2005; Tables 2.28 and 2.29). WACCM includes all of the physical parameterisations of the CAM model. A mass-conserving finite volume dynamical core (Lin, 2004) is used exclusively in WACCM. Compared to CAM3.5, only the GWD and vertical diffusion parameterisations are modified. WACCM includes chemical heating; mesospheric NO_x production by cosmic rays/solar particles, mesospheric / lower thermospheric ion chemistry; ion drag and auroral processes; and parameterisations of short wave heating at extreme ultraviolet (EUV) wavelengths and NLTE infrared transfer (Garcia *et al*., 2007; Collins *et al*., 2004). The chemistry is based on MOZART3 (Kinnison *et al*., 2007), involving a combined explicit and implicit backward-Euler solver. Heterogeneous processes on sulfate aerosols and polar stratospheric clouds are included following the approach of Considine *et al*. (2000).

Changes since CCMVal-1:

- The gas-phase chemical reaction rates and photolysis rates were updated to the recommendations of JPL (2006).
- Volcanic heating was added for the REF-B1 simulations (see below). This heating is derived from the SPARC SAD time-series.
- The wavelength dependent exo-atmospheric flux was updated following Lean *et al*. (2005).
- The GWD parameterisation was updated based on Richter *et al*. (2010).
- Relaxation of tropical winds towards observations was added for the REF-B1 simulations (see below; Table 2.9).
- The underlying tropospheric climate model has a different closure for the deep convective parameterisation and added convective momentum transport (Neale *et al*., 2008).

Table 2.18: Implementation of volcanic effects in REF-B1.

CCM	SADs for heterogeneous chemistry	Direct radiative effects	Comment / reference
AMTRAC3	Derived from aerosol properties used for radiation[1]		
CAM3.5	SPARC ASAP[3]	None	
CCSRNIES	SPARC ASAP	Online derived from GISS[2]	*Hansen et al. (2002); Sato et al. (1993)*
CMAM	SPARC ASAP	Online derived from SPARC SAD	*Thomason et al. (1997)*
CNRM-ACM	SPARC ASAP	Calculated online using monthly optical depths at 0.55 μm of *Amman et al. (2003)*	Aerosol optical properties in REF-B1 lead to too strong sensitivity to volcanic eruptions. Different properties have been adopted since then (A. Voldoire, pers. comm.).
E39CA	CCMVal-1[4]	Prescribed heating rate anomalies[5]	
EMAC	Derived H_2SO_4 from SAGE measurements	Prescribed heating rate anomalies[5]	
GEOSCCM	Perpetual 1979 conditions (from CCMVal-1)	None	
LMDZrepro	SPARC ASAP	None	
MRI	SPARC ASAP	Online derived from GISS	
Niwa-SOCOL	SAGE I and II	SAGE and GISS based offline calculations	*Schraner et al. (2008); Thomason and Peter (2006)*
SOCOL	GISS (1960-1978) SAGE (1979-2006)	GISS (1960-1978) SAGE (1979-2006)	*Schraner et al. (2008); Fischer et al. (2008*
ULAQ	SPARC ASAP	Online using volcanic SO_2 estimates and gas/particle conversion	*Pitari (1993)*
UMETRAC UMUKCA-METO	SPARC ASAP	Online derived from GISS	*Sato et al. (1993)*
UMSLIMCAT UKUKCA-UCAM	SPARC ASAP	None	
WACCM	SPARC ASAP	Online derived from SPARC SAD	

Notes:

[1]*SADs are inferred from multi-wavelength extinction values, as in Stenchikov et al. (2006).*

[2]*GISS provides optical thickness at 550 nm and effective radius from 1850—2000, available from http://data.giss.nasa.gov/model-force/strataer/. This data set is based on SAGE observations and was introduced by Sato et al. (1993), with updates and minor improvements announced by Hansen et al. (2002).*

[3]*SPARC ASAP refers to data made available through the SPARC Assessment of Stratospheric Aerosol Properties (ASAP) report (Thomason and Peter, 2006), based primarily on SAGE measurements. Data available at http://www.sparc.sunysb.edu/asap/SAGE-ASAP%20Data%20Products.htm*

[4]*CCMVal-1 SADs were specified from a monthly climatology based on satellite data, similar to that used by Jackman et al. (1996) and updated by D. B. Considine (NASA Langley Research Center).*

[5]*The heating rates are monthly means from January 1950 to December 1999 for all-sky condition, and were calculated using GISS ModelE (Schmidt et al. 2006) radiative routines and volcanic aerosol parameters from the GISS data set (Stenchikov et al., 2006).*

2.5 Definitions of simulations and external forcings

In this section, we motivate and state the definitions of the model simulations conducted for CCMVal-2, discuss the associated forcings, and list the differences between the definitions and the actual simulations conducted by the modelling groups.

2.5.1 Internal and external modelling uncertainties

A source of error in CCMVal integrations relates to deficiencies in model formulation. Using identical boundary conditions, differences in the formulation of CCMs will lead to differences in their common prognostic or diagnostic fields. These differences will represent the internal uncertainties in dynamics, physics and chemistry in CCMs as used here. The CCMVal-2 simulations "REF-B0" and "REF-B1" (Section 2.5.2), covering the near-present and the past, respectively, have been designed primarily to address internal modelling uncertainties since SSTs, sea ice, and other external forcings such as volcanic eruptions and variations of solar irradiation, are prescribed based on observations. By contrast, the "REF-B2" simulations, covering the past and future, also include external uncertainty because here SST and sea ice data are obtained from climate simulations, with associated biases (Section 2.5.3.1). Further external uncertainties are associated with the future GHG and ODS forcings assumed in REF-B2.

2.5.2 CCMVal-2 simulations

The three reference simulations noted above and six control and sensitivity experiments have been proposed (Eyring *et al*., 2008). Most groups have completed the 3 reference simulations, some (CMAM, MRI, SOCOL, ULAQ, WACCM, for the REF-B2 simulations) with more than one ensemble member. A few of the sensitivity studies have been performed, although the coverage across the models is much less consistent than for the reference simulations (Tables O.1 – O.3 in the supplemental material). Since this report exclusively uses data from the reference simulations, only these are documented below, following Eyring *et al*. (2008).

2.5.2.1. REF-B0: Year 2000 time-slice simulation

REF-B0 is a time-slice simulation for 2000 conditions, designed to facilitate the comparison of model output against constituent data sets from various high-quality observational data sources and meteorological analyses under a period of high chlorine loading. Each simulation is integrated over 20 annual cycles following 10 years of spin-up.

- **Trace gas forcings:** The surface concentrations of GHGs are based on SRES scenario A1b of IPCC (2001) while the surface halogens are based on Table 8-5 (scenario A1) of WMO (2007) for the year 2000. Both ODSs and GHGs repeat every year.
- **Background aerosol** is prescribed from the extended SPARC (2006) SAD data set (Section 2.5.3.4) for the year 2000.
- **Solar irradiance** is averaged over one solar cycle to provide a mean solar flux for the year 2000.
- **Sea surface temperatures (SSTs) and sea ice concentrations (SICs)** in this simulation are prescribed as a mean annual cycle derived from the years 1995 to 2004 of the HadISST1 data set (Rayner *et al*., 2003).
- The **QBO** is not externally forced.
- **Emissions of ozone and aerosol precursors** (CO, NMVOC, NO_x and SO_2) are averaged over the years 1998 to 2000 and are taken from an extended data set of the REanalysis of the TROpospheric chemical composition (RETRO) project (Schultz *et al*., 2007; ***http://retro.enes.org***). In case of SO_2, RETRO only provides biomass burning related emissions. Therefore, this data is combined with an interpolated version of EDGAR-HYDE 1.3 (Van Aardenne *et al*., 2001) and EDGAR 32FT2000 (Olivier *et al*., 2005; Van Aardenne *et al*., 2005).

2.5.2.2. REF-B1: Reproducing the past

REF-B1 (1960-2006) is defined as a transient run from 1960 (with a 10-year spin-up period) to the present. All forcings in this simulation are taken from observations, and are mostly identical to those used by Eyring *et al*. (2006). This transient simulation includes all anthropogenic and natural forcings based on changes in trace gases, solar variability, volcanic eruptions, QBO, and SSTs/SICs.

- **GHGs** (N_2O, CH_4, and CO_2) between 1950 and 1996 are taken from IPCC (2001) and merged with the NOAA observations forward through 2006. NOAA CO_2, CH_4, and N_2O are scaled to agree on January 1996 with the historical IPCC data (Section 2.5.3.2).
- **ODSs** (CFC-10, CFC-11, CFC-12, CFC-113, CFC-114, CFC-115, CH_3CCl_3, HCFC-22, HCFC-141b, HCFC-142b, Halon-1211, Halon-1202, Halon-1301, and Halon-2402) are prescribed at the surface according to Table 8-5 of WMO (2007). For models that do not represent all the species listed here, the halogen content of species that are considered should be adjusted such that model inputs for total chlorine and total bromine match the time series of total chlorine and bromine given in this table (Section 2.5.3.2). This

also applies to the other simulations.

- **SSTs and SICs** are prescribed as monthly-mean boundary conditions following the observed global SIC and SST data set HadISST1 (Rayner *et al*., 2003; Section 2.5.3.1). To correct for the loss of variance due to the time interpolation of monthly-mean data, a variance correction is applied (http://grads.iges.org/c20c/c20c_forcing/karling_instruct.html).
- **Aerosol Surface Area Densities** (SADs) from observations are considered in REF-B1 (Section 2.5.3.4; Eyring *et al*., 2008).
- **Stratospheric warming and tropospheric-surface cooling** due to volcanic eruptions are either calculated on line by using aerosol data or by prescribing heating rates and surface forcing (Section 2.5.3.4).
- **Solar variability**. Daily spectrally resolved solar irradiance data from 1 January 1950 to 31 Dec 2006 (in $W/m^2/nm$) are provided at ***http://www.geo.fu-berlin.de/en/met/ag/strat/research/SOLARIS/Input_data/index.html***. The data are derived with the method described by Lean *et al*. (2005). Each modelling group is required to integrate the data over the individual wavelength intervals used in their radiation and photolysis schemes. This approach supersedes the parameterisation with the F10.7 cm radio flux previously used (Section 2.5.3.6).
- **The QBO:** Models that do not produce an internally generated QBO are asked externally impose a QBO for REF-B1 (Sections 2.3.1.3 and 2.5.3.5).
- **Ozone and aerosol precursors** (CO, NMVOC, NO_x and SO_2) from 1960 to 1999 are taken from the extended data set of the RETRO project (Schultz *et al*., 2007). For the spin-up period from 1950 to 1959 the 1960 values from this data set are used cyclically. After 2000 trend estimates taken from IIASA are used to extend the data set (P. Rafaj, personal communication; ***http://www.ozone-sec.ch.cam.ac.uk/ccmval_emissions***; Section 2.5.3.3).

2.5.2.3. REF-B2: Making Predictions

REF-B2 is an internally consistent simulation covering 1960-2100, using only anthropogenic forcings. The objective of REF-B2 is to produce best estimates of the future ozone-climate change assuming scenario SRES A1b for GHGs and decreases in halogen emissions (adjusted Scenario A1).

- **GHGs** follow the IPCC (2001) SRES A1b scenario, as in Eyring *et al*. (2007) (Section 2.5.3.2).
- **ODSs** are based on scenario A1 from WMO (2007). However, at the 2007 Meeting of the Parties to the Montreal Protocol, the Parties agreed to an earlier phase out of HCFCs (http://ozone.unep.org/Meeting_Documents/mop/19mop/Adjustments_on_HCFCs.pdf). Scenario A1 does not include this phase out. Hence, a new scenario has been developed that includes this phase out (hereafter referred to as the "adjusted scenario A1"). CFCs, Halons, and other

Table 2.19: Solar cycle by experiment with reference. Models not listed here do not impose a solar cycle.

CCM	REF-B0	REF-B1	REF-B2	SCN-B2d	Reference
AMTRAC3	N/A	YES	YES	N/A	
CAM3.5	YES,1996-2006 Avg	YES	Mean of Solar Cycles 19-23	N/A	Includes SPE's. *Lean (2005)*
CCSRNIES	NO	YES	NO	N/A	*Lean et al. (1997)* and flux at 10.7 cm *(Akiyoshi et al., 2009)*
CMAM	NO	YES	NO	N/A	Lean (2005)
CNRM-ACM		YES	NO	N/A	GCM : *Solanki and Krivova (2003)*. Chemistry : *Lean (2005)*
E39CA	N/A	YES	N/A	YES	*Lean et al. (1997)*
EMAC	N/A	YES	N/A	N/A	*Nissen et al. (2007)*
LMDZrepro	NO	YES	NO	N/A	
MRI	NO	YES	NO	N/A	
Niwa-SOCOL SOCOL	NO	YES	NO	N/A	*Lean (2005)* as defined in CCMVal forcing data
UMSLIMCAT	NO	YES	NO	N/A	GCM: *Zhong et al. (2001)*; chemistry: *Lean et al. (1997)*
WACCM	YES,1996-2006 Avg	YES	Mean of Solar Cycles 19-23	N/A	Includes SPE's. *Lean (2005)*

non-HCFC species remain as in the original scenario A1 (Section 2.5.3.2).

- **Background aerosol** is the same as in REF-B0 (Section 2.5.2.1), *i.e.* background, non-volcanic aerosol loading is assumed (Section 2.5.3.4).
- **SSTs and SICs.** Due to potential discontinuities between the observed and modelled data record, the REF-B2 runs use simulated SSTs and SICs for the entire period, using GCM simulations forced with the SRES A1b GHG scenario (Table 2.21; Section 2.5.3.1), or in the case of the CMAM model an interactive ocean.
- **Ozone and aerosol precursors** are identical to REF-B1 until 2000 and use the adjusted IIASA scenario through to 2100 (P. Rafai, personal communication). Models span a wide spectrum in how they represent tropospheric composition. Consequently, the usage of tropospheric emissions varies widely across the models (**Table 2.1**9; Section 2.5.3.3).

2.5.3 External forcings

2.5.3.1 SSTs and sea ice

REF-B0, REF-B1, and CNTL-B0 are using the HadISST1 observational SST/sea ice data set (***http://www.metoffice.com/hadisst***; Rayner *et al*., 2003). It covers the period of 1870-present. Climate change over the oceans documented in IPCC (2007) is largely diagnosed from the HadISST1 data set. Almost all simulations in these categories use HadISST1 (Table 2.14). There is a distinct warming trend in the HadISST1 SSTs (Figure 2.2), starting in around 1970. Since then, the sea surface has warmed by 0.2 to 0.3 K. Associated with this is a decline in the maximum monthly-mean sea-ice extent of both polar regions. For the Antarctic, sea ice coverage before 1970 is poorly known, explaining the lack of variability before 1962 and the linear trend in the late 1960s.

For the REF-B2 simulations modellers use a variety of different data sets, or, in the case of CMAM, an interactive ocean model. Mean SSTs from the HadGEM1 climate model (Johns *et al*., 2007) are displayed in **Figure 2.2**, right. A cold bias of around 2 K *versus* HadISST1 is apparent. This bias, and various other biases found in other climate model data, are the reason why a seamless simulation of past and future climate and ozone, such as REF-B2, cannot be performed based on a combination of analysed and simulated SSTs. Two groups of models sharing the same ocean surface forcing in REF-B2 appear, namely CAM3.5, GEOSCCM, ULAQ, and WACCM all use CCSM3 data, and E39CA, Niwa-SOCOL for parts of REF-B2, UMSLIMCAT, and the UMUKCA models use HadGEM1 data (Table 2.13). Niwa-SOCOL uses a combination of HadISST1 and HadGEM1 SSTs for its ocean forcing of REF-B2, introducing a discontinuity into this simulation.

For the LMDZrepro REF-B2 simulation, sea surface conditions are taken from the A1b simulation produced with the IPSL AOGCM (Dufresne *et al*., 2005). Since this simulation exhibits biases with respect to the AMIP2 data set (Taylor *et al*., 2000), the mean biases for the 1985-2005 period are first removed from the entire A1b simulation and then the corrected SST and sea ice forcing is used to force LMDZrepro.

2.5.3.2 Long-lived greenhouse gases and ozone-depleting substances

Figure 2.3 displays the time evolution of the major

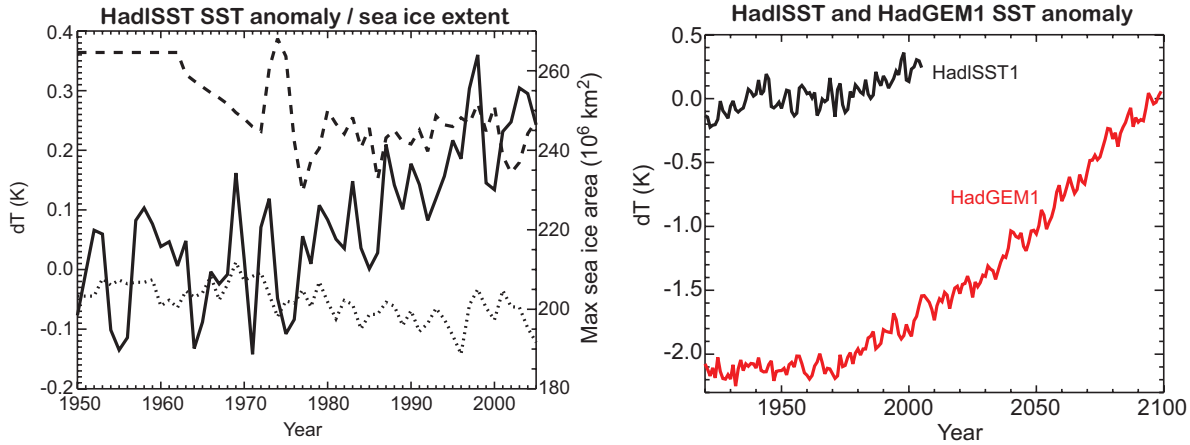

Figure 2.2: (left) Solid: anomaly in annual-mean, ocean-mean sea-surface temperature, relative to the 1950-1969 mean, in the HadISST1 data set. Dashed and dotted: Antarctic and Arctic maximum monthly-mean sea ice coverage (10^6 km^2). (right) HadISST1 and HadGEM1 SSTs, relative to the 1950-1969 mean of HadISST1, from 1920 to 2099.

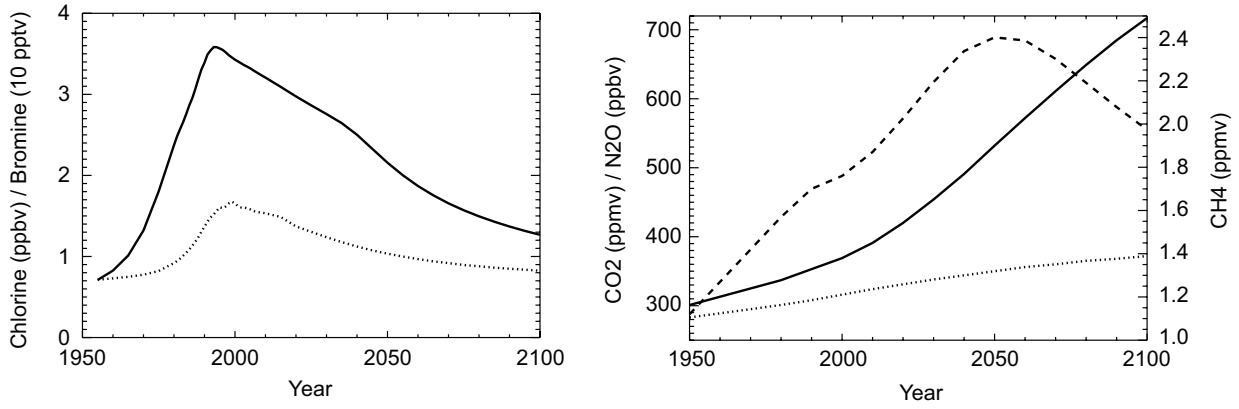

Figure 2.3: (left) Surface total chlorine (solid) and total bromine (dotted) as defined in the A1 scenario. (right) Surface CO_2 (solid), N_2O (dotted), and CH_4 (dashed) as defined in the SRES A1b scenario.

GHGs, total chlorine and total bromine, as specified in the SRES A1b (IPCC, 2001) and A1 (WMO, 2007) scenarios. The ODSs increase sharply during the 1970s and 1980s, resulting in an approximate 6-folding of organic chlorine and a doubling of organic bromine at peak abundances in the 1990, relative to pre-industrial times. For the 21st century, a continuous decline, in accordance with the Montreal Protocol, is anticipated. The decline is substantially slower than the increase in the 20th century. By contrast, for the leading greenhouse gas CO_2 a steady increase is anticipated, leading to a more than doubling by 2100, compared to 1950. N_2O follows a similar trend, *albeit* with smaller growth rates. CH_4, by contrast, is anticipated to undergo a trend reversal around 2050.

2.5.3.3 Ozone precursors

Surface emissions of NO_x, CO, and CH_2O, as used by many models, are displayed in **Figure 2.4**. For the period from 1960 to 1999 the data are from the RETRO database (***http://retro.enes.org/reports/D1-6_final.pdf***). Note the general increase of NO_x, CO, and CH_2O emissions during the 20th century. During the 21st century, however, the IIASA SRES A1b scenario forecasts a general reduction in CO emissions and a trend reversal for NO_x around 2020, followed by a sharp decrease. Emissions of CH_2O are forecast to increase then stabilize during the second half of the century. Evidently the interannual variability characterizing the RETRO emissions is absent in the 21st century. The IIASA emissions are courtesy of Peter Rafaj, IIASA (***http://www.atm.ch.cam.ac.uk/~om207/Download_emission_files.html***). Not included in Figure 2.4 is lightning-produced NO_x which is included in most models and is determined using a variety of different parameterisations (Section 2.3.3.7; Table 2.12).

2.5.3.4 Stratospheric aerosol surface area densities and direct aerosol-related heating

The SPARC aerosol data set is constructed from SAGE profile measurements of aerosols, beginning in 1983. Unlike in IPCC modelling, stratospheric CCMs require height-resolved aerosol forcing data due to the importance of heterogeneous chemical processing. Four big volcanic events are obvious, Agung in 1963, El Chichón in 1982, Nevado del Ruiz in 1985 and Mt Pinatubo in 1991 (**Figure 2.5**). Also some smaller events are apparent. Data before 1983 are constructed based on assumptions of background aerosol and, in the case of Agung, assuming a similar distribution of aerosol as after later volcanic eruptions. A problem is apparent at high latitudes in the Southern Hemisphere, where the satellite sensor cannot distinguish between sulfate aerosols and PSCs. In these areas, sometimes a very low SAD of sulfate aerosol is assumed. With

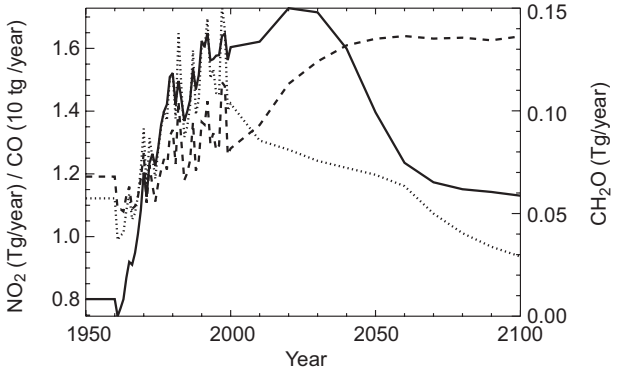

Figure 2.4: Surface emissions of (solid) NO_x (displayed as TG/year of NO_2), CO (dotted) and CH_2O (dashed) as used for CCMVal-2 simulations. From 1960 to 1999, data are from the RETRO emissions database (see text), after 1999 they are extrapolated using an IIASA scenario. Before 1960 they are repeated 1960 RETRO emissions.

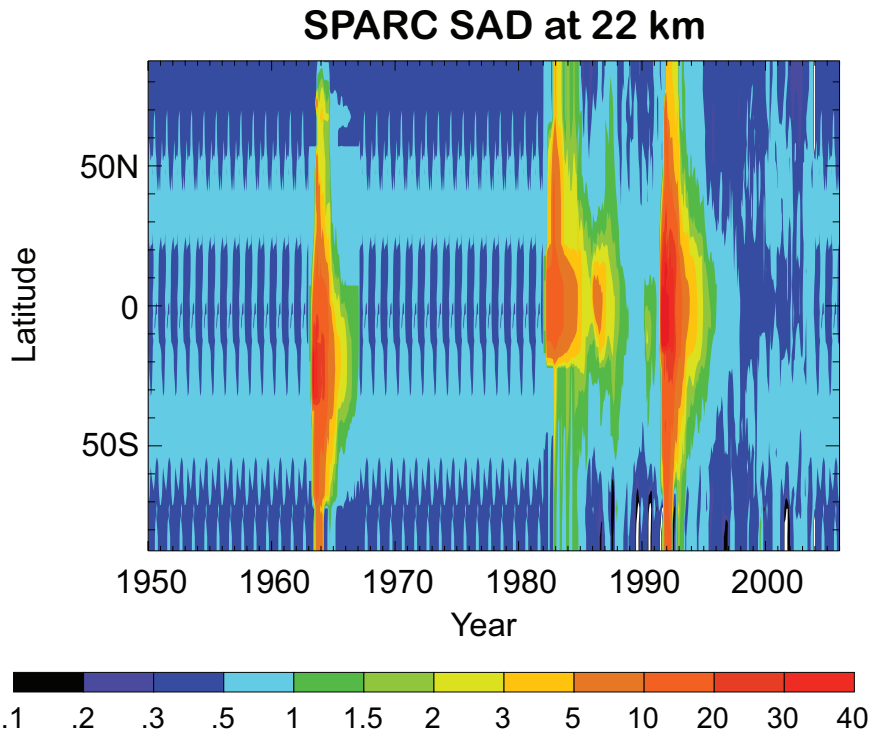

Figure 2.5: Aerosol surface area density ($\mu m^2/cm^3$) at 22 km, reconstructed from SAGE data.

the exception of (Niwa-)SOCOL (using a combination of SAGE and GISS data), all models use this data set for the REF-B1 simulations. For REF-B0 and REF-B2, background (year-2000) data are used cyclically throughout the simulations.

Aerosols cause a perturbation to the heating/cooling profiles of the troposphere and stratosphere, particularly during volcanic periods, and also cause the Earth's surface to warm or cool (Sato *et al*., 1993; Robock, 2002). Several different approaches have been taken by the CCMVal-2 models regarding this effect: Two models derive heating rates consistent with the prescribed SAD data set (CMAM, WACCM). Others use independent data sets such as the GISS data (CCSRNIES, MRI, UMETRAC, UMUKCA-METO). E39CA and EMAC use precalculated rates (Stenchikov *et al*., 2006; Eyring *et al*., 2008). The SOCOL models use a mixture of different sources. One (of 4) ULAQ REF-B1 simulation uses estimates of volcanic injections of SO_2, and an interactive aerosol calculation to infer heating rates. CNRM-ACM reports problems with

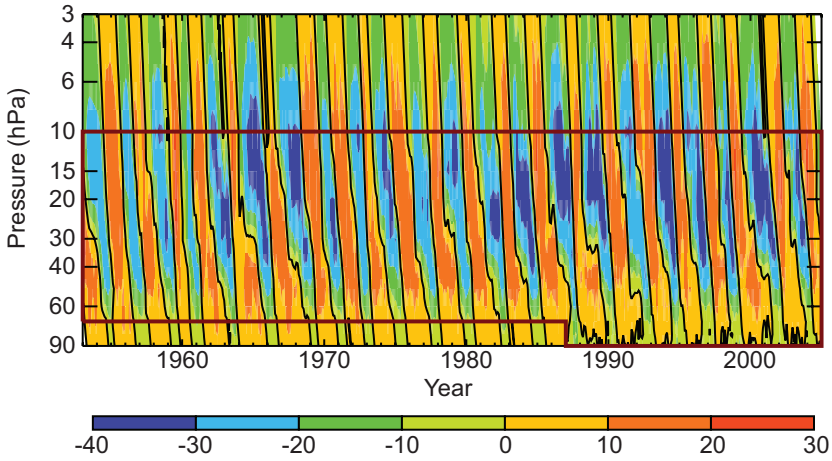

Figure 2.6: Zonal wind (u) from merged observations at Canton Island, Gan and Singapore, vertically extended. (http://www.pa.op.dlr.de/CCMVal/Forcings/qbo_data_ccmval/u_profile_195301_200412.html). The violet box denotes the area constrained by the observations. In the areas outside the box the data are extrapolated, assuming a phase speed of 2 km/month (above 10 hPa) and 1 km/month (below 70 hPa, before 1987).

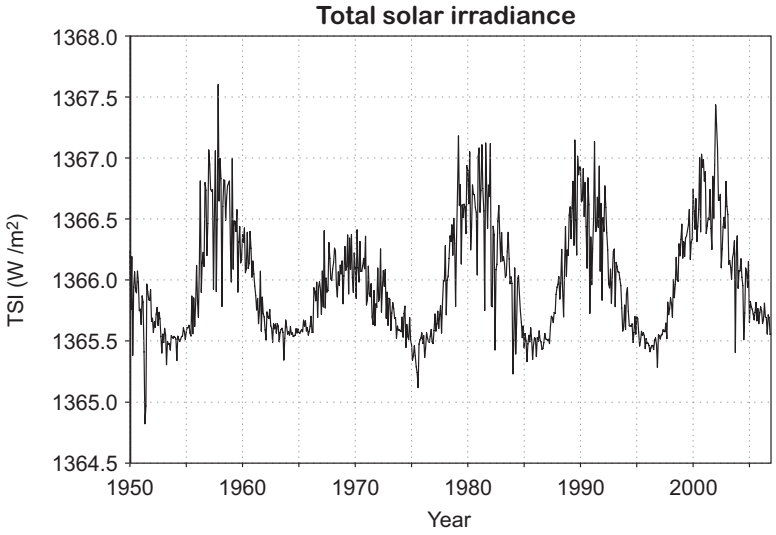

Figure 2.7: Total solar irradiance (W/m^2) updated from Lean et al. (2005).

their calculation, which is based on observed optical depth (Table 2.10, and references therein). Five CCMVal-2 models do not represent heating due to volcanic aerosol.

2.5.3.5 QBO time series

In the REF-B1 simulations, the QBO is imposed in the tropical region in various models. **Figure 2.6** shows a depiction of the QBO. Table 2.5 summarizes the different ways in which these models impose the QBO (Section 2.3.1.3).

2.5.3.6 Solar irradiance

Solar output varies with sunspot numbers and other parameters. Most of the atmospherically relevant variability is in the 11-year solar cycle. CCMVal-2 modellers have been asked to use the data by Lean *et al*. (2005) for their REF-B1 simulations. **Figure 2.7** shows total solar irradiance; it varies by about 1 W/m^2 on a background of around 1366 W/m^2. However, most of the variability is at short wavelengths, where the solar cycle is relatively more important than for the spectrally integrated solar output (the "solar constant").

2.5.4 Deviations from simulation definitions

The following is a model-by-model listing of the various ways in which model setups deviate from the definitions (Eyring *et al*., 2008) as summarized above:

AMTRAC3:
- REF-B2 includes an 11-year solar cycle.
- In REF-B1 there is no nudging of the QBO.

CAM3.5
- Direct radiative forcing by volcanic aerosols (impacting heating and photolysis) is not implemented in REF-B1.
- No variance correction is applied to the SSTs.

CCSRNIES:
- 1.8 pptv of $CHBr_3$ is assumed at the surface.
- Some photolysis cross sections stem from JPL (2002) and JPL (1997).
- The variance correction for SSTs is not applied.

CMAM:
- The REF-B1 simulations did not include a spontaneous or nudged QBO.
- The variance correction for SSTs was not performed.
- Heterogeneous reaction rates have not been updated to JPL (2006).

CNRM-ACM:
- There is no QBO in REF-B1.
- The variance correction for SSTs was not performed.

E39CA:
- In REF-B1 halogen loadings from WMO (2003) are used.
- In REF-B1: for 2000-2004, stratospheric aerosol from 1999 is used, otherwise as CCMVal definitions.
- In SCN-B2d, the future scenario of NO_x emissions from industry and traffic is set up as follows:
- 8 different regions (Europe, USA, Australia, Asia, India, South America, Africa) are defined. They are broken up into two categories: Industrialized (Europe, USA, Australia) and developing (Africa, Asia, India, South America). For the industrialized countries the

linear trend between 1990 and 2000 is extrapolated until 2015, and constant NO_x emissions are assumed from 2015. For the developing countries a linear trend between 1990 and 2000 is extrapolated until 2030, and constant NO_x emissions are assumed from 2030. This scenario assumes that developing countries will adopt technological advance 15 years later then industrialized countries.

EMAC:
- Chemical kinetics are mostly based on JPL (2002).
- Lumping is not performed for organic bromine, meaning there is slightly less bromine due to non-represenation of compounds other than CH_3Br, Halon-1211, and Halon-1301.
- Stratospheric aerosol is as in CCMVal-1.

GEOSCCM:
- All runs use JPL(2002) chemical kinetics.
- All runs use trace gas forcings prescribed for CCMVal-1 (*i.e.*, they are not updated to CCMVal-2). For ODSs, annual means were prescribed following scenario Ab (WMO, 2003, Table 1-16).
- All runs use background (1979) surface area densities from a data set created by D. Considine.
- Direct radiative forcing by volcanic aerosol (on heating and photolysis) is not implemented in REF-B1.
- All runs ignore the solar cycle for photolysis.
- The REF-B1 run does not include QBO forcing.

LMDZrepro:
- No heating from volcanic aerosol was imposed in REF- B1.
- No QBO was imposed in REF-B1.
- REF-B0 and REF-B1 are forced with AMIP-II sea surface conditions.
- Halon-1211 and Halon-1301 surface mixing ratios are set to 1 pptv where the A1 scenario implies less than 1 pptv (before about 1980 and after about 2040).
- A constant surface mixing ratio of 3 pptv is imposed for CH_2Br_2.

MRI:
- Members 1, 2, and 3 of REF-B1 use SST and sea-ice modelled by MRI-CGCM 2.3.2.
- These simulations also do not include the CH_4 changes after 2002.

Niwa-SOCOL:
- The parameters associated with sulfate aerosol are as in Schraner *et al*. (2008), covering 1975-2002. The only change to this data set was to set the single-scattering albedo to 0.995 instead of 1.0 in the solar/shortwave spectral region, as recommended by Fischer *et al*. (2008).
- For REF-B1 and SCN-B1 the SAD data set is defined as follows:
  - 1950-1962 and 1967-1974: 1975 annual mean of SAD data set
  - 1963-1966: 1991-1994 SAD data (to simulate the Agung volcano event, similar to Pinatubo)
  - 2003-2005: 2002 SAD data set.
- For REF-B0 , REF-B2 and SCN-B2x the 2000 annual mean of the SAD data is used cyclically.
- For CTL0: The 1975 annual mean of SAD data set is used cyclically.
- Volcanic aerosol does not affect the photolysis rates.
- The Niwa-SOCOL halogen chemistry includes $CHBr_3$ and CH_2Br_2 at 1.63 and 1.21 pptv in 2000, respectively.

SOCOL:
- The future scenarios for CO and NO_x emissions differ from those recommended. Future CO and NO_x emissions use the RETRO data set scaled by the SRES prediction of the future anthropogenic activities.
- JPL (2006) rates were used where applicable. Also data from earlier JPL versions, IUPAC (2005) and analytic expressions were used.
- SAD (background aerosol): see Niwa-SOCOL. The influence of stratospheric sulfate aerosol on the short- and longwave radiation has been directly taken into account, *i.e.*, the model radiation code calculates online the changes in the radiation fields due to stratospheric aerosol.
- Photolysis rates are not affected by volcanic aerosol.
- The SOCOL halogen chemistry includes $CHBr_3$ and CH_2Br_2 at 1.63 and 1.21 pptv in 2000, respectively.

ULAQ:
- Three REF-B1 integrations do not include diabatic heating rates from volcanoes.
- A fourth REF-B1 run includes the volcanic forcing, calculated online from the aerosol microphysics code of the ULAQ-CCM.

UMETRAC:
- There is no solar cycle in UMETRAC.
- The photochemistry has not been updated to JPL (2006).
- The SSTs have not been manipulated to account for a loss of variance.
- Photolysis rates do not account for the presence of volcanic aerosol.

UMSLIMCAT:
- Direct radiative (on photolysis and heating) due to volcanic impacts is not represented in REF-B1.

Table 2.20: Three-dimensional instantaneous (T3I) diagnostics produced by model, for REF-B2. Models not listed did not produce any T3I diagnostics. For the meaning of names see Table 1 of http://www.pa.op.dlr.de/CCMVal/DataRequests/CCMVal-2_Datarequest_FINAL.pdf.

CCM	T3I diagnostics
AMTRAC3 (REF-B1)	va, ua, ta, ps, plev, O3, N2O, H2O, CO, CH4
CCSRNIES	zg, wap, vorpot, va, ua, tntsw, tntlw, ta, sad-sulf, sad-nat, sad-ice, plev, OH, OClO, O3P, O3, NOy, NO2, NO, N2O5, N2O, N, HOCl, HOBr, HO2, HNO4, HNO3, HNO3s, HCl, HBr, H2O2, H2O, CO, Cly, ClONO2, ClO, Cl2O2, CHBr3, CH3OOH, CH3Cl, CH3Br, CH2O, CFCl3, CF2Cl2, Bry, BrONO2, BrO, BrCl, Br
CMAM	zg, wap, va, ua, tntsw, tntlw, ta, plev, OH, OClO, O3P, O3, O1D, NOy, NO2, NO, N2O5, N2O, N, mean_age, HOCl, HOBr, HO2, HNO4, HNO3, HCl, HBr, H2O2, H2, CO, Cly, clt, ClONO2, CO, Cl2O2, Cl, CH4, CH3OOH, CH3OOH, CH3Cl, CH3Br, CH2O, CFCl3, CF2Cl2, Bry, BrONO2, BrO, BrCl, Br
CNRM-ACM	sad-sulf, sad-nat, sad-ice, psc, OH, OClO, O3P, O3, O1D, NOy, NO, NO2, N, N2O, N2O5, jO2, jCl2O2, HOCl, HOBr, HO2, HNO4, HNO3, HCl,, HBr, H2SO4, H2O, H2O2, CO, Cly, ClONO2, ClO, Cl, Cl2O2, CH4, CH3OOH, CH3Cl, CH3Br, CH2O, CFCl3, CF2Cl2, CCl4, CCl2FCCl2F, CBrF3, CBrClF2, Bry, BrONO2, BrO, BrCl, Br
EMAC (REF-B1)	zg, vorpot, va, ua, ta, OH, OClO, O3P, O3, O1D, NOy, NO2, NO, N2O5, N2O, ice, HO2, HNO3_NAT, HNO3_liq, HNO3, HCl, H2O, CO2, CO, Cly, ClO, ClNO3, Cl2O2, CH4, CFCl3, CF2Cl2, Bry, BrO, BrNO3
GEOSCCM	zg, wap, va, ua, tntsw, tntlw, ta, plev, OH, OClO, O3, O(3P), O(1D), NOy, NO2, NO, N2O5, N2O, N, mean_age, HOCl, HOBr, HO2, HNO4, HNO3, HCl, HBr, H2O2, H2O, CO, Cly, ClONO2, ClO, Cl2O2, Cl, CH4, CH3OOH, CH3Cl, CH3Br, CH2O, CFCl3, CF2Cl2, Bry, BrONO2, BrO, BrCl, Br
LMDZrepro	zg, wap, vorpot, va, ua, tntsw, tntlw, ta, sad-sulf, sad-nat, sad-ice, plev, OH, OClO, O3s, O3, NOy, NO2, NO, N2O5, N2O, N, mean_age, HOCl, HOBr, HO2, HNO3, HCl, HBr, H2O2, H2O, convclt, CO, Cly, clt, ClONO2, ClO, Cl2O2, Cl, CH4, CH3OOH, CH3Cl, CH3Br, CH2O, CH2Br2, CFCl3, CF2Cl2, Bry, BrONO2, BrO, BrCl, Br
MRI	OH, OClO, O3, NOy, NO2, NO, N2O5, N2O, N, HOCl, HOBr, HO2, HNO4, HNO3, HCl, HBr, H2O2, H2O, CO2, CO, Cly, ClONO2, ClO, Cl2O2, Cl, CH4, CH3Cl, CH3Br, CFCl3, CF2Cl2, Bry, BrONO2, BrO, BrCl, Br
Niwa-SOCOL (REF-B1)	va, ua, ta, O3, NAT-SAD, NAT, N2O, ICE-SAD, ICE, HNO3, HCl, H2O, CO, ClO, Cl2O2, CH4
UMUKCA-METO	zg, va, ua, tntsw, tntlw, ta, plev, OH, OClO, O3s, O3P, O3, NOy, NOx, NO, N2O, N2O5, mean_age, HOCl, HOBr, HO2, HNO4, HNO3, HCl, HBr, H2O, H2O2, H2, CO, Cly, ClONO2, ClO, Cl, Cl2O2, CH4, CH3Br, CFCl3, CF2Cl2, Bry, BrONO2, BrO, BrCl, Br
WACCM	zg, wap, va, ua, tntsw, ta, sad-sulf, sad-nat, sad-ice, OH, OClO, O3, O1D, NOy, NO, NO2, N, N2O, N2O5, mean_age, JCl2O2, HOCl, HOCl, HOBr, HO2, HNO3, HCl, HBr, H2O, H2O2, H2, convclt, CO, CO2, Cly, clt, ClONO2, ClO, Cl, Cl2O2, CH4, CH3OOH, CH3Cl, CH3Br, CH2O, CFCl3, CF2Cl2, Bry, BrONO2, BrO, BrCl, Br

- The photolysis cross-section data was not updated to JPL (2006).
- The REF-B1 and REF-B2 simulations use an extra 6 pptv of Br_y.
- The SSTs have not been manipulated to account for a loss of variance.

UMUKCA-METO:

- There is no solar cycle in the UMUKCA-METO simulations.
- SSTs are not manipulated to increase day-to-day variability.
- Photolysis cross sections and heterogeneous reaction data are not updated to JPL (2006).
- Photolysis rates are not affected by volcanic aerosol.
- For ODSs, in REF-B2 the unadjusted scenario A1

Table 2.21: Three- and two-dimensional surface monthly-mean (T3M, T2Ms) diagnostics produced by model, for REF-B2.

CCM	T3M diagnostics	T2Ms diagnostics
AMTRAC3 (REF-B1)	zg, ua, tntsw, ta, H2O	toz,slp
CAM3.5	zg, va, ua, ta	toz, sic, ps, hfss, hfsl
CCSRNIES	zg, wap, va, ua, TRACER, tntsw, tntlw, ta, O3, NO2, N2O, HCl, H2O, CO, CH4	ztp, toz, tatp, ptp, ps, nufl
CMAM	zg, wa, va, ua, tntsw, tntlw, ta, O3P, O3, O1D, NO2, NO, N2O, mean_age, HCl, H2O, CO, clt, CH4	ztp, toz, tatp, ptp, ps, nufl
CNRM-ACM	zg, wap, va, ua, ta, O3, NO, NO2, N2O, mean_age, HCl, H2O, CO, CH4	toz, tatp, ptp, ps, pr, hfss, hfls, conclt, clt
E39CA (REF-B1)	va, ua, ta, O3, H2O	toz
EMAC (REF-B1)	zg, va, ua, ta, O3, HNO3, H2O, CO, Cly, CH4, Bry	toz
GEOSCCM	zg, va, ua, tntsw, tntlw, ta, O3, N2O, mean_age, inst_wap, inst_NOx, inst_HCl, inst_CO, H2O, convclt, clt, CH4	ztp, toz, tatp, ptp, ps, pr, clt
LMDZrepro	zg, wa, va, ua, tntsw, tntlw, ta, O3, NO2, NO, N2O, mean_age, HCl, H2O, convclt, CO, clt, CH4	toz, tatp, ptp, ps, pr, ogw_flux, nufl, hfss, hfls
MRI	zg, wa, va, ua, tntsw, tntlw, ta, O3, N2O, HCl, H2O, CH4	toz, rsdscs, rsds, ps
Niwa-SOCOL (REF-B1)	zg, va, ua, ta, O3, NO2, NO, N2O, HCl, H2O, CO, ClONO2, CH4	toz, ps
SOCOL	zg, wap, va, ua, ta, O3, NOx, N2O, mean_age, HCl, H2O, CO, CH4	ztp, toz, tatp, ptp, ps, pr, hfss, hfls, clt
ULAQ	zg, va, ua, ta, O3, N2O, mean_age, H2O, CO2, CO, CH4	toz
UMSLIMCAT	zg, wa, va, ua, ta, OH, OClO, O3, NOy, NO, NO3, NO2, N2O, N2O5, HOCl, HOBr, HO2, HNO4, HNO3, HCl, HBr, H2O, H2O2, CO, Cly, ClONO2, ClO, Cl2O2, CH4, CH3Br, CH2O, BrONO2, BrCl	toz, tos, snd, rsdscs, rsds, ps, nufl, convclt, clt
UMETRAC (REF-B1)	ua, ta, O3, NOy, mean_age, HOCl, HOBr, HCl, HBr, H2O, CO, Cly, ClONO2, CH3OOH, Bry, BrONO	ztp, toz, tatp, ptp, ps, clt
UMUKCA-METO	zg, wa, ua, tntsw, tntlw, ta, O3, NOx, N2O, mean_age, HCl, CO, Cly, CH4	ztp, toz, tatp, ptp, ps
UMUKCA-UCAM	zg, wa, va, ua, tntsw, tntlw, ta, O3, N2O, mean_age, H2O, CO, Cly, ClONO2, CH4	toz
WACCM	zg, wa, va, ua, tntsw, tntlw, ta, O3, N2O, mean_age, H2O, CO, Cly, ClONO2, CH4	toz, sic, ps, precl, precc, nufl, hfss, hfls

(WMO, 2006) is used.

UMUKCA-UCAM:

- UMUKCA-UCAM does not have a representation of the solar cycle.
- There is no direct volcanic aerosol effect implemented in UMUKCA-UCAM for REF-B1 (neither on heating nor photolysis).
- SSTs are not manipulated to increase day-to-day variability.
- Kinetic data are not updated to JPL (2006).
- For ODSs, in REF- B2 the unadjusted scenario A1 (WMO, 2006) is used.

WACCM

- No variance correction is applied to the SSTs.

2.6 Diagnostic output requested for CCMVal-2

In comparison with CCMVal-1, a much more com-

Table 2.22: Zonal-monthly-mean (T2Mz) diagnostics produced by model, for REF-B2.

CCM	T2Mz diagnostics
AMTRAC3 (REF-B1)	va, ua, ta, O3, NOy, N2O, mean_age, HNO3, HCl, H2O, Cly, CH4, Bry
CAM3.5	zg, wstar, vstar, va, ua, ta, OH, OClO, O3, NOy, NO, NO2, N, N2O, N2O5, mean_age, HOCl, HOBr, HO2, HNO3, HCl, HBr, H2O, H2O2, H2, Cly, ClONO2, ClO, Cl, Cl2O2, Cl2, CHClF2, CH4, CH3Cl, CH3CCl3, CFCl3, CF2Cl2, CCl4, BrONO2, BrO, BrCl, Br
CCSRNIES	zg, wstar, vstar, va, ua, TRACER, ta, OH, OClO, O3, NOy, NO, NO2, N, N2O, N2O5, HOCl, HOBr, HO2, HNO4, HNO3, HCl, HBr, H2O, H2O2, fz, fy, CO, Cly, ClONO2, ClO, Cl2O2, CHClF2, CHBr3, CH4, CH3OOH, CH3Cl, CH3CCl3, CH3Br, CH2O, CFCl3, CF2Cl2, CCl4, CCl2FCClF2, CBrF3, CBrClF2, Bry, BrO, BrCl, Br, accel_ogw, accel_gw, accel_divf
CMAM	zg, wstar, vstar, va, ua, ta, OH, ogw_flux, OClO, O3P, O3, O1D, NOy, nogw_w_flux, nogw_e_flux, NO, NO2, N, N2O, N2O5, mean_age, HOCl, HOBr, HO2, HNO4, HNO3, HCl, HBr, H2O, H2O2, H2, fz, fy, CO, Cly, ClONO2, ClO, Cl2O2, Cl, CHF2Cl, CH4, CH3OOH, CH3Cl, CH3CCl3, CH3Br, CH2O, CFCl3, CF2Cl2, CCl4, Bry, BrONO2, BrO, BrCl, Br, accel_ogw, accel_nogw, accel_gw, accel_divf
CNRM-ACM	zg, wstar, va, ua, ta, OH, OClO, O3, NOy, NO, NO2, N, N2O, N2O5, mean_age, HOCl, HOBr, HO2, HNO4, HNO3, HCl, HBr, H2O, H2O2, CO, Cly, ClONO2, ClO, Cl2O2, Cl, CH4, CH3OOH, CH3Cl, CH3CCl3, CH3Br, CH2O, CFCl3, CF2Cl2, CCl4, CCl2FCClF2, CBrF3, CBrClF2, Bry, BrONO2, BrO, BrCl, Br
E39CA (REF-B1)	zg, wstar, vstar, va, ua, ta, O3, NO2, N2O, HNO3, HCl, H2O, fz, fy, CO, Cly, ClONO2, CH4, accel_divf
EMAC (REF-B1)	zgm, zg, wstar, vstar, va, ua, tntsw, ta, SF6, OH, O3P, O3, NOy, NO2, NO, N2O5, N2O, HO2, HNO3, HCl, H2O, fz, fy, CO, Cly, ClONO2, ClO, CH4, CFCl3, CF2Cl2, Bry, BrO, accel_divf
GEOSCCM	zg, wstar, va, ua, ta, OH, OClO, O3, NOy, NO, NO2, N, N2O, N2O5, mean_age, HOCl, HOBr, HO2, HNO4, HNO3, HCFC-22, HCl, HBr, H2O, H2O2, fz, fy, Cly, ClONO2, ClO, Cl2O2, Cl, CH4, CH3Cl, CH3CCl3, CH3Br, CFCl3, CF2Cl2, CCl4, CBrF3, Bry, BrONO2, BrO, BrCl, Br, accel_ogw, accel_nogw, accel_gw, accel_divf
LMDZrepro	g, wstar, vstar, va, ua, ta, OH, OClO, O3, NOy, NO, NO2, N, N2O, N2O5, mean_age, HOCl, HOBr, HO2, HNO3, HCl, HBr, H2O, H2O2, fz, fy, CO, Cly, ClONO2, ClO, Cl2O2, Cl, CH4, CH3OOH, CH3Cl, CH3Br, CH2O, CH2Br2, CFCl3, CF2Cl2, CCl4, CBrF3, CBrClF2, Bry, BrONO2, BrO, BrCl, Br, accel_ogw, accel_nogw, accel_gw, accel_divf
MRI	zg, wstar, vstar, va, ua, ta, OH, OClO, O3, NOy, NO, NO2, N, N2O, N2O5, mean_age, HOCl, HOBr, HO2, HNO4, HNO3, HCl, HBr, H2O, H2O2, fz, fy, CO2, CO, Cly, ClONO2, ClO, Cl2O2, Cl, CH4, CH3Cl, CH3Br, CFCl3, CF2Cl2, Bry, BrONO2, BrO, BrCl, Br, accel_ogw, accel_gw, accel_divf
Niwa-SOCOL (REF-B1)	zg, wstar, vstar, va, ua, ta, sad-sulf, sad-nd, OH, odscls, odscll, O3, NOy, NO, NO2, N, N2O, N2O5, mean_age, HOCl, HOBr, HO2, HNO4, HNO3, HCl, HBr, H2O, H2O2, H2, fz, fy, CO, Cly, ClONO2, ClO, Cl2O2, Cl2, Cl, CH4, Bry, BrONO2, BrO, BrCl, Br, accel_divf
SOCOL	zg, wstar, vstar, va, ua, ta, OH, O3, NOy, NO, NO2, N, N2O, N2O5, mean_age, HOCl, HOBr, HO2, HNO4, HNO3, HCl, HBr, H2O, H2O2, H2, fz, fy, CO, Cly, ClONO2, ClO, Cl2O2, Cl2, Cl, CH4, CH3OOH, CH2O, CFCl3, CF2Cl2, CBry, Bry, BrONO2, BrO, BrCl, Br, accel_ogw, accel_nogw, accek_gw, accel_divf
ULAQ	zg, wstar, vstar, va, ua, ta, OH, O3, NOy, NO, NO2, N2O, N2O5, mean_age, HO2, HNO4, HNO3, HCl, HBr, H2O, H2O2, H2, fz, fy, Cly, ClONO2, ClO, CHClF2, CH4, CH3Cl, CH3CCl3, CH3Br, CFCl3, CF2Cl2, CClF2CF3, CClF2CClF2, CCl4, CCl2FCClF2, CBrF3, CBrClF2, Bry, BrO, Br, accel_divf

Table 2.22 continued.

CCM	T2Mz diagnostics
UMSLIMCAT	zg, wstar, wa, vstar, va, ua, ta, OH, OClO, O3, NOy, NO, NO3, NO2, N2O, N2O5, HOCl, HOBr, HO2, HNO4, HNO3, HCl, HBr, H2O, H2O2, fz, fy, divf, CO, Cly, ClONO2, ClO, Cl2O2, CH4, CH3Br, CH2O, CFC-12, CFC-11, Bry, Brx, BrONO2, BrCl
UMETRAC (REF-B1)	zg, ua, ta, O3, NOy, N2O5, N2O, mean_age, HOCl, HOBr, HCl, HBr, H2O, CO, Cly, ClONO2, CH4, CH3OOH, Bry, BrONO2
UMUKCA-METO	zg, wstar, vstar, va, ua, ta, OH, ogw_flux, O3, NOy, NOx, nogw_w_flux, nogw_e_flux, NO, NO2, N, N2O, N2O5, mean_age, HOCl, HOBr, HO2, HNO4, HNO3, HCl, HBr, H2O, fz, fy, CO, Cly, ClONO2, ClO, Cl2O2, Cl, CH4, CH3Br, CH2Br2, CFCl3, Bry, BrONO2, BrO, BrCl, Br, acccel_ogw, accel_nogw, accel_divf
UMUKCA-UCAM	zg, wstar, vstar, va, ua, ta, O3, NOy, N2O, N2O5, mean_age, HNO3, H2O, Cly, ClONO2, CH4, accel_divf
WACCM	zg, wstar, vstar, va, ua, ta, OH, OClO, O3, NOy, NO, NO2, N, N2O, N2O5, mean_age, HOCl, HOBr, HO2, HNO3, HCl, HBr, H2O, H2O2, H2, Cly, ClONO2, ClO, Cl2O2, Cl, CHClF2, CH4, CHCl3, CH3CCl3, CFCl3, CF2Cl2, CCl4, Bry, BrONO2, BrO, BrCl, Br

Table 2.23: Surface and zonal-mean instantaneous (T2Is, T2Iz) diagnostics produced by model, for REF-B2.

CCM	T2Is diagnostics	T2Iz disgnostics
CAM3.5	toz, ta50	
CMAM	zg500, zg100, zg10, va100, va10, ua100, ua10, toz, ta100, ta10, ps	zg, ua, ta
CNRM-ACM	zg500, zg10, zg100, zg1000, vp_840K, vp_460K, va_10, va_100, va_1000, ua_10, ua_100, ua1000, toz, tasmin, tasmax, tas, ta_10, ta_100, ta_1000, ps, clt	zg, va, ua, ta
E39CA (REF-B1)	tas	zg
Niwa-SOCOL (REF-B1)	rsdscs, rsds	
UMSLIMCAT	zg500, zg10, zg100, va10, va100, ua10, ua100, toz, tos, ta10, ta100, snd, rsdscs, rsds, ps, nufl, convclt, clt	zg, va, ua, ta
UMUKCA-METO	zg500, zg10, zg100, zg1000, vorpot_840K, vorpot_460K, va10, va100, va1000, ua10, ua100, ua1000, toz, tasmin, tas-max, tas, ta10, ta100, ta1000, ps, nufl	

prehensive list of diagnostics has been requested (***http://www.pa.op.dlr.de/CCMVal/DataRequests/CCMVal-2_Datarequest_FINAL.pdf***). In particular, the process-oriented validation approach envisaged for CCMVal means that a lot of instantaneous fields have been produced; this class of diagnostics is missing in CCMVal-1. Monthly- and daily-mean diagnostics are given on 31 standard CCMVal-2 levels (1000, 850, 700, 500, 400, 300, 250, 200, 170, 150, 130, 115, 100, 90, 80, 70, 50, 30, 20, 15, 10, 7, 5, 3, 2, 1.5, 1, 0.5, 0.3, 0.2, and 0.1 hPa), whereas 3-dimensional instantaneous fields are given on model levels. In the horizontal, the data are requested on the native model grid. AMTRAC3 data are interpolated onto a regular latitude-longitude grid because of the unusual grid used in this model. The monthly-mean diagnostics fall into the categories T3M (3-dimensional), T2Ms (latitude-longitude), and T2Mz (zonal-mean). Instantaneous diagnostics likewise come in the categories T3I, T2Is, and T2Iz. For the T3I category, to reduce data volume, the diagnostics have been requested for specified periods, namely all years between 1990-2005, every 3-years before 1989, and every three years from 2005. Some diagnostics were requested as daily means (T2Ds, T2Dz). Finally, a few more diagnostics were 1- or 0-dimensional. **Tables 2.20-2.24** list the 3- and 2-dimensional diagnostics. (Note that the database (***ftp://ftp.badc.rl.ac.uk***) is updated frequently, so the reader is referred there for the most up-to-date listing.) CCMVal-1 data has originally been requested in ASCII format. This format is now considered outdated. For CCMVal-2, diagnostic output has been requested in Climate- and Forecast (CF)-compliant NetCDF format (http://www.unidata.ucar.edu/software/netcdf), and the CCMVal-1 data have also

Table 2.24: Daily zonal-mean (T2Dz), and daily surface (T2Ds) diagnostics produced by model, for REF-B2.

CCM	T2Dz diag.	T2Ds diagnostics
AMTRAC3 (REF-B1)	vptp, ua, ta	toz
CCSRNIES	zg, ua, ta	zg500, zg1000, zg100, zg10, vorpot840, vorpot460, va1000, va100, va10, ua1000, ua100, ua10, toz, ta1000, ta100, ta10, ps, nufl
CMAM		tasmin, tasmax, tas, snd, rsdscs, rsds
E39CA (REF-B1)		toz
EMAC (REF-B1)		va100, ua10, toz, tas, ta100
GEOSCCM	zg, ua, ta	zg500, zg1000, zg100, zg10, toz, tas, ta1000, ta100, ta10, ps, clt
LMDZrepro	zg, ua, ta	zg500, zg100, zg10, vorpot840, vorpot480, va100, va10, ua100, ua10, toz, tasmin, tasmax, tas, ta100, ta10, ps, nufl
MRI	zg, ua, ta	va100, va10, ua100, ua10, toz
Niwa-SOCOL (REF-B1)	zg, ua, ta	zg500, vorpot840, vorpot480, va100, va10, ua100, ua10, toz, tas, ta100, ta10, ps
SOCOL	zg, ua, ta	zg500, zg100, zg10, va100, va10, ua100, ua10, toz, tasmin, tasmax, tas, ta100, ta10, snd, rsdscs, rsds, ps, nufl, clt
ULAQ		toz
UMETRAC (REF-B1)		zg500, zg100, zg10, vorpot_840K, vorpot_460K, va100, va10, ua100, ua10, toz, tas, ta100, ta10, snw, rsds, ps, clt
UMUKCA-METO	zg, ua, ta	snw
UMUKCA-UCAM		ua10, toz, ta50
WACCM	zg, ua, ta	ps

been reprocessed into the same format for easier comparison with CCMVal-2. CF also defines the names for meteorological and chemical diagnostics which are generally used in CCMVal-2. See ***http://www.pa.op.dlr.de/CCMVal/DataRequests/CCMVal-2_Datarequest_FINAL.pdf*** for a list of the names of diagnostics listed here.

Special (offline) diagnostics have been requested for the photolysis and radiation chapters, using stand-alone versions of the photolysis and radiation modules used in the models (Chapters 3 and 6).

Acknowledgements

We would like to thank the 7 anonymous reviewers and José Rodriguez for constructive comments.

References

Adcroft, A., J.-M. Campin, C. Hill, and J. Marshall, 2007. Implementation of an atmosphere–ocean general circulation model on the expanded spherical cube, *Mon. Wea. Rev.*, **132**, 2845-2863.

Allen, M., and J. E. Frederick, 1982. Effective photodissociation cross sections for molecular oxygen and nitric oxide in the Schumann-Runge bands, *J. Atmos. Sci.*, **39**, 2066-2075.

Akiyoshi, H., 1997. Development of a global 1-D chemically radiatively coupled model and an introduction to the development of a chemically coupled general circulation model, GGER's supercomputer monograph report, 4, ISSN 1341-4356, 69pp.

Akiyoshi, H., 2000. Modeling of chemistry and chemistry-radiation coupling process for the middle atmosphere and a numerical experiment on CO2 doubling with a 1-D coupled model, *J. Meteorol. Soc. Jpn.*, **78**, 563-584.

Akiyoshi, H., T. Sugita, H. Kanzawa, and N. Kawamoto, 2004. Ozone perturbations in the Arctic summer lower stratosphere as a reflection of NOx chemistry and planetary scale wave activity, *J. Geophys. Res.*, **109**, doi:10.1029/2003JD003632.

Akiyoshi, H., L. B. Zhou, Y. Yamashita, K. Sakamoto, M. Yoshiki, T. Nagashima, M. Takahashi, J. Kurokawa, M. Takigawa, and T. Imamura, 2009. A CCM simulation of the breakup of the Antarctic polar vortex in the years 1980-2004 under the CCMVal scenarios, *J. Geophys. Res.*, **114**, doi:10.1029/2007JD009261.

Alexander, M. J., and T. J. Dunkerton, 1999. A spectral parameterization of mean flow forcing due to breaking gravity waves, *J. Atmos. Sci.*, **56**, 4167-4182.

Andrews, D. G., J. R. Holton, and B. Leovy, 1987. Middle Atmospheric Dynamics, Acad.Press.

Anstey, J. A., T. G. Shepherd, J. F. Scinocca (2010), Influence of the Quasi-Biennial Oscillation on the extratropical winter stratosphere in an atmospheric general circulation model and in reanalysis data. *J. Atmos. Sci.*, in press.

Arakawa, A., and W. H. Schubert, 1974. Interactions of cumulus cloud ensemble with the large-scale environment. Part I, *J. Atmos. Sci.*, **31**, 671-701.

Arora, V. K., G. J. Boer, J. R. Christian, C. L. Curry, K. L. Denman, K. Zahariev, G. M. Flato, J. F. Scinocca, W. J. Merryfield, and W. G. Lee, 2009. The effect of terrestrial photosynthesis down regulation on the twentieth-century carbon budget simulated with the CCCma Earth System model, *J. Clim.*, **22**, 6066-6088.

Austin, J., R. C. Pallister, J. A. Pyle, A. F. Tuck, and A. M. Zavody, 1987. Photochemical model comparisons with LIMS observations in a stratospheric trajectory coordinate system, *Quart. J. Roy. Meteorol. Soc.*, **113**, 361-392.

Austin J., 1991. On the explicit versus family solution of the fully diurnal photochemical equations of the stratosphere, *J. Geophys. Res.*, **96**, 12,941-12,975.

Austin, J., and N. Butchart, 2003. Coupled chemistry-climate model simulations of the period 1980-2020: Ozone depletion and the start of ozone recovery, *Quart. J. Roy. Meteorol. Soc.*, **129**, 3225-3249.

Austin, J. and R.J. Wilson, 2006. Ensemble simulations of the decline and recovery of stratospheric ozone, *J. Geophys. Res.*, **111**, doi: 10.1029/2005JD006907.

Austin, J., J. Wilson, F. Li, and H. Vömel, 2007. Evolution of Water Vapor Concentrations and stratospheric age of air in coupled chemistry-climate model simulations. *J. Atmos. Sci.*, **64**, 905–921.

Bacmeister, J. T., M. J. Suarez, and F. R. Robertson, 2006. Rain re-evaporation, boundary layer convection interactions, and Pacific rainfall patterns in an AGCM. *J. Atmos. Sci.*, **8**, SRef-ID: 1607-7962/gra/EGU06-A-08925.

Baldwin, M. P., L. J. Gray, T. J. Dunkerton, K. Hamilton, P. H. Haynes, W. J. Randel, J. R. Holton, M. J. Alexander, I. Hirota, T. Horinouchi, D. B. A. Jones, J. S. Kinnersley, C. Marquardt, K. Sato, and M. Takahashi, 2001. The Quasi-Biennial Oscillation, *Rev. Geophys.*, **39**, 179–229.

Baumgaertner, A. J. G., P. Jöckel, and C. Brühl, 2009. Energetic particle precipitation in ECHAM5/MESSy1 – Part 1: Downward transport of upper atmospheric NOx produced by low energy electrons, *Atmos. Chem. Phys.*, **9**, 2729-2740.

Bian, H., and M. J. Prather, 2002. Fast-J2: Accurate simulation of stratospheric photolysis in global chemical models, *J. Atmos. Chem.*, **41**, 281-296.

Blitz, M. A., D. E. Heard, M. J. Pilling, S. R. Arnold, and M. P. Chipperfield, 2004. Correction to pressure and temperature-dependent quantum yields for the photodissociation of acetone between 279 and 327.5 nm, *Geophys. Res. Lett.*, **31**, 2.

Bonan, G. B., K. W. Oleson, M. Vertenstein, S. Levis, X. Zeng, Y. Dai, R. E. Dickinson, and Z.-L. Yang (2002), The land surface climatology of the Community Land Model coupled to the NCAR Community Climate Model, *J. Clim.*, **15**, 3123–3149.

Blondin, C. and H. Böttger, 1987. The surface and subsurface parameterisation scheme in the ECMWF forecasting system. Revision and operational assessment of weather elements, *ECMWF Tech. Memo.*, **135**, 48 pp.

Bossuet C., M. Déqué, and D. Cariolle, 1998. Impact of a simple parameterization of convective gravity-wave drag in a stratosphere-troposphere general circulation model and its sensitivity to vertical resolution. *Ann. Geophys.*, **16**, 238-249.

Bougeault, P., 1985. A simple parameterization of the large-scale effects of cumulus convection, *Mon. Wea. Rev.*, **113**, 2108-2121.

Brasseur, G. P., J. J. Orlando, and G. S. Tyndall, 1999. Atmospheric Chemistry and Climate Change, Oxford University Press, 688 pp.

Briegleb, B. P., 1992. Delta-Eddington approximation for solar radiation in the NCAR Community Climate Model, *J. Geophys. Res.*, **97**, 7603-7612.

Brinkop, S., Inclusion of cloud processes in the ECHAM PBL parameterization; In: R. Sausen (Ed.) Studying Climate with the ECHAM Atmospheric Model. Large Scale Atmospheric Modelling, Report No. 9, 5-14, Meteorologisches Institut der Universität

Hamburg, 1991.

Brinkop, S., 1992. Parameterisierung von Grenzschichtwolken für Zirkulationsmodelle; Berichte aus dem Zentrum für Meeres- und Klimaforschung, Reihe A: Meteorologie, Nr. 2, Meteorologisches Institut der Universität Hamburg, 77 pp.

Brinkop, S., and E. Roeckner, 1995. Sensitivity of a general circulation model to parameterizations of cloud-turbulance interactions in the atmospheric boundary layer, *Tellus*, **47A**, 197–220.

Brinkop, S., and R. Sausen, 1997. A modified mass-flux scheme for convection which maintains positive tracer concentrations, *Beitr. Phys. Atmos.*, **70**, 245–248.

Buchholz, J., 2005. Simulations of physics and chemistry of polar stratospheric clouds with a general circulation model, Ph.D. thesis, University of Mainz, Germany, ***http://nbn-resolving.de/urn/resolver.pl?urn=urn:nbn:de:hebis:77-8187***.

Burkholder, J. B., J. J. Orlando, and C. J. Howard, 1990. Ultraviolet absorption cross-sections of Cl2O2, between 210 and 410nm, *J. Phys. Chem.*, **94**, 687-695.

Carslaw, K. S., B. Luo, and T. Peter, 1995. An analytic expression for the composition of aqueous HNO3-H2SO4 stratospheric aerosols including gas phase removal of HNO3, *Geophys. Res. Lett.*, **22**, 1877-1880.

Charron M., and E. Manzini, 2002. Gravity waves from fronts: Parameterization and middle atmosphere response in a general circulation model, *J. Atmos. Sci.*, **59**, 923-941.

Chipperfield, M. P., 1999. Multiannual simulations with a three-dimensional chemical transportmodel. *J. Geophys. Res.*, **104**, 1781-1805.

Chipperfield, M. P., 2006. New version of the TOMCAT/SLIMCAT off-line chemical transport model: Intercomparison of stratospheric tracer experiments, *Quart. J. Roy. Meteorol. Soc.*, **132**, 1179-1203, doi:10.1256/qj.05.51.

Chou, M.-D., M. J. Suarez, C.-H. Ho, M. M.-H. Yan, K.-T. Lee, (1997), Parameterizations for cloud overlapping and short-wave single-scattering properties for use in general circulation and cloud ensemble members, *J. Clim.*, **11**, 202-214.

Chou, M.-D., and M. J. Suarez, 1999. A Solar Radiation Parameterization for Atmospheric Studies, NASA Technical Report Series on Global Monitoring and Data Assimilation, 104606, v15, 40pp.

Chou, M.-D., M. J. Suarez, X. Z. Liang, and M. M.-H. Yan (2001), A thermal infrared radiations parameterization for atmospheric studies. NASA Technical Report Series on Global Monitoring and Data Assimilation, 104606, v19, 56pp.

Collins, W. D., P. J. Rasch, B. A. Boville, J. R. McCaa, D. L. Williamson, J. T. Kiehl, B. P. Briegleb, C. M. Bitz, S.-J. Lin, , M. Zhang, and Y. Dai, 2004. Description of the NCAR community atmosphere model (CAM3.0). Technical Report NCAR/TN-464+STR, National Center for Atmospheric Research, Boulder, CO, USA.

Collins, W. D., P. J. Rasch, B. A. Boville, J. J. Hack, J. R. McCaa, D. L. Williamson, B. P. Briegleb, C. M. Bitz, S.-J. Lin, and M. Zhang, 2006. The formulation and atmospheric simulation of the Community Atmosphere Model: CAM3. *J. Clim.*, **19**, 2122-2161.

Considine, D. B., A. R. Douglass, D. E. Kinnison, P. S. Connell, and D. A. Rotman, 2000. A polar stratospheric cloud parameterization for the three dimensional model of the global modeling initiative and its response to stratospheric aircraft emissions, *J. Geophys. Res.*, **105**, 3955-3975.

Cox, P., R. Betts, C. Bunton, R. Essery, P.R. Rowntree, and J. Smith, 1999. The impact of new land surface physics on the GCM simulation of climate and climate sensitivity. *Clim. Dyn.*, **15**, 183-203.

Cusack S., A. Slingo, J. M. Edwards, and M. Wild, 1998, The radiative impact of a simple aerosol climatology on the Hadley Centre GCM. *Quart. J. Roy. Meteorol. Soc.*, **124**, 2517-2526.

Dameris, M., V. Grewe, M. Ponater, R. Deckert, V. Eyring, F. Mager, S. Matthes, C. Schnadt, A. Stenke, B. Steil, C. Brühl, and M. Giorgetta, 2005. Long-term changes and variability in a transient simulation with a chemistry-climate model employing realistic forcing, *Atmos. Chem. Phys.*, **5**, 2121-2145.

Davies, T, M. J. P. Cullen, A. J. Malcolm, M. H. Mawson, A. Staniforth, A. A. White, and N. Wood, 2005. A new dynamical core for the Met Office's global and regional modelling of the atmosphere. *Quart. J Roy. Meteorol. Soc.*, **131**, 1759-1782.

de Grandpré, J., J. W. Sandilands, J. C. McConnell, S. R. Beagley, P. C. Croteau, and M. Y. Danilin, 1997. Ca-

nadian Middle Atmosphere Model: Preliminary results from the Chemical Transport Module, *Atmos. Ocean*, **35**, 385–431.

deGrandpré, J., S. R. Beagley, V. I. Fomichev, E. Griffioen, J. C. McConnell, A. S. Medvedev and T. G. Shepherd, 2000. Ozone climatology using interactive chemistry: Results from the Canadian Middle Atmosphere Model, *J. Geophys. Res.*, **105**, 26,475-26,491.

DeMore, W. B., Sander, S. P., Golden, D. M., Hampson, R. F., Kurylo, M. J., Howard, C. J., Ravishankara, A. R., Kolb, C. E., and Molina, M. J. (1997), Chemical kinetics and photochemical data for use in stratospheric modeling. Evaluation number 12, JPL Publication 97-4, Jet Propulsion Laboratory, Pasadena, CA, (referred to as JPL, 1997).

Delworth, T. L., A. Rosati, R. J. Stouffer, K. W. Dixon, J. Dunne, K. L. Findell, P. Ginoux, A. Gnanadesikan, C. T. Gordon, S. M. Griffies, R. Gudgel, M. J. Harrison, I. M. Held, R. S. Hemler, L. W. Horowitz, S. A. Klein, T. R. Knutson, S.-J. Lin, V. Ramaswamy, M. D. Schwarzkopf, J. J. Sirutis, M. J. Spelman, W. F. Stern, Michael Winton, A. T. Wittenberg, B. Wyman, A. J. Broccoli, V. Balaji, J. Russell, R. Zhang, J. A. Beesley, Jian Lu, William F. Cooke, J. W. Durachta, A. R. Langenhorst, H.-C. Lee, F. Zeng, K. A. Dunne, P. C. D. Milly, P. J. Kushner, Sergey L. Malyshev, E. Shevliakova, 2006. GFDL's CM2 global coupled climate models – Part 1: Formulation and simulation characteristics, *J. Clim.*, **19**, 643-674.

Déqué, M., 2007. Frequency of precipitation and temperature extremes over France in an anthropogenic scenario: model results and statistical correction according to observed values. *Global and Planetary Change*, **57**, 16-26.

Douglass, A. R., R. B. Rood, S. R. Kawa and D. J. Allen (1997), A three-dimensional simulation of the evolution of middle latitude winter ozone in the middle stratosphere, *J. Geophys. Res.*, **102**, 19,217-19,232.

Douglass, A. R., and S. R. Kawa, 1999. Contrast between 1992 and 1997 high-latitude spring Halogen Occultation Experiment observations of lower stratospheric HCl, *J. Geophys. Res.*, **104**, 18,739-18,754.

Douville H., S. Planton, J. F. Royer, D. B. Stephenson, S. Tyteca, L. Kergoat, S. Lafont, and R. A. Betts, 2000. Importance of vegetation feedbacks in doubled-CO2 climate experiments, *J. Geophys. Res.*, **105**, 14841-14861.

Dufresne, J.-L., J. Quaas, O. Boucher, F. Denvil, and L. Fairhead, 2005. Contrasts in the effects on climate of anthropogenic sulfate aerosols between the 20th and the 21st century, *Geophys. Res. Lett.,* **32**, doi: 10.1029/2005GL023619.

Dümenil, L., and E. Todini, 1992. A rainfall-runoff scheme for use in the Hamburg climate model, in: Advances in Theoretical Hydrology, A Tribute to James Dooge, edited by Kane, J. O., European Geophysical Society Series on Hydrological Sciences, pp. 129–157. Elsevier, Amsterdam.

Edwards, J.M. and A. Slingo, 1996. Studies with a flexible new radiation code. I: Choosing a configuration for a large scale model. *Quart. J. Roy. Meteorol. Soc.*, **122**, 689-719.

Egorova,T., E. Rozanov, V. Zubov, and I. Karol, 2003. Model for investigating ozone trends, Isv. *Atm. Ocean. Phys.*, **39**, 277-292.

Egorova T, E. Rozanov, E. Manzini, M. Haberreiter, W. Schmutz, V. Zubov, and T. Peter, 2004. Chemical and dynamical response to the 11-year variability of the solar irradiance simulated with a chemistry-climate model, *Geophys. Res. Lett.*, **31**, L06119.

Egorova, T., E. Rozanov, V. Zubov, E. Manzini, W. Schmutz, and T. Peter, 2005. Chemistry-climate model SOCOL: a validation of the present-day climatology, *Atm. Chem. Phys.*, **5**, 1557-1576.

Eluszkiewicz, J., R. S. Hemler, J. D. Mahlman, L. Bruhwiler and L. L. Takacs, 2000 Sensitivity of age-of-air calculations to the choice of advection scheme. *J. Atmos. Sci.*, **57**, 3185-3201.

Eyring, V., N. Butchart, D. W. Waugh, H. Akiyoshi, J. Austin, S. Bekki, G. E. Bodeker, B. A. Boville, C. Brühl, M. P. Chipperfield, E. Cordero, M. Dameris, M. Deushi, V. E. Fioletov, S. M. Frith, R. R. Garcia, A. Gettelman, M. A. Giorgetta, V. Grewe, L. Jourdain, D. E. Kinnison, E. Mancini, E. Manzini, M. Marchand, D. R. Marsh, T. Nagashima, P. A. Newman, J. E. Nielsen, S. Pawson, G. Pitari, D. A. Plummer, E. Rozanov, M. Schraner, T. G. Shepherd, K. Shibata, R. S. Stolarski, H. Struthers, W. Tian, and M. Yoshiki, 2006. Assessment of temperature, trace species and ozone in chemistry-climate model simulations of the recent past, *J. Geophys. Res.*, **111**, doi:10.1029/2006JD007327.

Eyring, V., D. W. Waugh, G. E. Bodeker, E. Cordero, H. Akiyoshi, J. Austin, S. R. Beagley, B. Boville, P. Braesicke, C. Brühl, N. Butchart, M. P. Chipperfield, M. Dameris, R. Deckert, M. Deushi, S. M. Frith, R. R. Garcia, A. Gettelman, M. Giorgetta, D. E. Kinnison, E. Mancini, E. Manzini, D. R. Marsh, S. Matthes, T. Nagashima, P. A. Newman, J. E. Nielsen, S. Pawson, G. Pitari, D. A. Plummer, E. Rozanov, M. Schraner, J. F. Scinocca, K. Semeniuk, T. G. Shepherd, K. Shibata, B. Steil, R. Stolarski, W. Tian, and M. Yoshiki, 2007. Multimodel projections of stratospheric ozone in the 21st century, *J. Geophys. Res.*, **112**, doi:10.1029/2006JD008332.

Eyring, V., M. P. Chipperfield, M. A. Giorgetta, D. E. Kinnison, E. Manzini, K. Matthes, P. A. Newman, S. Pawson, T. G. Shepherd, and D. W. Waugh (2008), Overview of the New CCMVal Reference and Sensitivity Simulations in Support of Upcoming Ozone and Climate Assessments and the Planned SPARC CCMVal Report, *SPARC Newsletter No. 30*, 20-26.

Farman, J. C., B. G. Gardiner, and J. D. Shanklin (1985), Large losses of total ozone in Antarctica reveal seasonal ClOx/NOx interaction, *Nature*, **315**, 207–210.

Fischer, A. M., M. Schraner, E. Rozanov, P. Kenzelmann, C. S. Poberaj, D. Brunner, A. Lustenberger, B. P. Luo, G. E. Bodeker, T. Egorova, W. Schmutz, T. Peter, and S. Brönnimann, 2008. Interannual-to-decadal variability of the stratosphere during the 20th century: Ensemble simulations with a chemistry-climate model. *Atmos. Chem. Phys.*, **8**, 7755-7777.

Fomichev, V. I., J. P. Blanchet, and D. S. Turner, 1998. Matrix parameterization of the 15 μm CO2 band cooling in the middle and upper atmosphere for variable CO2 concentration, *J. Geophys. Res.*, **103**, 11505–11528.

Fomichev, V. I., C. Fu, J. de Grandpré, S. R. Beagley, V. P. Ogibalov, and J. C. McConnell, 2004. Model thermal response to minor radiative energy sources and sinks in the middle atmosphere, *J. Geophys. Res.*, **109**, doi:10.1029/2004JD004892.

Fouquart, Y. and B. Bonnel, 1980. Computations of solar heating of the Earth's atmosphere: A new parameterization, *Beitr. Phys. Atmos.*, **53**, 35–62.

Garcia, R. R. and B. A. Boville, 1994. Downward control of the mean meridional circulation and temperature distribution of the polar winter stratosphere, *J. Atmos. Sci.*, **51**, 2238–2245.

Garcia, R. R., D. Marsh, D. E. Kinnison, B. Boville, and F. Sassi, 2007. Simulations of secular trends in the middle atmosphere, 1950-2003, *J. Geophys. Res.*, **112**, doi:10.1029/2006JD007485.

Garny, H., M. Dameris, and A. Stenke, 2009. Impact of prescribed SSTs on climatologies and long-term trends in CCM simulations, *Atmos. Chem. Phys.*, **9**, 6017-6031.

Gent, P. R., F. O. Bryan, G. Danabasoglu, S. C. Doney, W. R. Holland, W. G. Large, and J. C. McWilliams, 1998. The NCAR Climate System Model global ocean component, *J. Clim.*, **11**,1287-1306.

Gent, P. R., S. G. Yeager, R. B. Neale, S. Levis, and D. A. Bailey, 2009. Improvements in a half degree atmosphere/land version of the CCSM, *Clim. Dyn.*, in press, doi:10.1007/s00382-009-0614-8

Giorgetta, M. A., 1996. Der Einfluss der quasi-zweijährigen Oszillation: Modellrechnungen mit ECHAM4, Max-Planck-Institut für Meteorologie, Hamburg, Examensarbeit Nr. 40, MPI-Report 218.

Giorgetta, M., and L. Bengtsson, 1999. Potential role of the Quasi-Biennial Oscillation in the stratosphere-troposphere exchange as found in water vapor in general circulation model experiments, *J. Geophys. Res.*, **104**, 6003-6019.

Giorgetta, M. A., E. Manzini, and E. Roeckner (2002), Forcing of the Quasi-Biennial Oscillation from a broad spectrum of atmospheric waves, *Geophys. Res. Lett.*, **29**, doi:10.1029/2002GL014756.

Giorgetta, M. A., E. Manzini, E. Roeckner, M. Esch, and L. Bengtsson, 2006. Climatology and forcing of the quasi-biennial oscillation in the MAECHAM5 model, *J. Clim.*, **19**, 3882-3901.

Global Carbon Budget, 2009. Carbon budget and trends 2008. ***www.globalcarbonproject.org/carbonbudget***, released on 17 November 2009.

Gregory, D., R. Kershaw, and P. M. Inness, 1997. Parametrization of momentum transport by convection. II: Tests in single column and general circulation models. *Quart. J. Roy. Meteorol. Soc.*, **123**, 1153-1183.

Gregory, D., G. J. Shutts, and J. R. Mitchell, 1998. A new gravity wave drag scheme incorporating anisotropic orography and low level wave breaking: Impact upon the climate of the UK Meteorological Office Unified Model. *Quart. J. Roy. Meteorol. Soc.*, **124**, 463-493.

Gregory, A. R., and V. West, 2002. The sensitivity of a

model's stratospheric tape recorder to the choice of advection scheme. *Quart. J. Roy. Meteorol. Soc.*, **128**, 1827-1846.

Grewe, V., D. Brunner, M. Dameris, J. Grenfell, R. Hein, D. Shindell, J. Staehelin, 2001. Origin and variability of upper tropospheric nitrogen oxides and ozone at northern mid-latitudes, *Atmos. Env.*, **35**, 3421-3433.

Hack, J. J., 1994. Parameterization of moist convection in the NCAR community climate model (CCM2), *J. Geophys. Res.*, **99**, 5551-5568.

Hansen, J., M. Sato, L. Nazarenko, R. Ruedy, A. Lacis, D. Koch, I. Tegen, T. Hall, D. Shindell, B. Santer, P. Stone, T. Novakov, L. Thomason, R. Wang, Y. Wang, D. Yacob, S. Hollandsworth, L. Bishop, J. Logan, A. Thompson, R. Stolarski, J. Lean, R. Willson, S. Levitus, J. Antonov, N. Rayner, D. Parker, and J. Christy, 2002. Climate forcings in Goddard Institute for Space Studies SI2000 simulations, *J. Geophys. Res.*, **107**, 4347, doi:10.1029/2001JD001143.

Hines, C. O., 1997a. Doppler spread parameterization of gravity wave momentum deposition in the middle atmosphere. Part I: Basic formulation. *J. Atmos. Solar Terr. Phys.*, **59**, 371–386.

Hines, C. O., 1997b. Doppler spread parameterization of gravity wave momentum deposition in the middle atmosphere. Part II: Broad and quasi monochromatic spectra and implementation. *J. Atmos. Solar Terr. Phys.*, **59**, 387–400.

Hitchcock, P., T. G. Shepherd and C. McLandress, 2009. Past and future conditions for polar stratospheric cloud formation in the Canadian Middle Atmosphere Model. *Atmos. Chem. Phys.*, **9**, 483-495.

Holstag, A., and B. A. Boville, 1993. Local versus nonlocal boundary-layer diffusion in a global climate model, *J. Clim.*, **6**, 1825-1842.

Holton, J. R., 1992. An Introduction to Dynamical Meteorology, 3rd ed., Academic Press, San Diego, CA, 511pp.

Horinouchi, T., S. Pawson, K. Shibata, U. Langematz, E. Manzini, M. A. Giorgetta, F. Sassi, R. J. Wilson, K. Hamilton, J. de Grandpré, and A. A. Scaife, 2003. Tropical Cumulus Convection and Upward-Propagating Waves in Middle-Atmospheric GCMs, *J. Atmos. Sci.*, **60**, 2765–2782.

Hough, A. M., 1991. Development of a 2-dimensional global tropospheric model - Model chemistry, *J. Geophys. Res.*, **96**, 7325-7362.

Hourdin, F., and A. Armengaud, 1999. The use of finite-volume methods for atmospheric advection trace species: 1. Tests of various formulations in a general circulation model, *Mon. Weather Rev.*, **127**, 822–837.

Hourdin, F., I. Musat, S. Bony, P. Braconnot, F. Codron, J. L. Dufresne, L. Fairhead, M. A. Filiberti, P. Friedlingstein, J. Y. Grandpeix, G. Krinner, P. Levan, Z. X. Li and F. Lott, 2006. The LMDZ4 general circulation model: Climate performance and sensitivity to parametrized physics with emphasis on tropical convection, *Clim. Dyn.*, **27**, 787-813.

Hoyle, C. R., 2005. Three dimensional chemical transport model study of ozone and related gases 1960–2000, ETH Zürich, Dissertation No. 16271.

Intergovernmental Panel on Climate Change (IPCC) (2001), Climate Change 2001, The Scientific Basis, J. T. Houghton et al. (editors), Cambridge University Press, Cambridge UK and New York, USA, 881 pp.

IPCC, 2007: Climate Change 2007: The Physical Science Basis. Contribution of Working Group I to the Fourth Assessment Report of the Intergovernmental Panel on Climate Change [Solomon, S., D. Qin, M. Manning, Z. Chen, M. Marquis, K.B. Averyt, M.Tignor and H.L. Miller (eds.)]. Cambridge University Press, Cambridge, United Kingdom and New York, NY, USA, 996 pp.

International Union of Pure and Applied Chemistry (IUPAC) (various years), Evaluated kinetic data, ***http://www.iupac-kinetic.ch.cam.ac.uk/index.html***.

Iwasaki, T., S. Yamada, and K. Tada, 1989. A parameterization scheme of orographic gravity wave drag with the different vertical partitioning, part 1: Impact on medium range forecasts. *J. Meteor. Soc. Japan*, **67**, 11-41.

Jackman, C. H., E. L. Fleming, S. Chandra, D. B. Considine, and J. E. Rosenfield, 1996. Past, present, and future modeled ozone trends with comparisons to observed trends, *J. Geophys. Res.*, **101**, doi:10.1029/96JD00577.

Jacobson, M. Z., 1999. Fundamentals of Atmospheric Modeling, Cambridge Univ. Press, 656pp.

Jöckel, P., R. von Kuhlmann, M. G. Lawrence, B. Steil, C. A. M. Brenninkmeijer, P. J. Crutzen, P. J. Rasch, and B. Eaton, 2001. On a fundamental problem in implementing flux-form advection schemes for trac-

er transport in 3-dimensional general circulation and chemistry transport models. *Quart. J. Roy. Meteorol. Soc.*, **127**, 1035-1052.

Jöckel, P., H. Tost, A. Pozzer, C. Brühl, J. Buchholz, L. Ganzeveld, P. Hoor, A. Kerkweg, M. G. Lawrence, R. Sander, B. Steil, G. Stiller, M. Tanarhte, D. Taraborrelli, J. van Aardenne, and J. Lelieveld, 2006. The atmospheric chemistry general circulation model ECHAM5/MESSy1: Consistent simulation of ozone from the surface to the mesosphere, *Atmos. Chem. Phys.*, **6**, 5067– 5104.

Johns, T. C., C. F. Durman, H. T. Banks, M. J. Roberts, A. J. McLaren, J. K. Ridley, C. A. Senior, K. D. Williams, A. Jones, G. J. Rickard, S. Cusack, W. J. Ingram, M. Crucifix, D. M. H. Sexton, M. M. Joshi, B.-W. Dong, H. Spencer, R. S. R. Hill, J. M. Gregory, A. B. Keen, A. K. Pardaens, J. A. Lowe, A. Bodas-Salcedo, S. Stark, and Y. Searl, 2006. The new Hadley Centre climate model HadGEM1: Evaluation of coupled simulations, *J. Clim.*, **19**, 1327–1353.

Jonsson, A. I., V. I. Fomichev, and T. G. Shepherd, 2009. The effect of nonlinearity in CO2 heating rates on the attribution of stratospheric ozone and temperature changes, Atmos. Chem. Phys, 9, 8447-8452.

Jourdain, L., S. Bekki, F. Lott, and F. Lefèvre, 2008. The coupled chemistry-climate model LMDz-REPROBUS: description and evaluation of a transient simulation of the period 1980–1999, *Ann. Geophys.*, **26**, 1391-1413.

Kanae, S., K. Nishio, T. Oki, and K. Musiake, 1995. Hydrograph estimation by flow routing modeling from AGCM output in major basins of the world, *Proceedings of Hydraulic Engineering*, **39**, 97-102 (in Japanese with English abstract).

Kärcher, B, and U. Lohmann, 2001. The parameterization of cirrus cloud formation: homogeneous freezing of supercooled aerosols, *J. Geophys. Res.*, **108**, 4402-4415.

Kawa, S. R., R. M. Bevilacqua, J. J. Margitan, A. R. Douglass, M. R. Schoeberl, K. W. Hoppel, and B. Sen, 2002. Interaction between dynamics and chemistry of ozone in the setup phase of the Northern Hemisphere polar vortex, *J. Geophys. Res.*, **107**, doi:10.1029/2001JD001527.

Kinnison, D. E., G. P. Brasseur, S. Walters, R. R. Garcia, F. Sassi, B. A. Boville, D. Marsh, L. Harvey, C. Randall, W. Randel, J. F. Lamarque, L. K. Emmons, P. Hess, J. Orlando, J. Tyndall, and L. Pan, 2007. Sensitivity of chemical tracers to meteorological parameters in the MOZART-3 chemical transport model, *J. Geophys. Res.*, **112**, doi:10.1029/2006JD007879.

Kockarts, G. (1980), Nitric oxide cooling in the terrestrial thermosphere, *Geophys. Res. Lett.*, **7**, 137–140.

Koepke, P., M. Hess, I. Schult, and E. P. Shettle, 1997. Global Aerosol Data Set, Report No. 243, Max-Planck-Institut für Meteorologie, Hamburg, ISSN 0937-1060.

Koppers, G. A. A., and D. P. Murtagh, 1996. Model studies of the influence of O2 photodissociation parameterizations in the Schumann-Runge bands on ozone related photolysis in the upper atmosphere, *Ann. Geophys.*, **14**, 68-79.

Koshyk, J. N. and G. J. Boer, 1995. Parameterization of dynamical subgrid-scale processes in a spectral GCM, *J. Atmos. Sci.*, **52**, 965-976.

Koster, R. D., M. J. Suarez, A. Ducharne, M. Stieglitz, and P. Kumar, 2000. A catchment-based approach to modeling land surface processes in a general circulation model: 1. Model structure, *J. Geophys. Res.*, **105**, 24,809-24,822.

Kraus, E. B., and J. S. Turner, 1967. A one dimensional model of the seasonal thermocline. Part II, *Tellus*, **19**, 98-105.

Kurokawa, J., H. Akiyoshi, T. Nagashima, H. Masunaga, T. Nagajima, M. Takahashi, and H. Nakane, 2005. Effects of atmospheric sphericity on stratospheric chemistry and dynamics over Antarctica, *J. Geophys. Res.*, **110**, doi:10.1029/2005JD005798.

Lacis, A., J. E. Hansen, and M. Sato, 1992. Climate forcing by stratospheric aerosols, *Geophys. Res. Lett.*, **19**, 1607-1610.

Land, C., J. Feichter, and R. Sausen, 2002. Impact of vertical resolution on the transport of passive tracers in the ECHAM4 model, *Tellus*, **54B**, 344-360.

Lamarque J.-F., D. E. Kinnison, P. G. Hess, and F. M. Vitt, 2008. Simulated lower stratospheric trends between 1970 and 2005: Identifying the role of climate and composition changes, *J. Geophys. Res.*, **113**, doi:10.1029/2007JD009277.

Landgraf, J., and P. J. Crutzen, 1998 An efficient method for online calculations of photolysis and heating rates. *J. Atmos. Sci.* **55**, 863-878.

Lanser, D., J. G. Blom and J. G. Verwer, 2000. Spatial discretization of the shallow water equations in spherical geometry using Osher's Scheme, *J. Comp. Phys.*, **165**, 542-565.

Lary, D. and J. A. Pyle, 1991. Diffuse-radiation, twilight, and photochemistry. 1., *J. Atmos. Chem.*, **13**, 393–406.

Lawrence, M. G., R. von Kuhlmann, M. Salzmann, and P. J. Rasch, 2003. The balance of effects of deep convective mixing on tropospheric ozone, *Geophys. Res. Lett.*, **30**, doi:10.1029/2003GL017644.

Lean, J. L., G. J. Rottman, H. L. Kyle, T. N. Woods, J. R. Hickey, and L. C. Puga, 1997. Detection and parameterization of variations in solar mid and near ultraviolet radiation (200 to 400 nm), *J. Geophys. Res.*, **102**, 29,939-29,956.

Lean, J., G. Rottman, J. Harder, and G. Kopp, 2005. Source contributions to new understanding of global change and solar variability, *Solar Phys.,* **230**, 27–53.

Lefèvre, F., G. P. Brasseur, I. Folkins, A. K. Smith, and P. Simon, 1994. Chemistry of the 1991-1992 stratospheric winter: Three-dimensional model simulations, *J. Geophys. Res.*, **99**, 8183-8195.

Lefèvre, F., F. Figarol, K. S. Carslaw, and T. Peter, 1998. The 1997 Arctic ozone depletion quantified from three-dimensional model simulations, *Geophys. Res. Lett.*, **25**, 2425-2428, 10.1029/98GL51812.

Le Quéré, C., M. R. Raupach, J. G. Canadell, G. Marland, L. Bopp, P. Ciais, T. J. Conway, S. C. Doney, R. A. Feely, P. Foster, P. Friedlingstein, K. Gurney, R. A. Houghton, J. I. House, C. Huntingford, P. E. Levy, M. R. Lomas, J. Majkut, N. Metzl, J. P. Ometto, G. P. Peters, I. C. Prentice, J. T. Randerson, S. W. Running, J. L. Sarmiento, U. Schuster1, S. Sitch, T. Takahashi, N. Viovy, G. R. van der Werf, F. I. Woodward, 2009. Trends in the sources and sinks of carbon dioxide. *Nature Geosci.*, **2**, 831 - 836 doi: 10.1038/ngeo689.

Le Treut, H. and Z.-X. Li, 1991. Sensitivity of an atmospheric general circulation model to prescribed SST changes: feedback effects associated with the simulation of cloud optical properties, *Clim. Dyn.*, **5**, 175-187.

Lin, S.-J., and R. Rood, 1996. Multi-dimensional flux-form semi-Lagrangian transport schemes, *Mon. Wea. Rev.*, **124**, 2046–2070.

Lin, S.-J., and R. B. Rood, 1997. An explicit flux-form semi-Lagrangian shallow water model on the sphere, *Quart. J. Roy. Meteorol. Soc.*, **123**, 2477-2498.

Lin, S.-J. (2004), A "vertically Lagrangian" finite volume dynamical core for global models. *Mon. Wea. Rev.*, **132**, 2293–2307.

Logan, J. A., 1999. An analysis of ozonesonde data for the troposphere: Recommendations for testing 3-D models and development of a gridded climatology for tropospheric ozone, *J. Geophys. Res.*, **104**, 16115-16150.

Lock, A. P., A. R. Brown, M. R. Bush, G. M. Martin, and R. N. B. Smith, 2000. A new boundary layer mixing scheme. Part 1: Scheme description and single-column model tests. *Mon. Wea. Rev.*, **138**, 3187-3199.

Lott, F. and M. J. Miller, 1997. A new-subgrid-scale orographic drag parameterization: Its formulation and testing. *Quart. J. Roy. Meteor. Soc.*, **123**, 101–12.

Lott, F., 1999. Alleviation of stationary biases in a GCM through a mountain drag parameterization scheme and a simple representation of mountain lift forces. *Mon. Wea. Rev.*, **127**, 788–801.

Lott, F., L. Fairhead, F. Hourdin and P. Levan, 2005. The stratospheric version of LMDz: Dynamical climatologies, Arctic Oscillation, and impact on the surface climate. *Clim. Dyn.*, **25**, 851–868, doi: 10.1007/s00382-005-0064.

Louis, J., 1979. A parametric model of vertical eddy fluxes in the atmosphere, *Bound. Layer Meteor.*, **17**, 187-202.

Louis, J., M. Tiedtke, and J. Geleyn, 1982. A short history of the PBL parameterization at ECMWF. Proc. ECMWF Workshop on Planetary Boundary Layer Paramerization, Reading, United Kingdom, ECMWF, 59-80.

Madronich, S., and S. Flocke, 1998. The role of solar radiation in atmospheric chemistry, pp. 1-26, Springer-Verlag, New York.

Manabe, S., J. Smagorinski, and R. F. Strickler, 1965. Simulated climatology of a general circulation model with a hydrologic cycle, *Mon. Wea. Rev.*, **93**, 769-798.

Manzini, E., N. A. McFarlane, and C. McLandress, 1997. Impact of the Doppler spread parameterization on the simulation of the middle atmosphere circulation using the MA/ECHAM4 general circulation model, *J. Geophys. Res.*, **102**, 25,751–25,762.

Manzini, E., and N. McFarlane, 1998. The effect of varying the source spectrum of a gravity wave parameterization in the middle atmosphere general circulation model, *J. Geophys. Res.*, **103**, 31,523–31,539.

Marsh, D. R., R. R. Garcia, D. E. Kinnison, B. A. Boville, S. Walters, K. Matthes, and S.C. Solomon, 2007. Modeling the whole atmosphere response to solar cycle changes in radiative and geomagnetic forcing, *J. Geophys. Res.*, **112**, doi:10.1029/2006JD008306.

Martin, G. M., M. R. Bush, A. R. Brown, A. P. Lock, and R. N. B. Smith, 2000. A new boundary layer mixing scheme. Part II: Tests in climate and mesoscale models. *Mon. Wea. Rev.*, **128**, 3200-3217.

Martin, G. M., M. A. Ringer, V. D. Pope, A. Jones, C. Dearden, and T. J. Hinton, 2006. The physical properties of the atmosphere in the new Hadley Centre Global Environment Model (HadGEM1). Part I: Model description and global climatology. *J. Clim.*, **19**, 1274-1301.

Mascart P., J. Noilhan, and H. Giordani, 1995. A modified parameterization of flux profile relationships in the surface layer using different roughness length values for heat and momentum. *Bound. Layer Meteorol.*, **72**, 331-344.

McCalpin, J. D., 1988. A quantitative analysis of the dissipation inherent in semi-Lagrangian advection, *Mon. Wea. Rev.*, **116**, 2330-2336.

McIntyre, M. E., 1995. The stratospheric polar vortex and sub-vortex: fluid dynamics and midlatitude ozone loss, *Phil. Trans. Roy. Soc.*, **352**, 227-240.

McFarlane, N. A., 1987. The effect of orographically excited gravity wave drag on the general circulation of the lower stratosphere and troposphere, *J. Atmos. Sci.*, **44**, 1775 – 1800.

McLandress, C., 2002. Interannual variations of the diurnal tide in the mesosphere induced by a zonal-mean wind oscillation in the tropics, *Geophys. Res. Lett.*, **29**, doi:10.1029/2001GL014551.

McLandress, C., and J. F. Scinocca, 2005. The GCM response to current parameterizations of non-orographic gravity wave drag, *J. Atmos. Sci.*, **42**, 2394-2413.

Mellor, G. L., and T. Yamada, 1974. A hierarchy of turbulence closure models for planetary boundary layers. *J. Atmos. Sci.*, **31**, 1791-1806.

Miller, M. J., T. N. Palmer, and R. Swinbank, 1989. Parameterization and influence of sub-grid scale orography in general circulation and numerical weather prediction models, *Meteorol. Atmos. Phys.*, **40**, 84–109.

Mlawer, E. J. S. Taubman, P. Brown, M. Iacono, and S. Clough, 1997. Radiative transfer for inhomogeneous atmospheres: RRTM, a validated correlated-k model for the longwave. *J. Geophys. Res.*, **102**, 16,663-16,682.

Molina, M. J., and F. S. Rowland, 1974. Stratospheric sink for chlorofluoromethanes — Chlorine atomic-catalyzed destruction of ozone, *Nature*, **249**, 810–812.

Moorthi, S., and M. J. Suarez, 1992. Relaxed Arakawa-Schubert: A parameterization of moist convection for general circulation models, *Mon. Wea. Rev.*, **120**, 978-1002.

Morcrette, J.-J., 1989. Description of the radiative scheme in the ECMWF model, Technical Report, No. 260165, ECMWF, Reading, United Kingdom, 26 pp.

Morcrette, J.-J., 1990. Impact of changes to the radiation transfer parameterizations plus cloud optical properties in the ECMWF model. *Mon. Wea. Rev.*, **118**, 847-873.

Morcrette, J.-J., 1991. Radiation and cloud radiative properties in the ECMWF operational weather forecast model, *J. Geophys. Res.*, **96**, 9121– 9132.

Morgenstern, O., P. Braesicke, M. M. Hurwitz, F. M. O'Connor, A. C. Bushell, C. E. Johnson, and J. A. Pyle, 2008. The World Avoided by the Montreal Protocol, *Geophys. Res. Lett.*, **35**, doi: 10.1029/2008GL034590.

Morgenstern, O., P. Braesicke, F. M. O'Connor, A. C. Bushell, C. E. Johnson, S. M. Osprey, and J. A. Pyle, 2009. Evaluation of the new UKCA climate-composition model. Part 1: The stratosphere. *Geosci. Model Dev.*, **1**, 43-57.

Morgenstern, O., M. A. Giorgetta, K. Shibata, V. Eyring, D. W. Waugh, T. G. Shepherd, H. Akiyoshi, J. Austin, A. J. G. Baumgaertner, S. Bekki, P. Braesicke, C. Brühl, M. P. Chipperfield, D. Cugnet, M. Dameris, S. Dhomse, S. M. Frith, H. Garny, A. Gettelman, S. C. Hardiman, M. I. Hegglin, P. Jöckel, D. E. Kinnison, J.-F. Lamarque, E. Mancini, E. Manzini, M. Marchand, M. Michou, T. Nakamura, J. E. Nielsen, D. Olivié, G. Pitari, D. A. Plummer, E. Rozanov, J. F. Scinocca, D. Smale, H. Teyssèdre, M. Toohey, W. Tian, Y. Yamashita, 2010. Review of the formulation of present-generation stratospheric chemistry-

climate models and associated external forcings, *J. Geophys. Res.*, in press.

Mote, P. W., K. H. Rosenlof, M. E. Mclntyre, E. S. Carr, J. C. Gille, J. R. Holton, J. S. Kinnersley, H. C. Pumphrey, J. M. Russell, and J. W. Waters, 1996. An atmospheric tape recorder: The imprint of tropical tropopause temperatures on stratospheric water vapor, *J. Geophys. Res.*, **101**, 3989-4006.

Müller, J.-F., and G. Brasseur, 1995. IMAGES: A three dimensional chemical transport model of the global troposphere, *J. Geophys. Res.*, **100**, 16,445-16,490.

Nissen, K. M., K. Matthes, U. Langematz, and B. Mayer, 2007. Towards a better representation of the solar cycle in general circulationmodels, *Atmos. Chem. Phys.*, **7**, 5391–5400.

Nagashima, T., M. Takahashi, M. Takigawa, and H. Akiyoshi, 2002. Future development of the ozone layer calculated by a general circulation model with fully interactive chemistry, *Geophys. Res. Lett.*, **29**, doi:10.1029/2001GL014026.

Nakajima, T., and M. Tanaka, 1986. Matrix formulation for the transfer of solar radiation in a plane-parallel scattering atmosphere, *J. Quant. Spectrosc. Radiat. Transfer,* **35**, 13-21.

Nakajima, T., M. Tsukamoto, Y. Tsuhima, A. Numaguti, and T. Kimura, 2000. Modeling of the radiative process in an atmospheric general circulation model, *Appl. Opt.*, **39**, 4869-4878.

NASA, 1993. The atmospheric effects of stratospheric aircraft: Report of the 1992 Models and Measurements Workshop, NASA Publ. 1292.

Neale, R. B., J. H. Richter and M. Jochum, 2008. The impact of convection on ENSO: From a delayed oscillator to a series of events, *J. Clim.*, **21**, 5904-5924.

Noilhan, J. and S. Planton, 1989. A simple parameterization of land surface processes for meteorological models. *Mon. Wea. Rev.*, **117**, 536-549.

Nozawa, T., T. Nagashima, T. Ogura, T. Yokohata, N. Okada, and H. Shiogama, 2007. Climate change simulations with a coupled ocean-atmosphere GCM called the model for interdisciplinary research on climate: MIROC, CGER's supercomputer monograph report, 12, ISSN 1341-4356, 79pp.

Numaguti, A., 1993. Dynamics and energy balance of the Hadley circulation and the tropical precipitation zones: Significance of the distribution of evaporation, *J. Atmos. Sci.*, **50**, 1874–1887.

Numaguti, A., M. Takahashi, T. Nakajima, and A. Sumi, 1995. Development of an atmospheric general circulation model, in *Reports of a New Program for Creative Basic Research Studies, Studies of Global Environment Change to Asia and Pacific Regions*, Rep. I-3, pp. 1 – 27, CCSR, Tokyo.

Numaguti, A., S. Sugata, M. Takahashi, T. Nakajima, A. Sumi, 1997. Study on the climate system and mass transport by a climate model, *CGER's supercomputer monograph report*, **3**, CGER-I025-'97, NIES, Tsukuba, Japan, 91pp.

Olivier, J., et al., 2005. Recent trends in global greenhouse gas emissions: regional trends and spatial distribution of key sources, In: "Non-CO2 Greenhouse Gases (NCGG-4)", van Amstel, A. (coord.), 325-330, Millpress, Rotterdam, ISBN 90 5966 043 9.

Pawson, S., R. S. Stolarski, A. R. Douglass, P. A. Newman, J. E. Nielsen, S. M. Frith, and M. L. Gupta, 2008. Goddard Earth Observing System chemistry-climate model simulations of stratospheric ozone-temperature coupling between 1950 and 2005, *J. Geophys. Res.*, **113**, doi:10.1029/2007JD009511.

Phillips, V. T., and L. J. Donner, 2006. Cloud microphysics, radiation and vertical velocities in two- and three-dimensional simulations of deep convection, *Quart. J. Roy. Meteorol. Soc.*, **132**, doi:10.1256/qj05.171.

Pierrehumbert, R.T., 1986. An essay on the parameterization of orographic gravity wave drag. Proc. ECMWF 1986 Seminar, Vol. I, Reading, U.K., ECMWF, 251-282.

Pitari, G., 1993. A numerical study of the possible perturbation of stratospheric dynamics due to Pinatubo aerosols: Implications for tracer transport, *J. Atmos. Sci.*, **50**, 2443-2461.

Pitari G., E. Mancini, V. Rizi and D. T. Shindell, 2002. Impact of future climate and emission changes on stratospheric aerosols and ozone, *J. Atmos. Sci.*, **59**.

Price, C., and D. Rind, 1992. A simple parameterization for calculating global lightning distributions, *J. Geophys. Res.*, **97**, 9919-9933.

Price, C., and D. Rind, 1994. Modeling global lightning distributions in a general-circulation model, *Mon. Wea, Rev.*, **122**, 1930-1.

Priestley, A., 1993. A quasi-conservative version of the semi-Lagrangian advection scheme, *Mon. Wea. Rev.*,

121, 621-629. doi:10.1175/1520-0493.

Putman, W. M., and S.-J. Lin, 2007. Finite-volume transport on various cubed-sphere grids, *J. Comp. Phys.*, **227**, 55-78.

Ramaroson, R., M. Pirre, and D. Cariolle, 1992. A box model for online computations of diurnal variations in a 1-D model – Potential for ap*plication in multidimensional cases,* Ann. Geophys., **10**, 416-428.

Rasch, P. J., N. M. Mahowald, and B. E. Eaton, 1997. Representations of transport, convection, and the hydrological cycle in chemical transport models: Implications for the modeling of short-lived and soluble species, *J. Geophys. Res.*, **102**, 28,127-28,138.

Rasch, P. J., and J. E. Kristjánsson, 1998. A comparison of the CCM3 model climate using diagnosed and predicted condensate parameterizations, *J. Clim.*, **11**, 1587-1614.

Rasch, P. J., D. B. Coleman, N. Mahowald, D. L. Williamson, S.-J. Lin, B. A. Boville, and P. Hess, 2006 Characteristics of atmospheric transport using three numerical formulations for atmospheric dynamics in a single GCM framework, *J. Clim*, **19**, 2243-2266.

Rayner, N. A., P. Brohan, D. E. Parker, C. K. Folland, J. J. Kennedy, M. Vanicek, T. Ansell, and S. F. B. Tett, 2006. Improved analyses of changes and uncertainties in sea surface temperature measured in situ since the mid-nineteenth century: The HadISST2 data set, *J. Clim.*, **19**, 3, 446-469.

Reithmeier, C., and R. Sausen, 2002. ATTILA: atmospheric tracer transport in a Lagrangian model, *Tellus B*, **54**, 278-299.

Ricard, J.-L., and J.-F. Royer, 1993. A statistical cloud scheme for use in a AGCM, *Ann. Geophys.,* **11**, 1095-1115.

Richter, J. H., F. Sassi, and R. R. Garcia, 2010. Towards a physically based gravity wave source parameterization in a general circulation model, *J. Atmos. Sci.*, **67**, 136-156.

Rienecker M. M., et al. (2008) The GEOS-5 Data Assimilation System—Documentation of versions 5.0.1, 5.1.0, and 5.2.0. NASA/TM-2008-104606, Vol. 27, Tech. Rep. Series on Global Modeling and Data Assimilation, 118 pp. (available at ***http://gmao.gsfc.nasa.gov/systems/geos5/***)

Robock, A., 2002. Pinatubo eruption: The climatic aftermath, *Science*, **295**, 1242-1244.

Roeckner, E., K. Arpe, L. Bengtsson, S. Brinkop, L. Dümenil, M. Esch, E. Kirk, F. Lunkeit, M. Ponater, B. Rockel, R. Sausen, U. Schleese, S. Schubert, and M. Windelband, 1992. Simulation of the present-day climate with the ECHAM model: Impact of model physics and resolution, Max-Planck-Institut for Meteorology, MPI-Report No. 93.

Roeckner, E., 1995. Parameterization of cloud radiative properties in the ECHAM4 model, in Cloud microphysics parameterizations in global circulation models, Proceedings of the WCRP Workshop, WCRP Report No. 93, WMO/TD–No. 713, 105–116.

Roeckner, E., K. Arpe, L. Bengtsson, M. Christoph, M. Clausen, L. Dümenil, M. Esch, M. Giorgetta, U. Schlese, and U. Schulzweida, 1996. The atmospheric general circulation model ECHAM-4: Model description and simulation of present-day climate, Rep. 218, Max-Planck-Inst. für Meteorol., Hamburg, Germany.

Roeckner, E., et al., 2003. The atmospheric general circulation model ECHAM5. Part I: Model description, MPI Report No. 218, Max-Planck-Institut für Meteorologie, Hamburg, Germany, 90pp.

Roeckner, E., R. Brokopf, M. Esch, M. Giorgetta, S. Hagemann, L. Kornblueh, E. Manzini, U. Schlese, and U. Schulzweida, 2004. The atmospheric general circulation model ECHAM5 Part II: Sensitivity of simulated climate to horizontal and vertical resolution, Max-Planck-Institute for Meteorology, MPI-Report No. 354, 2004.

Roehl, C. M., S. A. Nizkorodov, H. Zhang, G. A. Blake, and P. O. Wennberg, 2002. Photodissociation of peroxynitric acid in the near-IR, *J. Phys. Chem. A*, **106**, 3766-3772.

Rossow, W. B., B. L. Garder, P. J. Lu, and A. W. Walker, 1987. Satellite cloud climatology project (ISCCP), Documentation on cloud data, WMO/TD-266, WMO, Geneva, 78.

Rozanov, E., M. E. Schlesinger, V. Zubov, F. Yang, and N. G. Andronova, 1999. The UIUC three-dimensional stratospheric chemical transport model: Description and evaluation of the simulated source gases and ozone, *J. Geophys. Res.*, **104**, 11,755-11,781.

Sander, S. P., R. R. Friedl, A. R. Ravishankara, D. M. Golden C. E. Kolb, M. J. Kurylo, R. E. Huie, V. L. Orkin, M. J. Molina, G. K. Moortgat, and B. J. Finlayson-

Pitts, 2002. Chemical kinetics and photochemical data for use in atmospheric studies, JPL Publications 02-25 (referred to as JPL, 2002)

Sander, S. P., R. R. Friedl, D. M. Golden, M. J. Kurylo, R. E. Huie, V. L. Orkin, G. K. Moortgat, A. R. Ravishankara, C. E. Kolb, M. J. Molina, and B. J. Finlayson-Pitts (2006), Chemical Kinetics and Photochemical Data for Use in Atmospheric Studies, Evaluation Number 15, JPL Publication, 06-2, Jet Propulsion Laboratory, Pasadena (referred to as JPL, 2006).

Sander, R., A. Kerkweg, P. Jöckel, and J. Lelieveld, 2005. Technical note: The new comprehensive atmospheric chemistry module MECCA, *Atmos. Chem. Phys.*, **5**, 445–450.

Sassi, F., B. A. Boville, D. Kinnison, and R. R. Garcia, 2005. The effects of interactive ozone chemistry on simulations of the middle atmosphere, *Geophys. Res., Lett.*, **32**, doi:10.1029/2004GL022131.

Sato, M., J. E. Hansen, M. P. McCormick, and J. B. Pollack, 1993. Stratospheric aerosol optical depths, 1850-1990, *J. Geophys. Res.*, **98**, 22,987-22,994.

Savage, N. H., K. S. Law, J. A. Pyle, A. Richter, H. Nuss, and J. P. Burrows, 2004. Using GOME NO2 satellite data to examine regional differences in TOMCAT model performance, *Atm. Chem. Phys.*, **4**, 1895-1912.

Scaife, A., N. Butchart, C. D. Warner, D. Stainforth, W. Norton, and J. Austin, 2000. Realistic Quasi-Biennial Oscillations in a simulation of the global climate. *Geophys. Res. Lett.*, **27**, 3481-3484.

Scaife, A. A., N. Butchart, C. D. Warner, and R. Swinbank, 2002. Impact of a spectral gravity wave parametrization on the stratosphere in the Met Office Unified Model. *J. Atmos. Sci.*, **59**, 1473-1489.

Schraner, M., E. Rozanov, C. Schnadt-Poberaj, P. Kenzelmann, A. Fischer, V. Zubov, B. P. Luo, C. Hoyle, T. Egorova, S. Fueglistaler, S. Brönnimann, W. Schmutz, and T. Peter, 2008. Technical Note: Chemistry-climate model SOCOL: Version 2.0 with improved transport and chemistry/microphysics schemes. *Atmos. Chem. Phys.*, **8**, 5957-5974.

Schultz, M., et al., 2007. Emission data sets and methodologies for estimating emissions (***http://retro.enes.org/reports/D1-6_final.pdf***), REanalysis of the TROpospheric chemical composition over the past 40 years, A long-term global modeling study of tropospheric chemistry funded under the 5th EU framework programme, EU-Contract No. EVK2-CT-2002-00170.

Scinocca, J. F., and N. A. McFarlane (2000), The parametrization of drag induced by stratified flow over anisotropic orography, *Quart. J. Roy. Meteorol. Soc.*, **126**, 2353-2393.

Scinocca, J.F., 2003. An accurate spectral nonorographic gravity wave drag parameterization for General Circulation Models, *J. Atmos. Sci.*, **60**, 667-682.

Scinocca, J. F., N. A. McFarlane, M. Lazare, J. Li and D. Plummer, 2008. Technical note: The CCCma third generation AGCM and its extension into the middle atmosphere, *Atmos. Chem. Phys.*, **8**, 7055-7074.

Seinfeld, J.H., and S. N. Pandis, 2006. Atmospheric Chemistry and Physics - From Air Pollution to Climate Change (2nd Edition).. John Wiley & Sons., ISBN: 0471720186.

Sellers, P. J., Y. Mintz, Y. C. Sud, and A. Dalcher, 1986. A simple biosphere model (Sib) for use within general circulation models, *J. Atmos. Sci.*, **43**, 505-531.

Sessler, J., P. Good, A. R. MacKenzie, and J. A. Pyle, 1996. What role do type I polar stratospheric cloud and aerosol parameterizations play in modeled lower stratospheric chlorine activation and ozone loss?, *J. Geophys. Res.*, **101**, 28,817-28,835.

Shaw, T. A., and T. G. Shepherd, 2007 Angular momentum conservation and gravity wave drag parameterization: Implications for climate models. *J. Atmos. Sci.*, **64**, 190-203.

Shaw, T. A., M. Sigmond, T. G. Shepherd, and J. F. Scinocca, 2009. Sensitivity of simulated climate to conservation of momentum in gravity wave drag parameterization, *J. Clim.*, **22**, 2726-2742.

Shepherd, T. G., K. Semeniuk, and J. N. Koshyk, 1996. Sponge layer feedbacks in middle-atmosphere models, *J. Geophys. Res.*, **101**, 23,447–23,464.

Shepherd, T. G., 2003. Large-scale atmospheric dynamics for atmospheric chemists, *Chem. Revs.,* **103**, 4509-4531.

Shepherd, T. G., and T. A. Shaw, 2004. The angular momentum constraint on climate sensitivity and downward influence in the middle atmosphere, *J. Atmos. Sci.*, **61**, 2899-2908.

Shepherd, T. G., 2007. Transport in the middle atmosphere, *J. Meteorol. Soc. Japan,* **85B**, 165-191.

Shibata, K., and T. Aoki, 1989. An infrared radiative

scheme for the numerical models of weather and climate, *J. Geophys. Res.*, **94**, 14,923-14,943.

Shibata, K., and A. Uchiyama, 1994. An application of the discrete ordinate method to terrestrial radiation in climate models, *J. Atmos. Sci.*, **51**, 3531-3538.

Shibata, K., M. Deushi, T. T. Sekiyama, and H. Yoshimura (2005), Development of an MRI chemical transport model for the study of stratospheric chemistry, *Papers Meteorol. Geophys.*, **55**, 75-119.

Shibata, K., and M. Deushi (2008a), Long-term variations and trends in the simulation of the middle atmosphere 1980-2004 by the chemistry-climate model of the Meteorological Research Institute, *Ann. Geophys.*, **26**, 1299-1326.

Shibata, K., and M. Deushi, 2008b. Simulation of the stratospheric circulation and ozone during the recent past (1980-2004) with the MRI chemistry-climate model, *CGER's Supercomputer Monograph Report,* **13,** NIES, Japan, 154 pp.

Shiogama, H., M. Watanabe, M. Kimoto, and T. Nozawa, 2005. Anthropogenic and natural forcing impacts on ENSO-like decadal variability during the second half of the 20th century, *Geophys. Res. Lett.*, **32**, doi:10.1029/2005GL023871.

Slingo, J. M., 1987. The development and verification of a cloud prediction scheme for the ECMWF model, *Quart. J. Roy. Meteorol. Soc.*, **113**, 899–927.

Smith, R. N. B., 1990. A scheme for predicting layer clouds and their water content in a general circulation model. *Quart. J. Roy. Meteorol. Soc.*, **116**, 435-460.

Solanki S. K. and N. A. Krivova, 2003. Can solar variability explain global warming since 1970?, *J. Geophys. Res.*, **108**, doi:10.1029/2002JA009753.

Steil, B., M. Dameris, C. Brühl, P. J. Crutzen, V. Grewe, M. Ponater, and R. Sausen, 1998. Development of a chemistry module for GCMs: First results of a multiannual integration, *Ann. Geophys.*, **16**, 205-228.

Stenchikov, G., K. Hamilton, R. J. Stouffer, A. Robock, V. Ramaswamy, B. Santer, and H.-F. Graf, 2006. Arctic Oscillation response to volcanic eruptions in the IPCC AR4 climate models, *J. Geophys. Res.*, **111**, D7, doi:10.1029/2005JD006286, 2006

Stenke, A., V. Grewe, and M. Ponater, 2008a. Lagrangian transport of water vapor and cloud water in the ECHAM4 GCM and its impact on the cold bias, *Clim Dyn.*, **31**, 491-506.

Stenke, A., M. Dameris, V. Grewe, and H. Garny, 2008b. Implications of Lagrangian transport for coupled chemistry-climate simulations, *Atmos. Chem. Phys.*, **9**, 5489-5504.

Stott, P., G. Jones, J. Lowe, P. Thorne, C. Durman, T. Johns, and J. Thelen, 2006. Transient climate simulations with the HadGEM1 climate model: Causes of past warming and future climate change, *J. Clim.*, **19**, 2763-2782.

Struthers, H., G. E. Bodeker, D. Smale, E. Rozanov, M. Schraner, and T. Peter, 2009. Evaluating how photochemistry and transport determine stratospheric inorganic chlorine in coupled chemistry-climate models. *Geophys. Res. Lett.*, **36**, doi:10.1029/2008GL036403.

Sud, Y. C., W. C. Chao, and G. K .Walker, 1993. Dependence of rainfall on vegetation: Theoretical consideration, simulation experiments, observations, and inferences from simulated atmospheric soundings, *J. Arid. Environ.*, **25**, 5-18.

Sud, Y. and G. K. Walker, 1999. Microphysics of clouds with the Relaxed Arakawa Schubert Scheme (McRAS). Part 1: Design and Evaluation with GATE Phase III Data. *J. Atmos. Sci.*, **56**, 3196-3220.

Sundqvist, H., 1978. A parameterization scheme for nonconvective condensation including prediction of cloud water content, *Quart. J. Roy. Meteorol. Soc.*, **104**, 677-690.

Sundqvist, H., E. Berge, and J. E. Kristjansson, 1989. Condensation and cloud parameterization studies with a mesoscale numerical weather prediction model, *Mon. Wea. Rev.*, **117**, 1641-1657.

Takahashi, M., 1996. Simulation of the stratospheric quasi-biennial oscillation using a general circulation model, *Geophys. Res. Lett.*, **23**, 661-664.

Takahashi, M., 1999. Simulation of the quasi-biennial oscillation in a general circulation model, *Geophys. Res. Lett.*, **26**, 1307-1310.

Takigawa, M., M. Takahashi, and H. Akiyoshi, 1999. Simulation of ozone and other chemical species using a Center for Climate System Research/National Institute for Environmental Studies atmospheric GCM with coupled stratospheric chemistry, *J. Geophys. Res.*, **104**, 14003-14018.

Talukdar, R. K., C. A. Longfellow, M. K. Gilles, and A. R. Ravishankara, 1998. Quantum yields of O(1D) in the photolysis of ozone between 289 and 329 nm as

a function of temperature, *Geophys. Res. Lett.*, **25**, 143-146.

Teyssèdre H., M. Michou, H. L. Clark, B. Josse, F. Karcher, D. Olivie, V.-H. Peuch, D. Saint-Martin, D. Cariolle, J.-L. Attié, P. Nédélec, P. Ricaud, V. Thouret, R. J. van der A, A. Volz-Thomas, and F. Cheroux, 2007. A new tropospheric and stratospheric chemistry and transport model MOCAGE-Climat for multi-year studies: Evaluation of the present-day climatology and sensitivity to surface processes, *Atmos. Chem. Phys.*, **7**, 5815-5860.

Tian, W., and M. P. Chipperfield, 2005. A new coupled chemistry-climate model for the stratosphere: the importance of coupling for future O3-climate predictions, *Quart. J. Roy. Meteorol. Soc.*, **131**, 281-303.

Tian, W., and M. P. Chipperfield, 2006. Stratospheric water vapor trends in a coupled chemistry-climate model, *Geophys. Res. Lett.*, **33**, doi:10.1029/2005GL024675.

Tiedtke, M., 1989. A comprehensive mass flux scheme for cumulus parameterization in large-scale models, *Mon. Wea, Rev.*, **117**, 1779–1800.

Thomason, L. W., L. R. Poole, and T. Deshler, 1997. A global climatology of stratospheric aerosol surface area density deduced from Stratospheric Aerosol and Gas Experiment II measurements: 1984–1994, *J. Geophys. Res.*, **102**, 8967–8976.

Thomason, L., and T. Peter, 2006. Assessment of Stratospheric Aerosol Properties (ASAP), SPARC Report No. 4., WCRP-124, WMO/TD-No. 1295.

Tompkins, A., 2002. A prognostic parameterization for the subgrid-scale variability of water vapor and clouds in large-scale models and its use to diagnose cloud cover. *J. Atmos. Sci.*, **59**, 1917–1942.

Tost, H. , P. Jöckel, and J. Lelieveld, 2007. Lightning and convection parameterisations – uncertainties in global modeling, *Atmos. Chem. Phys.*, **7**, 4553-4568.

Untch, A., A. Simmons, et al., 1998. Increased stratospheric resolution in the ECMWF forecasting system, ECMWF Newsletter, 82, 2-8.

Uno, I., X.-M. Cai, D. G. Steyn, and S. Emori (1995), A simple extention of the Louis method for rough surface layer modeling, *Bound. Layer Meteorol.*, **76**, 395-409.

Van Aardenne, J., et al., 2005. The EDGAR 3.2 Fast Track 2000 dataset (32FT2000), Technical documentation, ***http://www.mnp.nl/edgar/model/v32ft2000edgar***.

Vogel, B., P. Konopka, J.-U. Grooss, R. Müller, B. Funke, M. Lopez-Puertas, T. Reddmann, G. Stiller, T. von Clarmann, and M. Riese (2008), Model simulations of stratospheric ozone loss caused by enhanced mesospheric NOx during Arctic winter 2003/2004, *Atmos. Chem. Phys.*, **8**, 5279-5293.

Walcek, C. J., R. A. Brost, J. S. Chang, and M. L. Wesely (1986), SO2, sulfate and HNO3 deposition velocities computed using regional landuse and meteorological data, *Atmos. Env.*, **20**, 949-964.

Warner, C. D., and M. E. McIntyre, 2001. An ultrasimple spectral parameterization for non-orographic gravity waves, *J. Atmos. Sci.*, **58**, 1837-1857.

Warrilow, D.A., A. B. Sangster, and A. Slingo, 1986. Modelling of land surface processes and their influence on European climate; Meteorological Office, Met O 20 Tech. Note DCTN 38, Bracknell, U.K..

Waugh, D. W., L. Oman, S. R. Kawa, R. S. Stolarski, S. Pawson, A. R. Douglass, P. A. Newman, and J. E. Nielsen. 2009. Impacts of climate change on stratospheric ozone recovery, *Geophys. Res. Lett.*, **36**, doi:10.1029/2008GL036223.

Webster, S., A. R. Brown, D. R. Cameron, and C. P. Jones, 2003. Improvements to the representation of orography in the Met Office Unified Model. *Quart. J. Roy. Meteorol. Soc.*, **129**, 1989-2010. doi:10.1256/qj.02.133.

Williamson, D. L., and P. J. Rasch, 1989. Two-dimensional semi-Lagrangian transport with shape-preserving interpolation, *Mon. Wea. Rev.*, **117**, 102–129.

World Meteorological Organisation Scientific assessment of ozone depletion, Global Ozone Res. Monit. Rep. 16, Geneva, 1992.

World Meteorological Organization (WMO)/United Nations Environment Programme (UNEP), 2007. *Scientific Assessment of Ozone Depletion: 2006*, World Meteorological Organization, Global Ozone Research and Monitoring Project, Report No. 50, Geneva, Switzerland.

Xiao, F., and X. Peng, 2004. A convexity preserving scheme for conservative advection transport, *J. Comput. Phys.*, **198**, 389-402, doi:10.1016/j.jcp.2004.01.013.

Yessad, K., 2001. Horizontal diffusion computations in the cycle 24T1 of ARPEGE/IFS. ARPEGE Technical Documentation, 96pp.

Yukimoto, S., A. Noda, A. Kitoh, M. Hosaka, H. Yo-

shimura, T. Uchiyama, K. Shibata, O. Arakawa, and S. Kusunoki, 2006. Present-day climate and climate sensitivity in the Meteorological Research Institute coupled GCM version 2.3 (MRI-CGCM2.3), *J. Meteorol. Soc. Japan*, **84**, 333-363.

Zdunkowski, W. G., R. M. Welch, and G. Korb, 1980. An investigation of the structure of typical two-stream-methods for the calculation of solar fluxes and heating rates in clouds. *Contr. Phys. Atmos.,* **53**, 147-166.

Zhong, W. and J. D. Haigh, 2001. An efficient and accurate correlated-k parameterization of infrared radiative transfer for troposphere-stratosphere-mesosphere GCMs, *Atmos. Sci. Lett.*, **1**, doi:10.1006/asle.2000.0022.

Zhong, W, J. D. Haigh, D. Belmiloud, R. Schermaul, and J. Tennyson, 2001. The impact of new water vapour spectral line parameters on the calculation of atmospheric absorption, *Quart. J. Roy. Meteorol. Soc.*, **127**, 1615-1626.

Zhong, W., S. M. Osprey, L. J. Gray, and J. D. Haigh, 2008. Influence of the prescribed solar spectrum on calculations of atmospheric temperature. *Geophys. Res. Lett.*, **35**, doi:10.1029/2008GL035993.

Zubov, V., E. Rozanov, and M. Schlesinger, 1999. Hybrid scheme for three-dimensional advective transport, *Mon. Wea. Rev.*, **127**, 1335-1346.